Caner Çuhac

# Wireless Sensor Network Applications in Military, Agricultural and Energy Research

ACTA WASAENSIA 431

Vaasan yliopisto
UNIVERSITY OF VAASA

ACADEMIC DISSERTATION

*To be presented, with the permission of the Board of the School of Technology and Innovations of the University of Vaasa, for public examination in Auditorium Nissi (K218) on the 11th of November, 2019, at noon.*

Reviewers

Prof. Hafız Alisoy
Tekirdağ Namık Kemal University, Faculty of Engineering
Electronics and Communication Department
Namık Kemal Üniversitesi - Çorlu Mühendislik Fakültesi
Silahtarağa Mahallesi Üniversite 1. Sokak No:13
59860 ÇORLU
TEKİRDAĞ
TURKEY

Prof. Francisco Vázquez
School of Engineering Sciences of Córdoba
Department of Computer Sciences and Numerical Analysis
University of Cordoba - Campus de Rabanales
Leonardo da Vinci Building
14071 CÓRDOBA
CÓRDOBA
SPAIN

| **Julkaisija** | **Julkaisupäivämäärä** |
|---|---|
| Vaasan yliopisto | Lokakuu 2019 |

| | | |
|---|---|---|
| **Tekijä(t)**<br>Caner Çuhac | **Julkaisun tyyppi**<br>Artikkeliväitöskirja | |
| **Orcid tunniste** | **Julkaisusarjan nimi, osan numero**<br>Acta Wasaensia, 431 | |
| **Yhteystiedot**<br>Vaasan yliopisto<br>Tekniikan ja<br>innovaatiojohtamisen yksikkö<br><br>PL 700<br>FI-65101 VAASA | **ISBN**<br>978-952-476-882-5 (painettu)<br>978-952-476-883-2 (verkkoaineisto) | |
| | **URN:ISBN:978-952-476-883-2** | |
| | **ISSN**<br>0355-2667 (Acta Wasaensia 431, painettu)<br>2323-9123 (Acta Wasaensia 431, verkkoaineisto) | |
| | **Sivumäärä**<br>128 | **Kieli**<br>englanti |

**Julkaisun nimike**
Langattomien anturiverkkojen sotilas-, agroteknologia- ja energiatutkimussovelluksia



**Tiivistelmä**
Fysikaaliset suureet mitataan nykyisin elektronisten anturien avulla. Langattomat anturiverkot ovat kustannustasoltaan edullisia, matalan tehonkulutuksen elektronisia laitteita, jotka kykenevät suorittamaan mittauksia niissä olevilla antureilla. Langattomat anturinoodit voidaan myös liittää toimilaitteisiin, jolloin ne voivat vaikuttaa fyysiseen ympäristöönsä. Koska langattomilla anturi- ja toimilaiteverkoilla voidaan vaikuttaa niiden fysikaalisen ympäristön tilaan, niiden avulla voidaan toteuttaa säätö- ja automaatiosovelluksia. Tässä väitöskirjatyössä suunnitellaan ja toteutetaan neljä erilaista langattomien anturi- ja toimilaiteverkkojen automaatiosovellusta. Ensimmäisenä tapauksena toteutetaan elektroniikka- ja ohjelmistosovellus, jolla integroidaan kamera langattomaan anturinoodiin. Kuvat tallennetaan ja prosessoidaan anturinoodissa vähän energiaa kuluttavia laskentamenetelmiä käyttäen. Toisessa sovelluksessa kahdesta erilaisesta langattomasta anturiverkosta koostuvalla järjestelmällä valvotaan siementen syöttöä kylvökoneessa. Kolmannessa sovelluksessa levitetään kaupunkiympäristössä kriisitilanteessa rakennuksen sisätiloihin langaton anturiverkko. Sen anturinoodit välittävät paikkatietoa rakennuksessa operoiville omille joukoille, jotka voivat tilanteesta riippuen olla esimerkiksi sotilaita, palomiehiä tai lääkintähenkilökuntaa. Neljännessä sovelluksessa toteutetaan langaton anturiverkko, jonka keräämää mittausdataa käytetään arvioitaessa lämpöenergian keräämismahdollisuuksia asfalttipinnoilta.



**Asiasanat**
langaton, anturi, sovellus, automaatio, mittaus

| **Publisher** | **Date of publication** | |
|---|---|---|
| University of Vaasa | October 2019 | |
| **Author(s)**<br>Caner Çuhac | **Type of publication**<br>Doctoral thesis by publication | |
| **Orcid identifier** | **Name, and number of series**<br>Acta Wasaensia, 431 | |
| **Contact information**<br>University of Vaasa<br>School of Technology and Innovations<br>Department of Computer Science<br><br>P.O. Box 700<br>FI-65101 VAASA | **ISBN**<br>978-952-476-882-5 (print)<br>978-952-476-883-2 (online) | |
| | **URN:ISBN:978-952-476-883-2** | |
| | **ISSN**<br>0355-2667 (Acta Wasaensia 431, print)<br>2323-9123 (Acta Wasaensia 431, online) | |
| | **Number of pages**<br>128 | **Language**<br>English |

**Title of publication**
Wireless Sensor Network Applications in Military, Agricultural and Energy Research



**Abstract**
The physical quantities nowadays are widely measured by using electronic sensors. Wireless sensor networks (WSNs) are low-cost, low-power electronic devices capable of collecting data using their onboard sensors. Some wireless sensor nodes are equipped with actuators, providing the possibility to change the state of the physical world. The ability to change the state of a physical system means that WSNs can be used in control and automation applications. This research focuses on appropriate system design for four different wireless measurement and control cases. The first case provides a hardware and software solution for camera integration to a wireless sensor node. The images are captured and processed inside the sensor node using low power computational techniques. In the second application, two different wireless sensor networks function in cooperation to overcome seeding problems in agricultural machinery. The third case focuses on indoor deployment of the wireless sensor nodes into an area of urban crisis, where the nodes supply localization information to friendly assets such as soldiers, firefighters and medical personnel. The last application focuses on a feasibility study for energy harvesting from asphalt surfaces in the form of heat.



**Keywords**
wireless, sensor, application, automation, measurement

# ACKNOWLEDGEMENTS

Dedicated to all children

# CONTENTS

# LIST OF FIGURES

# LIST OF TABLES

# LIST OF ACRONYMS

| | |
|---|---|
| **IoT** | Internet of Things |
| **OSI** | Open Systems Interconnection |
| **WISMII** | Wireless Indoor Situation Modeling II |
| **RSSI** | Received Signal Strength Indicator |
| **VEI** | Vaasa Energy Institute |
| **MCU** | Microcontroller Unit |
| **SNR** | Signal to Noise Ratio |
| **PCB** | Printed Circuit Board |
| **AGC** | Automatic Gain Control |
| **RAM** | Random Access Memory |
| **ADC** | Analog to Digital Converter |
| **COP** | Common Operational Picture |
| **I2C** | Inter-Integrated Circuit |
| **SRAM** | Static Random Access Memory |
| **SeAMK** | Seinäjoki University of Applied Sciences |
| **DFL** | Device Free Localization |
| **DTS** | Distributed Temperature Sensing |
| **EEA** | European Environment Agency |
| **CoAP** | Constrained Application Protocol |
| **6LoWPAN** | IPv6 over Low-Power Wireless Personal Area Networks |
| **FRAM** | Ferroelectric Random Access Memory |

# LIST OF PUBLICATIONS

The dissertation is based on the following four refereed articles:

(I) Çuhac, C., Yiğitler, H., Virrankoski, R. & Elmusrati, M. (2010). Camera Integration to Wireless Sensor Node. *Aalto University Workshop on Wireless Sensor Systems*. Aalto University Wireless Systems Group, Helsinki.

(II) Çuhac, C., Virrankoski, R., Hänninen, P., Elmusrati, M., Hööpakka, H., Palomäki H. (2012). Seed Flow Monitoring in Wireless Sensor Networks. *Aalto University Workshop on Wireless Sensor Systems*. Aalto University Wireless Systems Group, Helsinki.

(III) Björkbom M., Timonen J., Yiğitler H., Kaltiokallio O., García J. M. V., Myrsky M., Saarinen J., Korkalainen M, Çuhac C., Jäntti R., Virrankoski R., Vankka J., and Koivo H. N. (2013) Localization Services for Online Common Operational Picture and Situation Awareness, *IEEE Access*, vol. 1, pp. 742-757.

(IV) Çuhac, C., Mäkiranta, A., Välisuo P., Hiltunen, E., Elmusrati, M., (2019) Feasibility Study on Solar Energy Harvesting from Asphalt Surface in Cold Climate Region, *Renewable Energy*, Preprint submitted to Elsevier.

# AUTHOR'S CONTRIBUTION

### Publication I: "Camera Integration to Wireless Sensor Node"

The wireless sensor platform "UWASA Node" was designed by researchers in University of Vaasa. The author has designed a new hardware architecture for adding computer vision capabilities to this existing wireless sensor platform. The proof of concept for tilt and pan capable camera integration was analyzed and data acquisition methods were introduced. Later, this research was further developed and the vision capability was implemented. New image processing techniques and a more efficient image transmission method was introduced.

### Publication II: "Seed Flow Monitoring in Wireless Sensor Networks"

In this publication, wireless sensor devices were used to monitor the seed flow rates of an agricultural machinery in real time. The data measurement system was added to seed drill machine and an LCD screen based monitoring system was implemented for tractor side. The author has established communication between two different types of wireless sensor platforms. A partial seed drill machine prototype was equipped with wireless devices and measurements were made by the author. The acquired data was analyzed, monitored and the author provided software for both visualization and statistical analysis.

### Publication III: "Localization Services for Online Common Operational Picture and Situation Awareness"

This research presents a localization and online situation awareness system for military use. In case of an urban crisis, it is very important to know how many people are inside as well as their location. For this purpose, the research team has developed localization methods based on wireless devices. As a member of the team the author has worked on development of a wireless sensor node distribution system

integrated into a mobile robot. The wireless sensor nodes were deployed in certain locations inside a building, then provided data acquisition for localization services.

### Publication IV: "Feasibility Study on Solar Energy Harvesting from Asphalt Surface in Cold Climate Region"

Heat flux measurements were obtained by placing a sensor under the asphalt. Captured data was timestamped, compared and analyzed together with solar power that reaches the earth directly. In addition to those, temperatures at different depths of the ground were measured. The author has designed a new wireless sensor platform including both the hardware and software. These devices were then used in heat flux data acquisition over wireless network. The author has analyzed the acquired data, then constructed a physical model theory that explains the energy transfer between sun, ground surface and the deeper layers of the soil.

# 1 INTRODUCTION

This section briefly provides background information and introduces the research work and novelty covered within the context of this thesis.

## 1.1 Background Information

During the last two decades, there has been great advancements in wireless sensor network technologies. As defined in Diamond and Ceruti (2007) the concept of wireless sensor systems originates from the descendants of wireless ad hoc networks used in military monitoring and communication systems. Following developments started to cover wireless automation as well. This includes the internet of things (IoT) devices as well as larger platforms. In industrial automation there are many cases where the cabling is not possible due to rotating machinery parts or where the mobility is crucial. Certain agricultural applications also require mobility and distributed data acquisition. It is obvious that wireless network devices help reducing the implementation costs compared to cabled systems. On the other hand, in military applications low cost is not the primary factor but time and mobility is extremely valuable instead. Emergency situations such as urban violence or kidnapping cases require the ease of deployment and shorter installation time as emphasized in Virrankoski (2013). Wireless automation devices in this context, offer optimal solutions for variety of applications.

Referring to Akyildiz et al. (2002) a wireless sensor node is equipped with radio a communication interface, a processor or in most cases a microcontroller, one or more sensors and a power source. There is an important trade off between the functionality of the node and the power consumption. Some applications require extremely low power usage whereas some applications are more demanding of computational power. There are cases where the wireless sensor nodes could charge their batteries using natural sources like solar power. In order to address this trade off, many hardware developers prefer to offer a generic wireless sensor platform for integration stage, and later designs result in a customized application specific device.

The advancements in the industrial automation require proper collection of data and sharing. Data sharing does not necessarily cover only sharing between individuals but it also includes machine to machine communication. Wireless sensor networks provide methods to collect data about the environment such as temperature, motion, speed, humidity, luminosity etc. and are also capable of changing the physical states in the environment. In machine to machine communication, as defined in Jung et al. (2013), wireless sensor platforms are not solely responsible of collecting and

transferring the data, but they are usually responsible also of making important decisions in real time. During the progress of this research work, many physical quantities were measured and analyzed. The work consists of solutions such as collection of timestamped data, implementing distributed computation techniques, overcoming cable installation costs and implementation of wireless networks where cabling was not possible.

Applications represented in this thesis solve multiple problems that would either be very difficult to address due to implementation methods, or impossible to put in practice without using wireless sensor networks.

## 1.2 Practical Applications

Wireless sensor networks in present day are quite advanced and are widely used in conjunction with the IoT technologies. Regarding to Gomes et al. (2019), over the development years, variety of communication protocols and synchronization mechanisms have been developed for more efficient power utilization. The complexity of those protocols along with the importance of the critical applications such as tactical WSNs requires protection against cyber attacks referring to Thulasiraman et al. (2019).

Furthermore about security, in future it is highly possible that electronic commerce will rely on IoT technologies and wireless sensor networks. Cryptocurrencies are expected to replace banknotes and metal coins thus the adaptation of WSNs to e-commerce becomes necessary. Practical challenges defined in Makhdoom et al. (2019) need to be addressed and security measures need be standardized.

As of 2019, the development of the WSNs focus on network security, cloud computing, protection against cyber attacks, IoT privacy. Those issues are all related to higher layers of the OSI model, which means that the development of the hardware is not rapid nowadays. Back in 2000s the WSNs were mainly developed with simpler communication protocols while the main focus was on hardware side such as physical size, battery types and charging possibilities.

In present day, wireless sensor networks have proven their importance in many different areas such as smart grids, health monitoring systems, military, transportation, agriculture and more.

In this part, the realized wireless sensor applications during the author's research period are introduced.

### 1.2.1 UWASA Node and Additional Vision Capabilities

As described in Yiğitler et al. (2010), the development of the first version of UWASA Node wireless sensor platform was started in University of Vaasa, Communications and System Engineering department in 2009. The extensions for this platform and additional capabilities were discussed and addressed already during the development period. One of those planned extensions was a camera integration.

The author's specific work related to this development was to integrate a camera to this wireless device. One of the biggest challenges has been the lack of computing power. After theoretical studies the limitations were clarified and prototypes were started to be built.

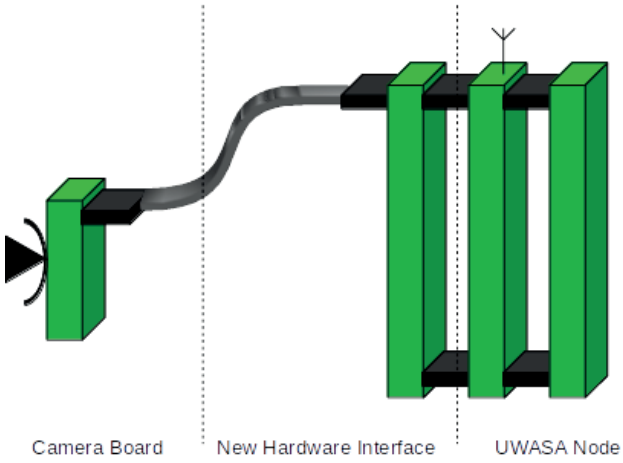


**Figure 1.** The proposed vision hardware extension for UWASA Node.

Another great challenge was the selection of the vision sensor and the image quality. An appropriate camera was not easy to choose during the time of the research. The hardware interface between the node and the camera was specific for the camera board and could not be replaced without changing the hardware interface. The camera had to be small and had to provide interface with sufficient documentation to receive images.

UWASA Node was later developed into second version and was used in multiple industrial, agricultural and military applications that some of those are not covered within the context of this thesis.

### 1.2.2 Agricultural Application in Seed Drill Machines

One important application of UWASA Node has been the agricultural use in seed drill machines. An industrial company expressed their need for wireless monitoring system to measure the seed drop rates in their machinery. When the tractor operates in humid fields it is possible that mud gets stuck into one or more pipes. This prevents germination in some of the rows. If the driver would be informed about the problem, or could see the seed flow rates in real time, it would be possible to take action as soon as the failure occurs.

**Figure 2.** Some rows are not germinated because of the problems occurred during the seeding.

The offered solution was using light based sensors, monitored by a small and low power wireless sensor platform called SURFbutton. SURFbutton was then bridged with a UWASA Node that acts as a gateway for data collection. Taking into consideration that a standard seed drill machine has 24 different seeding channels, the cost and the installation complexity would be very high using traditional cabled based methods. Furthermore it would be impossible to lay cables along rotating machinery parts.

### 1.2.3 Urban Crisis Usage

Within the context of Wireless Sensor Systems in Indoor Situtaion Modeling II (WISMII) project, UWASA Nodes were used for device-free human localization services. In case of an indoor urban crisis or an emergency situation, it is very important for the government units to locate where the people are inside the building. The proposed solution has been that wireless nodes were deployed by a mobile robot at certain locations inside the building, and the received signal strength indicator (RSSI) between each node to every other node was used for localizing. The author and Tobias Glocker who was also a researcher in University of Vaasa have been implementing the node distribution mechanism. Another group of researchers have been working on localization algorithms based on RSSI. Both the hardware and software has been integrated on a mobile robot. This application also addresses a research gap where the solution could be filled by the usage of wireless sensor networks.

### 1.2.4 Energy Research Application

In 2013, the development of Aldere wireless sensor platform was started by the author. Two different commercial models were produced. Both models use the same radio interface and the same network protocol. One of the models called ”Emin” is mainly built for such applications where the power requirements are not strict and the continuous power resource is present. Another smaller model is designed in a smaller form to be used in simple and very low power applications. Both models run an embedded operating system called ”FreeRTOS”.

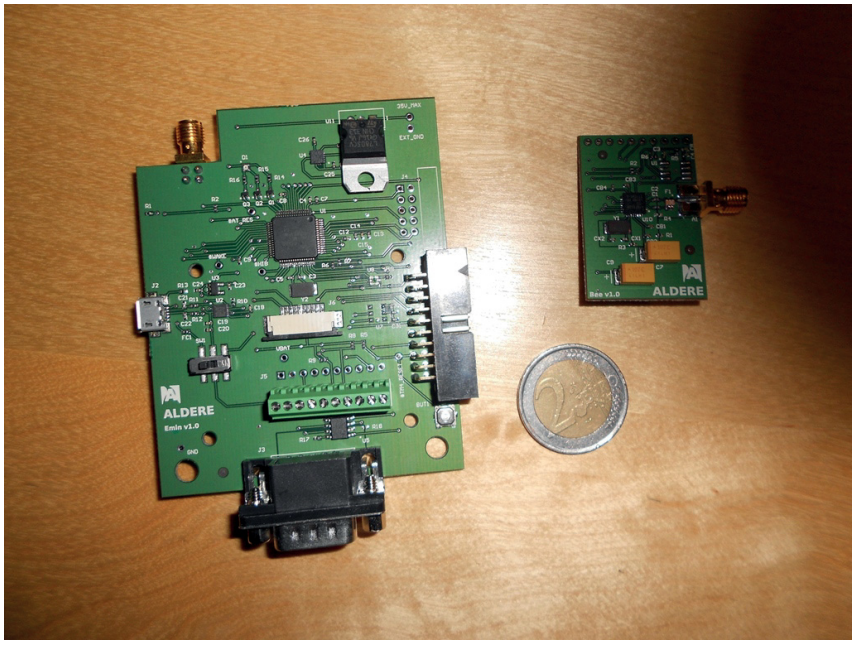


**Figure 3.** Both types of Aldere Platforms. The model on the left called ”Emin” contains multiple physical interfaces. Shown on the right side, ”Bee” model contains only few on-board sensors and interfaces.

During summer days the sunlight is so strong that it causes the temperatures on the asphalt surface to rise dramatically. Vaasa Energy Institute (VEI) has been researching possibilities to harvest thermal energy from the asphalt surface. For this purpose, the research group has decided to measure the solar power using a pyranometer. Although the solar power can directly be measured by pyranometer, the next question was how much of that energy is absorbed by the ground. In order to answer that, a heat flux plate was installed under the asphalt surface to compare and analyze the heat flow along with the solar power strength. The chosen location has been the parking yard behind the Fabriikki building of University of Vaasa.


**Figure 4.** The sensor is placed just below the asphalt layer.

**Figure 5.** The heat flux sensor is connected to Aldere Wireless Sensor Platform which is located inside the box.

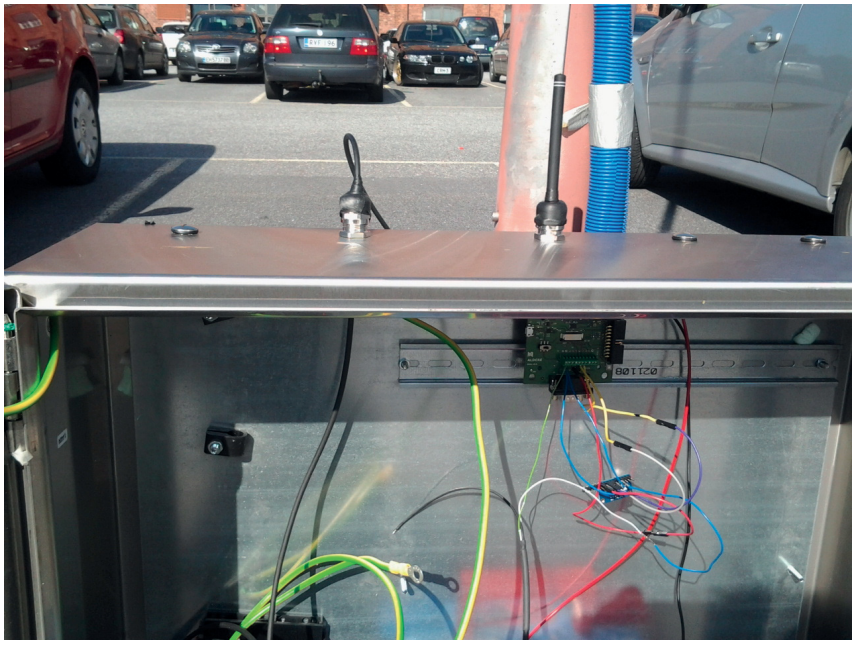

**Figure 6.** The wireless sensor platform is connected to the sensor. The device reads the date from the sensor and transmits to the gateway platform.

**Figure 7.** The gateway node is located inside the University. It collects and logs the data into an embedded Linux PC.

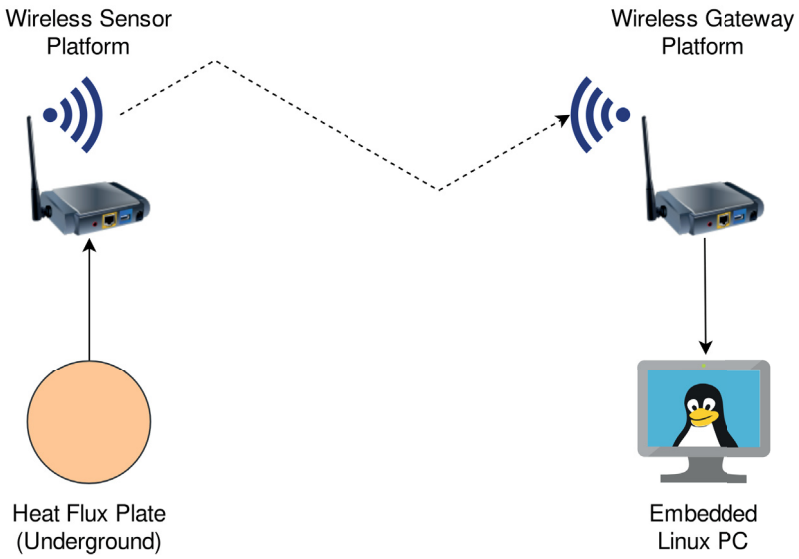


**Figure 8.** Network structure of the heat flux measurement system using wireless sensor platforms.

One of the Aldere wireless sensor platforms was placed outdoors to read the heat flux data, and the other one was placed indoors, acting as a gateway for data collection and storage. All the collected data has been timestamped and stored for further analysis.

After the design requirements are clarified the circuit is modeled on the PC.

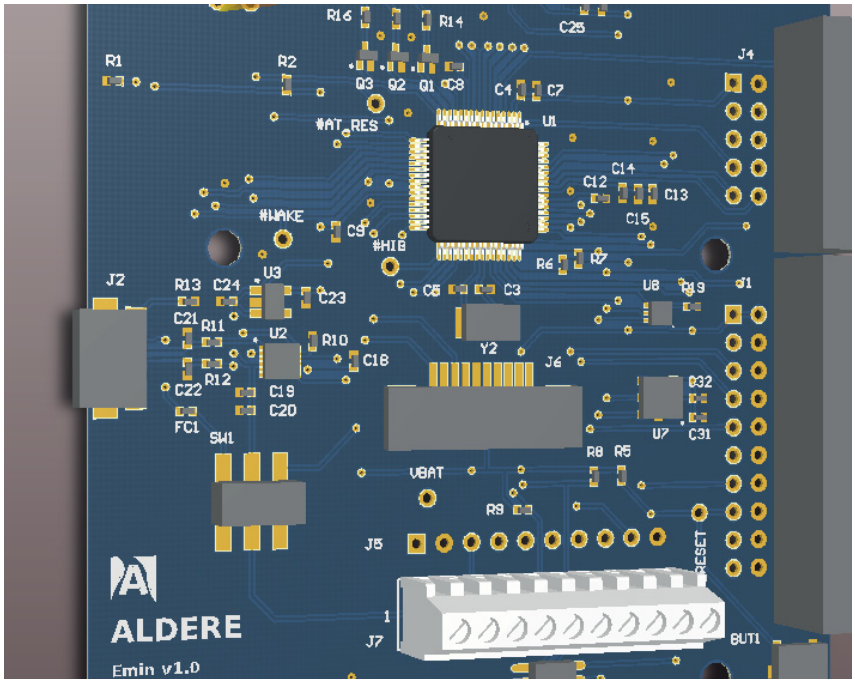


**Figure 9.** After the hardware requirements are portrayed, the electronic components were selected and modeled on computer. Component choice and placement plays a key role in low noise PCB design.

After the hardware design is completed, the productions files are generated and forwarded to production company.

Although the embedded software at this point is not used at all, the hardware design must strictly be done with the capabilities of embedded software in mind. In other words, the hardware should impose no unnecessary restrictions to software. For example, in case there would be a hardware fault in microcontroller programming interface, or in radio interface, there is no possibility to fix this problem from software part.

The software should also be well structured and the software architecture was designed as generic and flexible. Low level software relies on the stability of widely used FreeRTOS. As defined in Zagan et al. (2019), the operating system allows the tasks to be prioritized so that in case the microcontroller is busy with any event, it can store the unfinished task and do the more important task immediately. For example if there is some data coming from the radio and needs to be handled fast, the microcontroller can pause its current job and switch to higher priority task. All those events could be done within a millisecond.

The author's contribution to the research covered in this thesis is not only limited to device design and production. The application software and necessary external

hardware additions as well as computer simulations and data analysis were performed in all individual research works.

In this chapter the definitions of each research problem and requirements were introduced. The purpose of the camera integration to sensor node and proposed hardware solution is defined. In agricultural application, the problems related to the seeding machines is represented and a monitoring solution using wireless sensor networks is described. For military applications, the localization method by using distributed wireless sensors is described. Finally for energy research the wireless sensors are used for data collection and transmission where laying cables is not possible.

All those wireless applications introduced above will be explained and discussed in the following sections.

## 1.3 Thesis Contributions

During the doctoral studies the author has been working on various improvements related to wireless sensor networks. Every research work has been a unique design from the hardware point of view.

Firstly, the camera integration to a wireless sensor network used to be a very recent concept during the time of development. The commercially available embedded cameras were not advanced and were not suitable for wireless usage. Additionally the development of the protocols for wireless sensor networks focused mainly on low power usage and network coordination.

The author has developed a new hardware architecture for adding vision capabilities to UWASA Node. The design includes an SRAM and a FIFO chip for image capturing and fast image processing using limited computational power. Those image processing algorithms were based on already existing methods like monochrome image transformation and edge detection. The standard C library and the API of the microcontroller did not allow the usage of math library. However, the author has integrated the Babylonian square root method for fast computation, creating a unique algorithm that demands very low computational power. The solution has provided satisfactory results. Moreover the transmission size of the image was dramatically reduced by transmitting only the coordinates of interesting pixels instead of the entire picture.

In seed flow monitoring case, the author and the research team has designed a new automation system for agricultural use. The proposed architecture consists of data capturing from the seed drill implement and transmitting to the tractor for monitoring. Two different wireless sensor types are used. First one, the SURFbutton

is located only on the implement side, while the UWASA Node is located in both tractor side and the seed drill implement side. SURFbuttons were responsible for capturing the events for each falling seed. The captured data was then passed on another SURFbutton mounted on a UWASA Node, and finally the results were monitor inside the tractor.

The author has performed numerical analysis on seed falling events. By studying the possibilities for successful detection, the research team decided to use light based method. Although much of the work has been engineering and technical work, the novelty has been the statistical analysis and system design. During the time of the research there were no commercially available solutions, so in that context the design has been pioneering research work.

In third research case, the wireless sensor networks are mainly responsible for localization services in urban crisis such as kidnapping, fire or terrorist activities. The localization services are then used for building the common operational picture for all friendly assets. The author has implemented the software for node distribution mechanism and the integration of this subsystem to the common operational picture.

After working on several research projects, the author has designed a new wireless sensor platform. This platform was created in response to the shortages of the existing solutions. The research work related to energy harvesting application necessitated long range transmission and high precision measurements so the new platform met the demands. Data collection required on-site setup and transmission to a PC for post-analysis. During the new wireless sensor platform design process, the author has designed unique packet format and high layer data exchange protocol for both the wireless medium and peripheral communication like UART.

After the data collection system was setup, the solar power and heat flux has been monitored together for over a year. Data analysis were then performed in mathematical software. The energy coming from sun was analyzed together with a heat flux measurements obtained from the asphalt surface. The relation between the solar power and the absorbed heat was modeled and explained on concrete results. The properties of the soil was extracted from European Environment Agency EEA (2012) and the effect of solar power was analyzed even further; together with the temperature measurements in deeper layers of the soil. This entire model helped the research team to discover how much energy is absorbed and how it is transferred between the surface and deeper layers. The team has also measured the radiative losses during night times. By combining those results, the team has successfully estimated how much solar power could be harvested from the asphalt layer.

# 2 WIRELESS SENSOR NETWORKS IN AUTOMATION

In this section the general overview of the wireless sensor networks and structure of wireless sensor platforms will be represented. The hardware and software architecture as well as network protocols and real-time operating systems will be discussed.

## 2.1 Overview of Wireless Sensor Networks

Wireless sensor nodes are typically small-scale devices that exchange data over wireless medium and external peripheral interfaces. These devices operate on low power to extend the battery lifetime as much as possible. Wireless sensor networks are able to monitor the physical quantities such as temperature, humidity, light, pressure, sound, vibrations, movements in a co-operative way.

Batteries are the primary source of energy for wireless sensor nodes. Depending on the design, there could be additional energy scavenging systems for battery charging such as solar panels or any other vibration or motion based subsystems. In order to keep operational for a longer lifetime, wireless nodes in a network wake up for a short time of communication and then go to sleep mode to save power as described in Akyildiz et al. (2002). These rules depend on the application requirements and communication protocol. For example, a room temperature measuring sensor node might use very low power during the sleep mode and wake up once in an hour to transmit its last reading but a temperature sensor that monitors an engine block would need to wake up, measure and transmit more often.

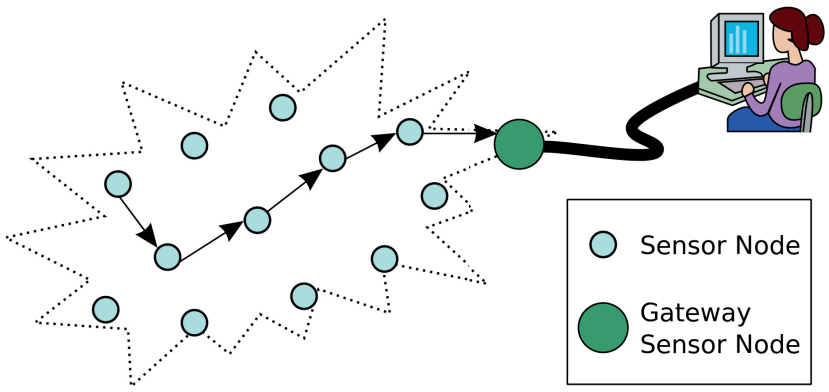


**Figure 10.** Architecture of a typical wireless sensor network. Wikipedia (2018).

The number of nodes in a wireless network may vary from 2 up to tens or even hundreds. At least one of those nodes is responsible for data collection and it is usually called gateway node or sink node.

The spatial density of the nodes in a network depends on the communication range. UWASA Node uses 2.4 GHz ISM band and the communication range is approximately 120 meters outdoors. Aldere nodes use 868 MHz European ISM band and have a communication range is approximately 1 kilometers outdoors.

Usually the most lightweight operating systems are used inside the wireless sensors. Examples to those include TinyOS and Contiki operating systems.

## 2.2 Real Time Operating Systems

An operating system is a computer program responsible for fundamental functions of the computer and provides background services to other running applications. On personal computers the operating systems gets the mouse and keyboard inputs, provides services for web browsing, file operations. In other words, it optimizes the allocations and scheduling of computation resources for applications. To the user, all those applications seem to work seamlessly at the same time but in fact the processor handles the tasks one at a time. The task switching happens so rapidly that the user is not able to perceive the scheduling. This is called multitasking.

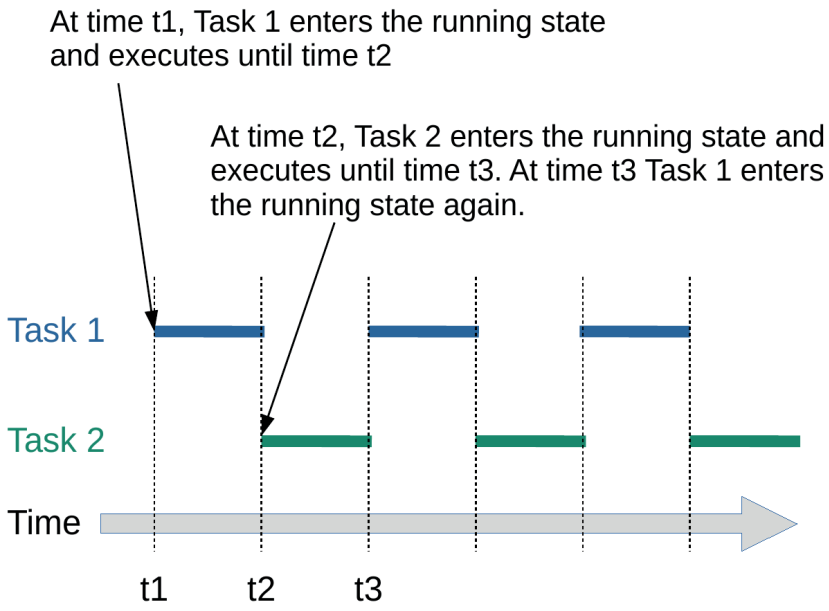


**Figure 11.** Task scheduling in real time embedded operating systems.

The difference between an ordinary operating system and a real time operating system is that, Real Time Operating System (RTOS) guarantees that a certain event will be handled within a strictly defined time. As expressed in Zagan et al. (2019), RTOS achieves deterministic thread execution by assigning priorities to tasks. Embedded systems usually have real time requirements thus implementation of RTOS is necessary for tasks like network synchronization or any other time critical tasks.

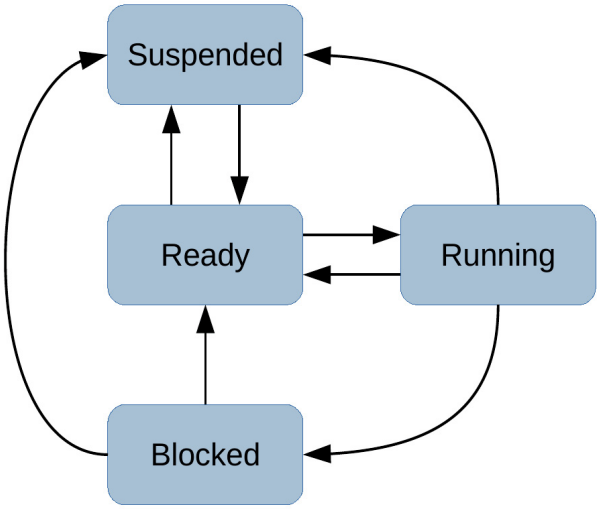


**Figure 12.** Task states and task switching in FreeRTOS. FreeRTOS (2018).

A task can be in one of the four states:

- Running State: At a given time, when a task is actually being executed it is in the Running state.
- Ready State: A task is in the Ready state if another task with a same or higher priority is being executed.
- Blocked State: A task is in Blocked state if it is waiting for a certain time delay or an external event.
- Suspended State: Tasks which are Suspended do not have a timeout and will not be utilized in processor scheduling unless explicitly commanded to resume.

In the research covered by this thesis, both the UWASA Node and Aldere wireless sensor platform uses FreeRTOS as a real time operating system. For network operations the tasks stay in blocked state until a radio interrupt occurs or timeout is reached.

One important aspect of having an operating system is the ability to use queues and semaphores to synchronize tasks and ensure that resources are handled appropriately. For example, if the radio resources are currently used by a task, no other task should intervene its operation. So the semaphores are needed to prevent possible conflicts. In case a resource is busy, the queues of the operating system will allow the programmer to put everything in order. Below is an example of the radio package handling in Aldere sensor node.

```
if(xQueueReceive(radio_receiver_queue,
&radio_receiver_message, portMAX_DELAY) == pdPASS){
    if(radio_receiver_message == RX_START){
        xSemaphoreTake(radio_semaphore, portMAX_DELAY);
        // Allow some time to receive the whole frame.
        vTaskDelay(1); // Arbitrary
        frame_ptr = receive_frame_emin();
        // First byte of the received frame is the status,
        // next is length, and next is the first data byte.
        switch ((unsigned char) *(frame_ptr+2)){
            ...
            case 0x68:
                temp=(unsigned char) *(frame_ptr+3);
                sendTempMeasToPC(temp);
                break;
            ...
            default:
            break;
        }
        xSemaphoreGive(radio_semaphore);
    }
}
```

In this example it can be seen that the reception of the packages happens with queuing system and utilization of the semaphores. Although not very obvious in this particular example, the transmission of the temperature measurement to PC also utilizes queuing system. In case other tasks are currently sending, this operation would wait for them to finish.

## 2.3 Communication Protocols

Communication protocols define the rules on how the devices exchange the data. For low layer network operations the IEEE 802.15.4 standard is used. This standard

is very common in low layer protocol stack and the hardware components have built-in support for it.

On top of the IEEE 802.15.4 standard, additional upper layer communication protocol is defined by the author. Aldere uses its own communication protocol for upper layer of network operations. Same protocol is also used for communication between the wireless sensor platform and the PC.

**Table 1.** Communication Protocol for Aldere Wireless Sensor Platform.

| Byte Number | 0 | 1 | 2 | 3 | ... | 127 |
|---|---|---|---|---|---|---|
| Data Package | 0x50 | length | data | data | ... | chcsum |
| Command Package | 0x50 | length | cmdID | val(opt) | ... | chcsum |

The first byte of the package is always hexadecimal 0x50 which corresponds to letter 'P' in ASCII table. The next byte indicates the number of remaining bytes in the package. There is two types of packages. Data package or command package. Data packages are intended for transmitting big amounts of data such as text or a series of measurements. Command packages are designed for handling specific events such as turning on a led, setting the motor speed, sending acknowledgments, reading sensor data. For example, a node can send a servo motor position command to set the motor rotational position to a certain value.

## 2.4 Hardware Design Considerations

The hardware design is one of the most exhaustive aspects of embedded engineering. Selection of components, schematic design, component placement and routing, power calculations and noise considerations are key objectives during the design process.

### 2.4.1 Design Objectives

The objectives of the hardware design has been efficient power usage, smaller form factor, high computational power, long range communication, security, more external interfaces, real-time operation, and the ability for modifications.

There are already existing solutions on the market but none of those devices were able to meet application specific requirements. Those devices are mostly for stu-

dents, hobby users and testers. At some point, a commercially available candidate device was considered for usage, but it had a very small form, had very low power usage but it lacked computational power. Moreover it had only 50 meters reliable communication range and offered only few pins for external additions. Thus the solution had to be rejected since it did not meet application demands. Another device had good range but lacked high computation power and operating system. Lack of an operating system and low computational power imposes serious limitations on real-time automation.

32-bit microcontrollers were used in both the UWASA Node and Aldere Wireless Sensor Platform and both runs an operating system. UWASA Node lacked long range while Aldere had communication range up to 1 km.

There are many possibilities like using a Raspberry Pi and an additional radio module. Solutions similar to those have high power usage, huge form and lacks security. In professional applications, these solutions do not offer good security and reliability. Most of those designs have open source hardware and software and are not suitable for certification and commercial usage. Some software licenses force all commercial applications to open source their own work.

### 2.4.2 Efficient Power Usage

Power considerations must be evaluated during the hardware design together with the capabilities offered by the software. The interrupt circuitry should be designed carefully for most efficient power usage. Hardware interrupts play the key role in software operation because those interrupts cause the processor to wake up. The software handles the hardware triggered interrupts as higher priority than the tasks.

Task scheduling in software determines the power consumed by the processor. Software can also set the transmission power levels, activate or deactivate the radio block, switch the power usage of sensors and other peripherals.

### 2.4.3 Noise elimination

Elimination of the noise is extremely important for longer distance communication because the signal strength is not the only factor for assessing radio link's quality. The term Signal to Noise Ratio (SNR) is used to determine the quality of a radio link.

If the noise level becomes very low, the transmit signal strength can also be kept in low levels. When both the noise and the signal levels are low, still a good SNR

can be achieved. This allows a longer operation lifetime by using less power and saving more battery. Another benefit of having lower level noise and using lower level transmission power is that our systems would have less interference to other networks.

In order to keep the noise in minimum levels, four separate grounds were used in Aldere wireless sensor platform. In lumped parameter model circuit analysis, having different grounds on a same device has no meaning. But since wireless devices operate on high frequencies, the design approach for distributed parameter model is applied. In Aldere radio logic design, those four separate grounds were isolated from each other by placing 0 Ω resistors in between.

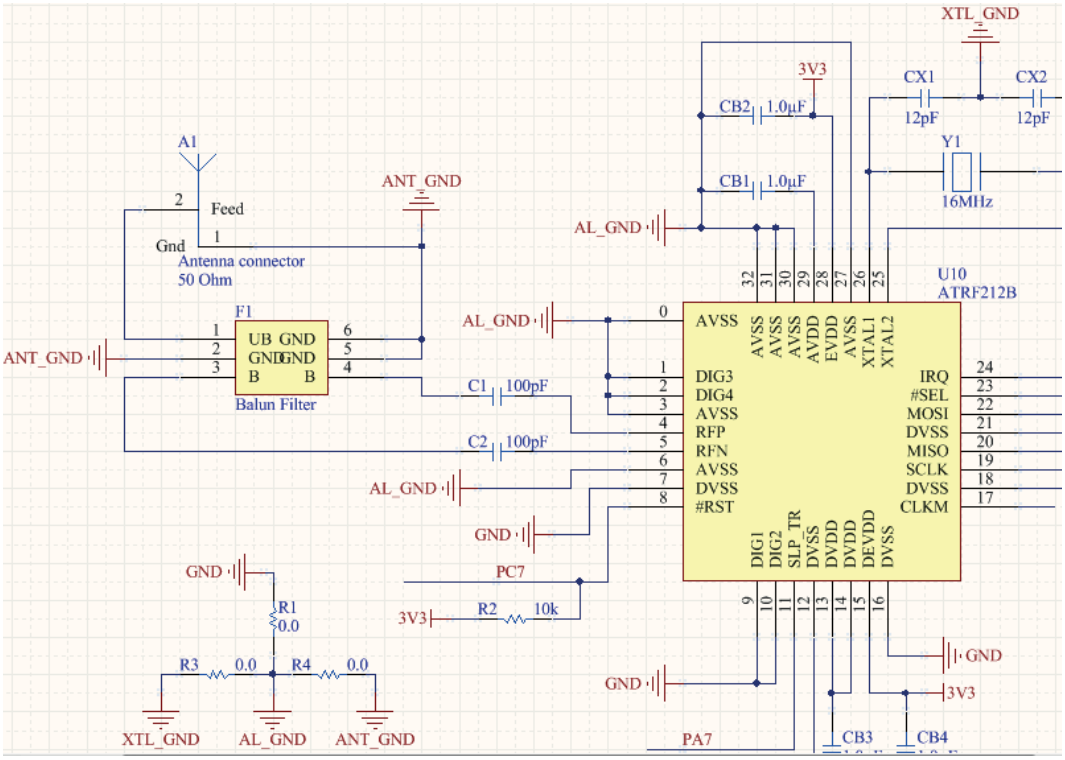


**Figure 13.** Four different grounds were connected to each other via 0 Ω resistors.

Those four grounds were used for crystal, analog radio, antenna and the rest of other components. During component placement and routing phase these 0 Ω resistors were placed close to the outer edge of the board.

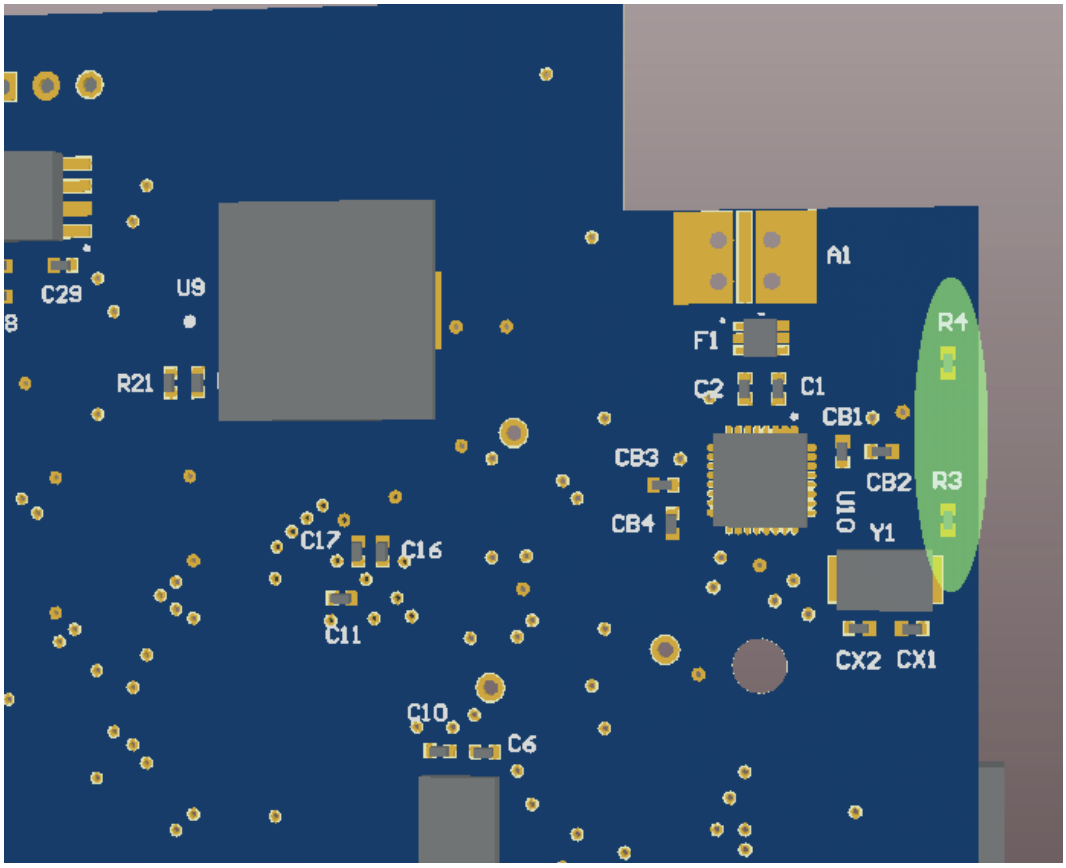


**Figure 14.** In order to keep the noise in minimum levels, the 0 Ω resistors were placed near the board edge.

Symmetry in component placement, simplicity and electromagnetic isolation provides better SNR. In Figure 14 the component A1 corresponds to antenna location. All the radio circuitry and crystal were placed in the same area having as small distance as possible. Keeping some components in more distant locations would cause the Printed Circuit Board (PCB) routes to behave similar to a microstrip antenna.

Routing is a tedious process and usually requires relocation of some components. It is also important to know beforehand the technological capabilities of the production company. All those issues together with software design are somehow correlated with each other and designer should iterate several times over the design to avoid faulty or noisy production.

# 3 APPLICATION CHALLENGES AND REQUIREMENTS

This section discusses the challenged issues and limitations for each research covered in this thesis.

## 3.1 Wireless Vision Sensor Capability

Integration of camera to UWASA Node has been challenging task due to the vision sensor limitations and the lack of configuration options. The work has started in 2010 and the commercially available vision sensor technology during that time was not as advanced as today.

The vision sensor was limited only to 352 x 288 resolution. Although for embedded devices the computation power and the memory is limited, the author has added additional Random Access Memory (RAM) and First-In-First-Out (FIFO) chips for image storage. The sensor behavior in dark environments was not satisfactory and posed certain limitations regardless of the Automatic Gain Control (AGC) mechanism.

One other tedious problem was that the output from the camera module always contained unstable data at the beginning of a frame. This problem is mentioned in the camera module manual and the only way to discover the correct start byte was to use a debugger and sequence based detection mechanism in software.

The output of the vision sensor was provided from 32 different pins that represent 16 bits for RGB color and another 16 bits for control inputs and synchronization signals. Having too many connections resulted in a more complicated circuitry for the benefit of faster parallel reading.

The internal memory of the microcontroller unit was not enough for storage of a single picture so additional RAM chips were used. Still the memory was only limited to store a single image and in case some filtering would be applied, the original image needed to be overwritten and lost. Applying the image filtering algorithms required square root operation of 6 digit numbers. Although this operation can be done easily by calculators or PCs, the C code library of the microcontroller did not support such mathematical operation. To overcome this problem, the author applied an ancient and iterative and fast method called Babylonian square root which is explained in Dellajustina et al. (2014).

## 3.2 Seed Drill Case

In seed drill case, the funding company provided a part of the machinery to the research group. The block contained a seed chamber, rotating part and a pipe through which the seeds make their way into the soil.

After the research group has set up the rotation rates based on real values, it was found out that the rotating part of the machine does not always drop a single seed in a uniform manner. When two seeds fall simultaneously, the light sensor generated a single but slightly greater amplitude signal as an output. The sensor reading was based on a threshold triggered events (comparator interrupt) and those events were counted. The challenge was not solved because there was no way to differentiate between a normal signal and slightly higher amplitude signal while using a comparator.

The research group has repeated many experiments. The dropped seeds were counted by hand and compared to the count provided by the wireless sensor installation. It was concluded that simultaneous drops can be neglected because it rarely happened.

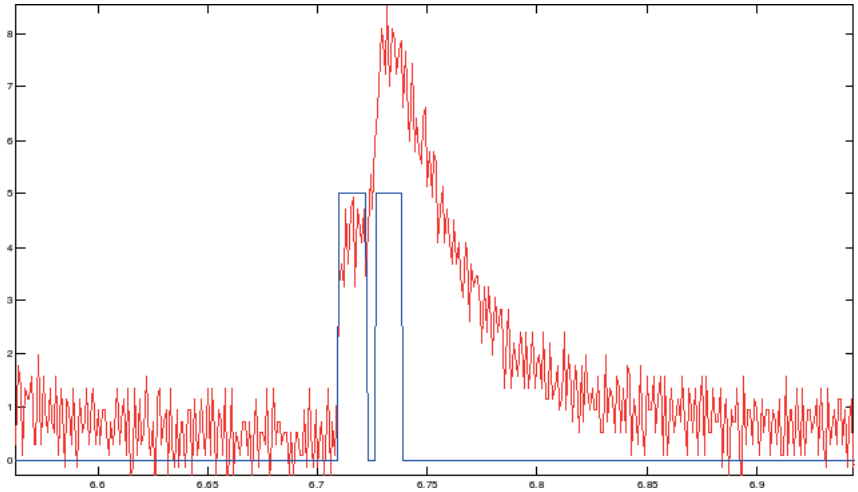


**Figure 15.** Detection of simultaneous seed dropping by applying peak detection algorithms.

There has also been experiment cases where the Analog to Digital Converter (ADC) kept measuring the signal output continuously. In case of an overlapping seeds it was possible to apply Fourier analysis and other peak detection methods to obtain more precise results as represented in Figure 15. In real life application keeping the ADC module always operational is not the best solution because the ADC periph-

eral consumes high power so it was better to rely on triggered interrupts.

## 3.3 Localization Services Case

In case of an urban crisis such as hostage rescue situations, urban combat or indoor fire it is very important to plan the operation and to be ready to execute the operation as soon as possible. This sort of emergency events are very reliant on time limits.

The author contributions in this part of the research covers the deployment of the wireless sensor nodes by using a mobile robot.

**Figure 16.** Mobile robot that deploys the wireless sensor nodes.

The robot shown in Figure 16 deploys the wireless nodes via the extension between the tank treads. The robot is remote controlled and it has on-board laser mapping module to construct the map of the interior structures such as walls and doors. Since the robot is not only responsible for node distribution, the path followed by the robot was not the optimal one for localization services.

The node deployment is triggered manually over the network. When a node is deployed, its location is marked on the Common Operational Picture (COP). However the location of the deployed nodes in real time does not offer the best solution for localization algorithms.

Another challenge during the installation has been the battery operations due to cold weather. Lithium batteries of the UWASA Node failed to operate in temperatures

close to 0°C. Hand warmers for outdoors camping was wrapped around the batteries during the testing period.

## 3.4 Heat Flux Measurements

The heat flux measurements along with the pyranometer data were logged for almost a period of 2 years. In case of a battery depletion or some software interruption, maintenance of the system during the whole research period was not immediately possible. This resulted in missing data for certain time periods.

Another challenge was the proper quantization of the measurements. The heat flux plate is a passive sensor and it has only two output pins generating a tiny amount of voltage depending on the heat flows through it. Although the sensor is precise and gives accurate measurements, the sampling resolution of the on-board ADC of the Aldere wireless sensor platform needed improvement. For this purpose the researchers decided to add a separate ADC module connected to Aldere node via Inter Integrated Circuit (I2C) interface. This modification has led to much more accurate measurements.

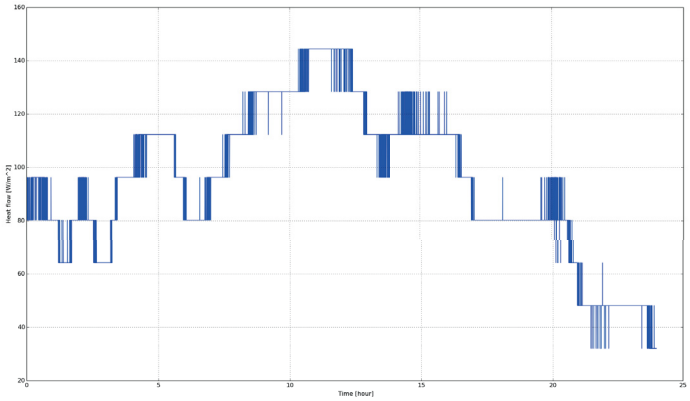


**Figure 17.** Heat flow measurements before ADC modification.

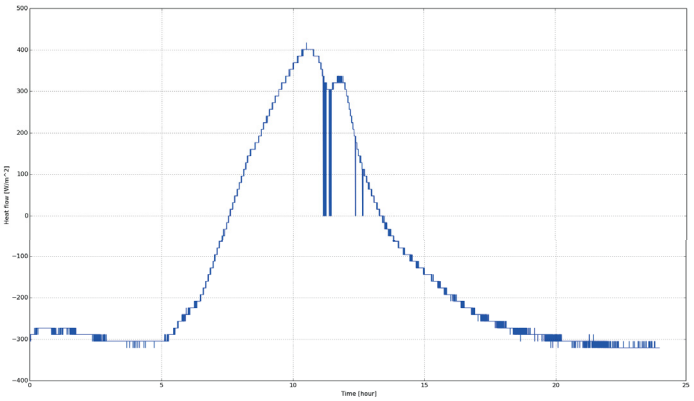


**Figure 18.** Heat flow measurements after ADC modification.

In Figure 17 and Figure 18 above, the accuracy of the sampling resolutions can be compared. This hardware extension allowed the research results to be more precise and reliable.

# 4 IMPLEMENTATION AND DESIGN METHODS

In this section detailed explanations are provided about how each research case was implemented, what methods were used and how the theoretical ideas were applied to real life.

## 4.1 Camera Integration to Wireless Sensor Node

The methods used during this research can be divided into two parts. Hardware design and the development of software algorithms. Building the hardware part consisted of engineering a completely new design from scratch. However, the greatest novelty of this part of research has been in the image processing algorithms.

There are of course plenty amounts of effective algorithms for image processing and those algorithms can be found in open source libraries such as OpenCV computer vision library. However, in UWASA Node the computation possibilities are very limited. For example, the software is based on C codes. In PCs the C compilers come with fundamental libraries such as math library. These functions were not available in UWASA Node. When an algorithm required utilization of a square root operation, it was not possible to apply it directly. The author has developed new algorithms for image processing by using simplified calculation techniques.

### 4.1.1 Building the Hardware

The preliminary plan for vision capability integration to UWASA Node was to design a new hardware interface that contains additional memory and logical circuits. Because UWASA Node has been designed as a generic platform, there are extension sockets on the master module for slave extensions. In that case the new hardware interface and the camera module would be an additional slave modules of the UWASA Node.

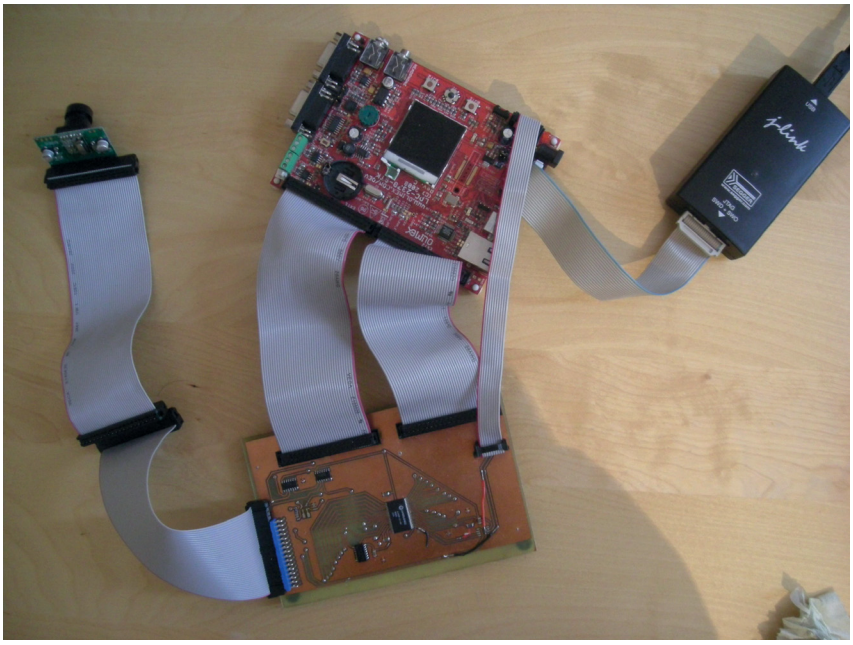

**Figure 19.** First prototype of the UWASA Node wireless sensor platform extension for adding vision capabilities. Prototype was based on development board that contains the same microcontroller on the UWASA Node.

The research started by experimenting with a development board as previously mentioned in introduction section. The new hardware interface that contains a FIFO chip was designed.

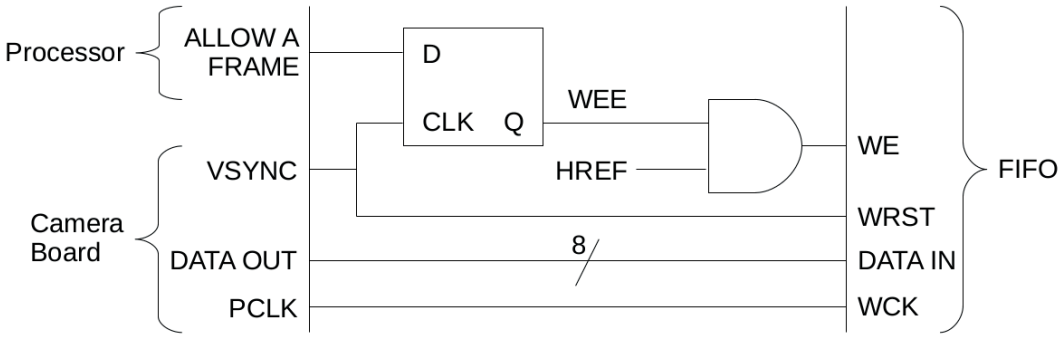


**Figure 20.** Connection of FIFO to the camera module.

The definitions of each signal in Figure 20 are represented in Table 2.

**Table 2.** Signals of the FIFO connection.

| **Signal** | **Definition** |
|---|---|
| ALLOW A FRAME | This signal requests the next image to be stored in the FIFO. |
| VSYNC | Marks the readiness of the next image. |
| DATA OUT | 8-bit data output. |
| PCLK | Pixel clock signal. |
| D | D input of a D-type flip-flop. |
| CLK | Clock signal of the flip-flop. |
| Q | Output of the flip-flop. |
| WEE | Write enable enable. |
| HREF | Horizontal reference. Marks each row of pixels. |
| WE | Write enable. |
| WRST | Write reset. |
| DATA IN | 8-bit data input. |
| WCK | Write clock. |

FIFO chip was used to capture the first available image from the camera module. However the FIFO is a read-only component for the microcontroller side. As the name implies the data located in FIFO must be read in arriving order, so addressing the data was not possible. In order to store the image and apply image processing techniques a Static Random Access Memory (SRAM) was needed.

The connection of the SRAM is represented in Figure 21.

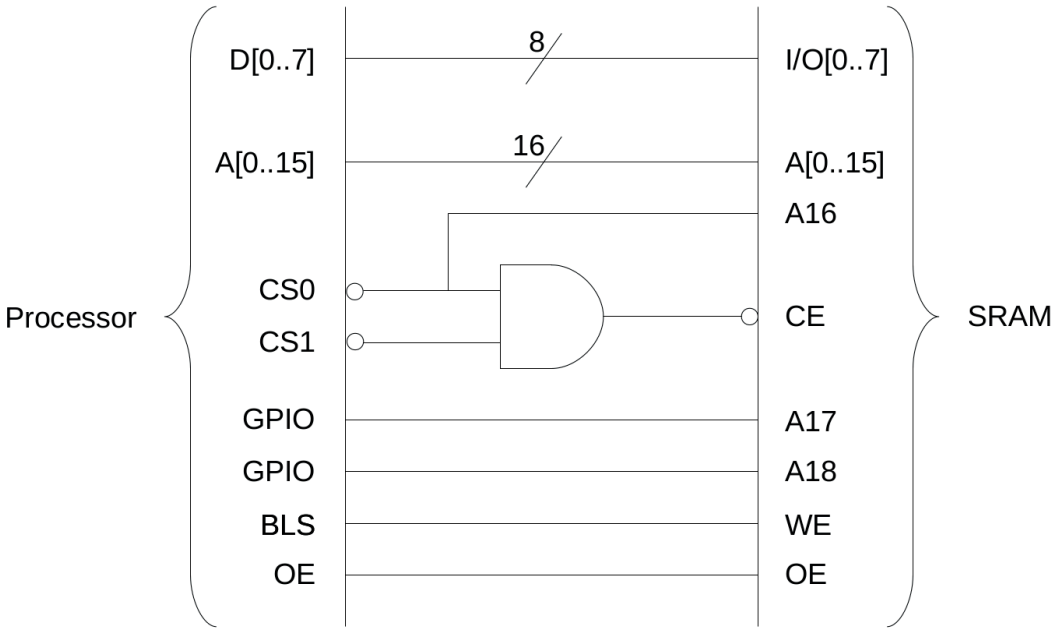


**Figure 21.** Connection between the processor and the SRAM.

Using the chip select pins the SRAM could store up to four images.

**Table 3.** Signals of the SRAM connection.

| **Signal** | **Definition** |
|---|---|
| D[0..7] | Data signals. |
| A[0..18] | Address signals. |
| CS[0,1] | Chip select 0 and 1. |
| GPIO | General purpose input-output. |
| BLS | Byte lane select. |
| OE | Output enable. |
| I/O[0..7] | SRAM data input and output. |
| CE | Chip enable. |
| WE | Write enable. |

### 4.1.2 Simplified Image Processing Methods

The experiments continued to find out the most efficient way to calculate the edges and gradients on the image. After the studies on edge detection and gradient algorithms, it was clear that those methods use high computational power. The author has developed the simplified versions of those image detection methods. The first and basic simplification has been the monochrome image generation. This was the first step for image processing in our case because both the edge detection and gradient calculation algorithms used monochrome images.

According to E. Demarsh and J. Giorgianni (1989), the transformation from RGB color space to monochrome is defined as:

$$Y = 0.2125 \cdot R + 0.7154 \cdot G + 0.0721 \cdot B \tag{4.1}$$

where Y represents the gamma, R, G and B represent red, green and blue colors respectively.

To avoid high processor usage caused by multiplication with floating point numbers, it was decided to approximate the equation as:

$$Y = \frac{1}{4} \cdot R + \frac{5}{8} \cdot G + \frac{1}{16} \cdot B \tag{4.2}$$

Applying equation 4.2 in embedded systems is extremely efficient compared to floating point number multiplication because the color component coefficients now can be obtained by using only two type of atomic instructions; bitwise right shift and addition. Bitwise right shift divides a number by 2 and addition operation gives the result for a given pixel.

After the monochrome image is constructed it is possible to generate gradient image. According to Kanopoulos et al. (1988) the Sobel operator for gradient calculations uses two dimensional convolution kernels. If we represent the pixel values of monochrome image laying under the kernel as a matrix A, the gradients for x and y dimensions are:

$$G_x = \begin{bmatrix} -1 & 0 & +1 \\ -2 & 0 & +2 \\ -1 & 0 & +1 \end{bmatrix} * A \tag{4.3}$$

and,

$$G_y = \begin{bmatrix} -1 & -2 & +1 \\ 0 & 0 & 0 \\ -1 & +2 & +1 \end{bmatrix} * A \tag{4.4}$$

Here the * denotes the convolution. And finally the gradient value at the center of the kernel is calculated as:

$$G_{xy} = \sqrt{{G_x}^2 + {G_y}^2} \tag{4.5}$$

Here the challenge for low computational power embedded devices is the square root operation. Inside the square root is a 32 bit number. Since this is not supported in embedded C libraries the author decided to apply Babylonian square root method.

Babylonian square root method is an iterative way to calculate the square root of a number. In case the square root of *S* is to be calculated, the algorithm starts with an initial guess $x_0$. If n denotes the number of iterations, Fowler and Robson (1998) defines the technique as:

$$x_0 \approx \sqrt{S} \tag{4.6}$$

$$x_{n+1} = \frac{1}{2}\left(x_n + \frac{S}{x_n}\right) \tag{4.7}$$

$$\sqrt{S} = \lim_{n \to \infty} x_n \tag{4.8}$$

The results from each pixel is calculated by this method and finally the gradient image is built.

Finding the edges is now relatively easy because edges represent the lines where the gradient values are relatively higher than in other pixels. Simply, a threshold value was selected, and the values below the threshold was coded as black.

## 4.2 Seed Flow Monitoring in Wireless Sensor Networks

Integration of wireless sensor devices to the agricultural machinery started by deciding what physical quantity could be measured. Finally the research team agreed that the best choice would be based on light measuring system.

In Seinäjoki University of Applied Sciences (SeAMK), researchers have developed a very small and low power wireless sensor node called SURFbutton. These devices are coin sized and operate on a coin type battery. Although these devices do not have many external interfaces they are better choice than UWASA Nodes in size constrained areas. The proposed solution for seed drill implementation is shown in Figure 22.

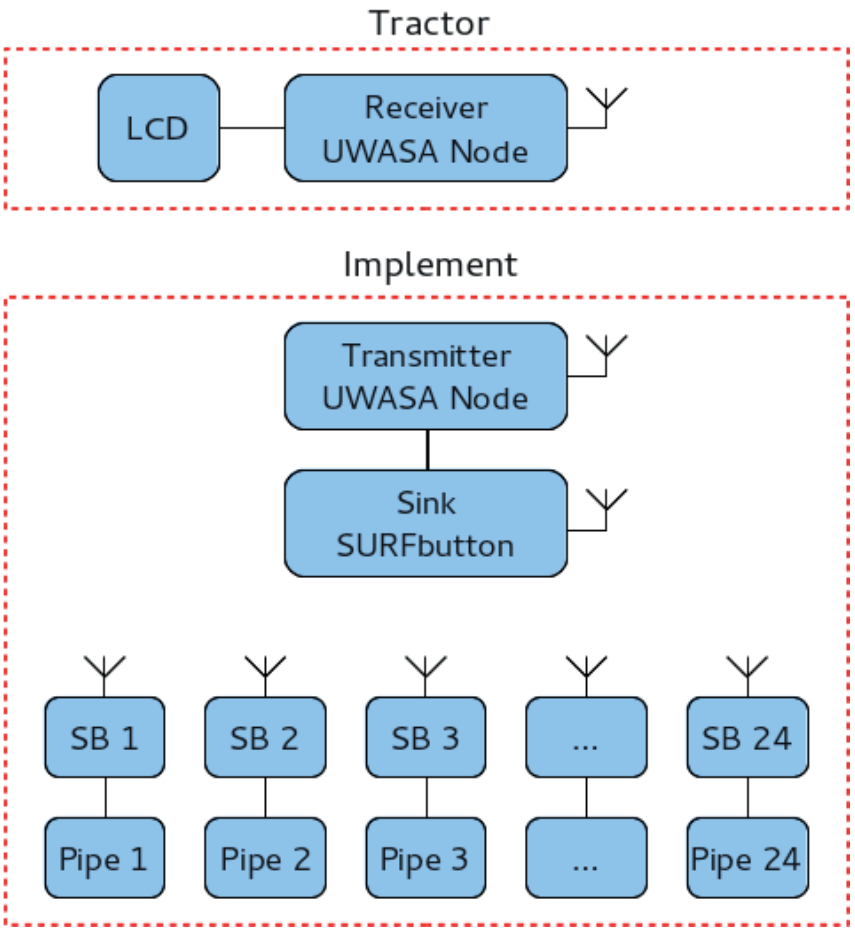


**Figure 22.** Solution for seed drill monitoring system using wireless sensor networks.

In this system architecture there is a SURFbutton connected to each pipe of the implement. The UWASA Node is not radio compatible with SURFbuttons, so one of the SURFbuttons act as a sink node. This sink node is bridged to UWASA Node via hardware connection as shown in Figure 23.

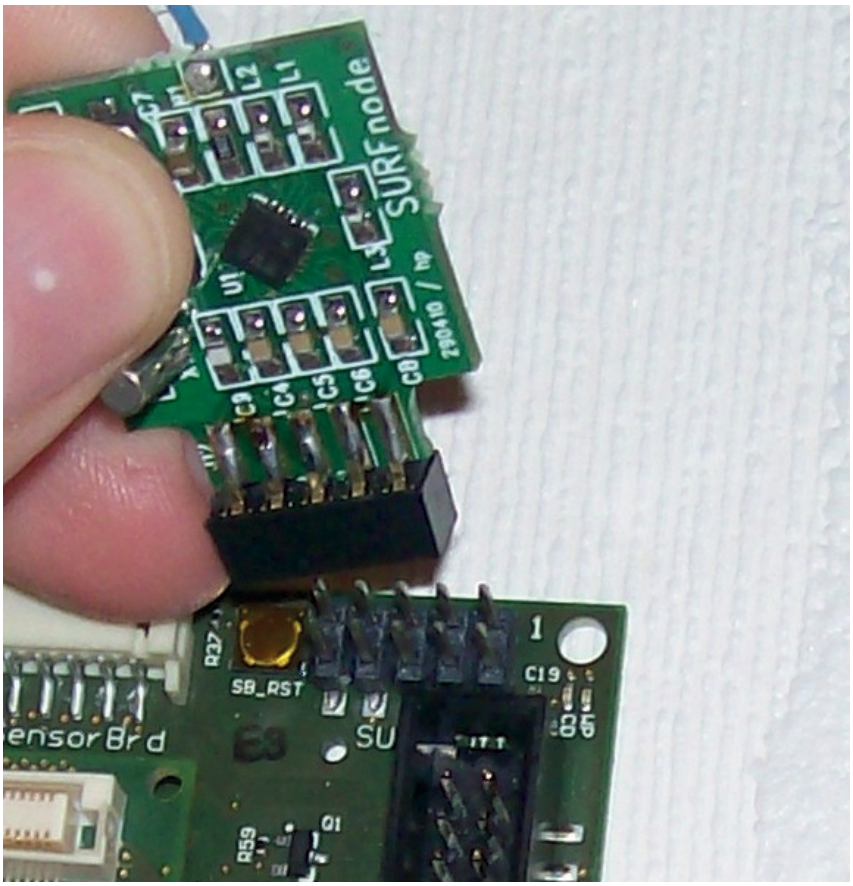


**Figure 23.** SURFbutton is bridged to UWASA Node by using header pins.

The collected data is then transferred to another receiver UWASA Node located inside the tractor. This node has an LCD extension to display the seed flow rates for each pipe. The values are updated continuously and the driver can monitor the situation in real time.

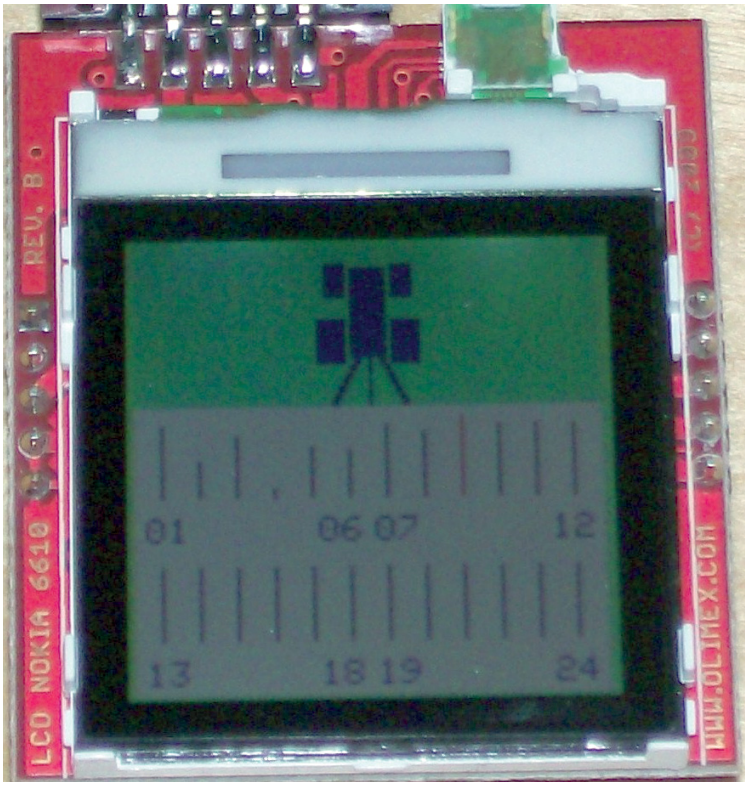


**Figure 24.** Seed flow rates can be monitored in an LCD display real time.

In Figure 24, the length of the pipe corresponds to the flow rate. In case the flow rate is zero, the pipe symbology turns to red which indicates that pipe is either stuck or there is some other reason to investigate manually. In this research the author has been implementing the codes for the Nokia 6610 LCD screen and also application codes for UWASA Nodes and performed data analysis which will to be presented in results section.


**Figure 25.** Tractor and the implement are attached to each other. Junkkari (2019).

After the preliminary tests of the system integrity and connectivity, the company has supplied the research team with a part of the seed drill machine. The light sensors were installed inside the pipes to monitor the flow rates.

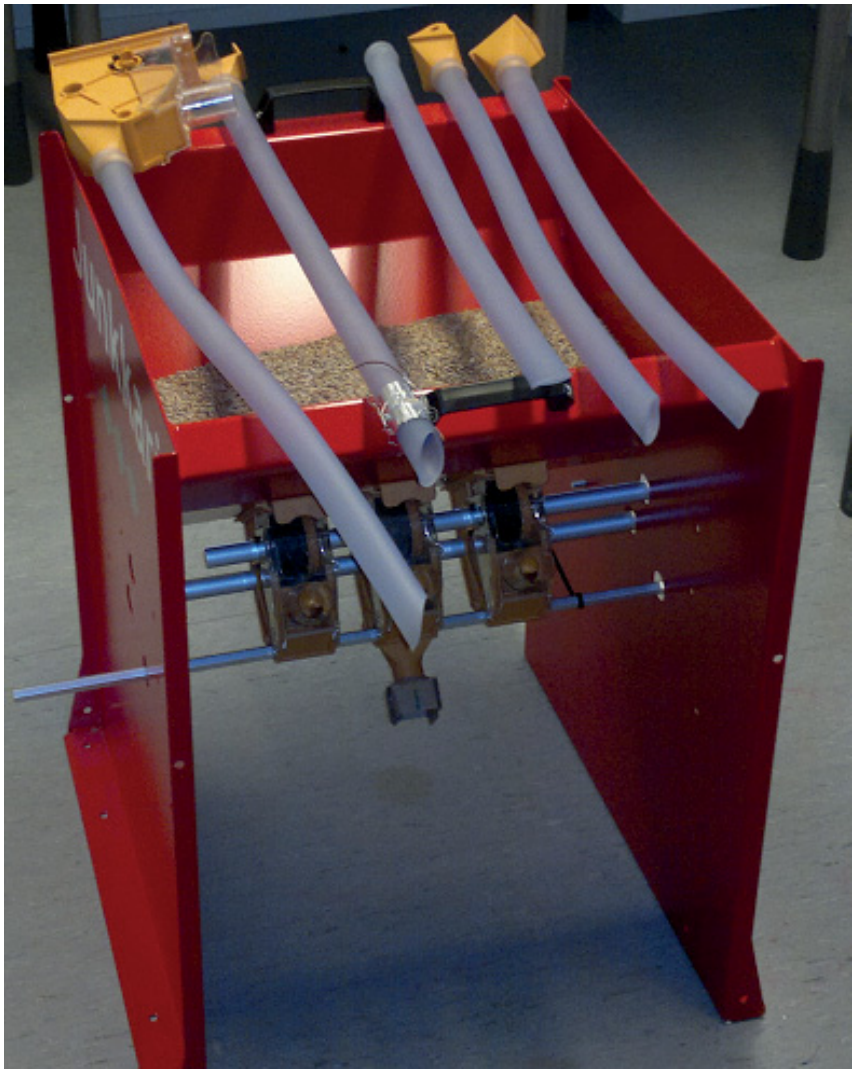

**Figure 26.** Part of the implement was built and delivered to the research team to carry out the experiments.

The software of the SURFbuttons were provided by SeAMK researchers. Data was captured from the pipes, collected and transmitted to receiver UWASA Node. UWASA Node logged the data to the PC over the USB interface. After repeating the tests with different flow rates the collected data was analyzed using mathematical software.

## 4.3 Localization Services for Online Common Operational Picture and Situation Awareness

Law enforcement units heavily rely on situational awareness to plan and execute the operation within strict time limits. In case of urban crisis the overall picture is quite dynamic and sudden changes would require changes of initial plans. For this reason friendly forces need to exchange information continuously in real time.

In order to present and update real time information, indoor sensing systems are needed. These monitoring systems include the radio based localization services. Radio signals are able to penetrate concrete and wooden walls He et al. (2006). Thus, those systems are capable of providing valuable information about indoor situation modeling where the satellite images or unmanned aerial vehicles would not help.

Within the context of WISMII project new algorithms were developed for device free localization Kaltiokallio et al. (2013). As described in Virrankoski (2013), three research organizations, six companies and Finnish Defense Forces participated in this project and the requirements were defined by Finnish National Defense University.

The distribution of the wireless sensor nodes was done by a mobile robot. Distribution mechanism was designed by Tobias Glocker who is a researcher in University of Vaasa. The mechanical integration of the node distribution mechanism as well as server and client software was done. The robot has successfully deployed the wireless sensor nodes to be used in Device Free Localization (DFL). The node dropping commands were issued manually over the ICE Storm software. ICE Storm is a networking middleware that provides object based data exchange between every network asset regardless of their programming language. This middleware helps building the common operational picture more rapidly and in a simpler way.

## 4.4 Feasibility Study on Solar Energy Harvesting from Asphalt Surface in Cold Climate Region

Geothermal heating systems deliver the natural thermal heat from underground up to surface via boreholes. Continuous heat transfer in the long run may cause the heat source to lose its total energy. However this problem could be compensated by harvesting some of the heat from the asphalt surface and storing underground.

During summer days the temperatures on the asphalt layer rise more than the current air temperature because the solar power is absorbed as heat due to black-body

behavior of asphalt. In this research the purpose is to quantify how much solar power arrives to the surface and how much of this energy is absorbed. In case the heat could be harvested and stored before it is dissipated back to the atmosphere, the long term effects of geothermal heating in deeper layers could be compensated.

The research team has decided to measure physical quantities from three different sources. First measurement source was pyranometer that measures solar power that directly arrives to earth. Second was the heat flux plate buried just below the asphalt surface. By using those two sources it has been possible to compare the absorbed power versus incoming power. The third source is the Distributed Temperature Sensing (DTS) system. This device measures the underground temperatures at different depths using a laser beam traveling through fiber optical cable.

Heat flux data was measured by a passive sensor that has two analog output pins. The voltage difference between the pins is sampled by ADC. Since the heat flux plate is a passive sensor, it generates a tiny voltage so the research team needed to use a very high resolution ADC.

Aldere platform is used to capture the heat flux data. The device is installed inside a small metal box next to the heat flux sensor installation site as shown in Figure 27.

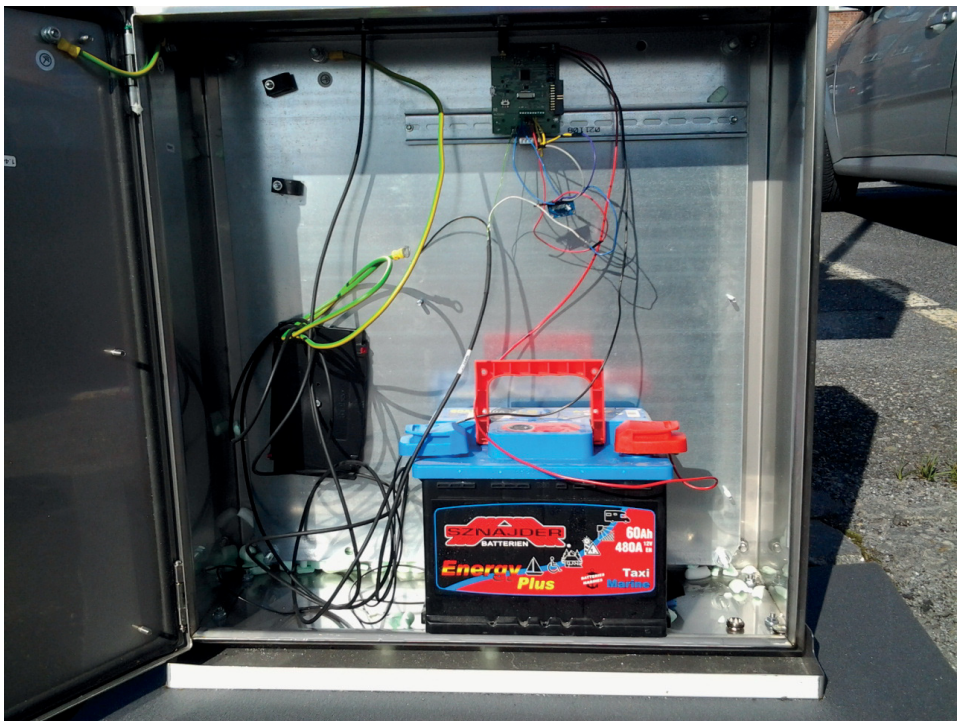


**Figure 27.** Aldere platform (on top) was powered by a car battery to withstand very cold temperatures during winter season.

The heat flux data was sampled every 10 seconds and transmitted to another Aldere gateway platform was installed inside the university. Then the gateway node logged the network data into an embedded Linux PC.

After the data was obtained the research team has built two mathematical models based on physics laws to describe the heat transfer between the sun, asphalt surface and the deeper layers of the soil.

### 4.4.1 Surface Heat Flow Model

To explain the model it is better to analyze a single day and compare the pyranometer data with heat flux data. The model explained here was then extended to cover multiple days of every season and will be presented in results section.

Solar power captured by the pyranometer on 23rd of April is given in Figure 28.

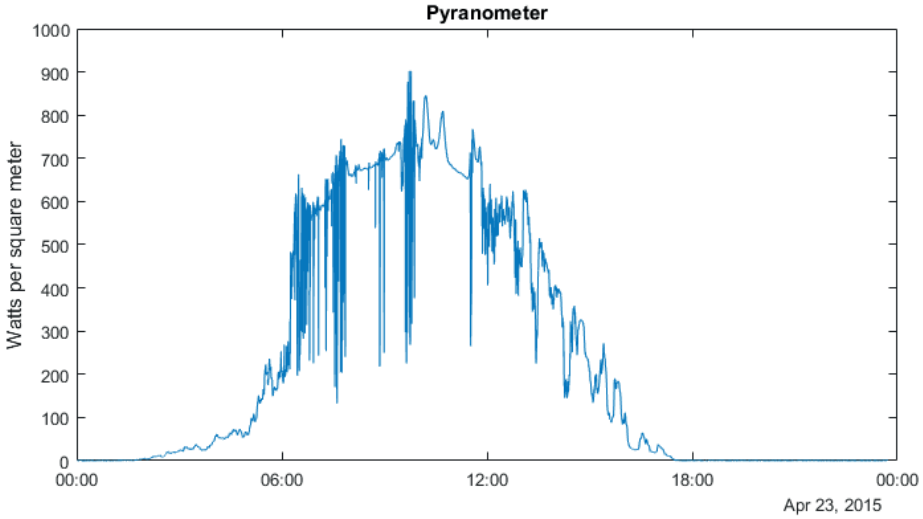


**Figure 28.** Pyranometer data for 23rd of April 2015.

The values of pyranometer data are always positive. The sunlight on 23rd of April 2015 starts to deliver energy starting approximately about 3:30 AM. The peak power is seen at 11:00AM and the last sunlight of the day hits the earth at about 17:00. Although this data is purely based on sunlight strength, sometimes clouds have caused instantaneous disturbances. This is a natural effect and it is not neglected during the research.

By applying the average over the whole day measurements, the mean sunlight power was calculated as 230 w/m$^2$.

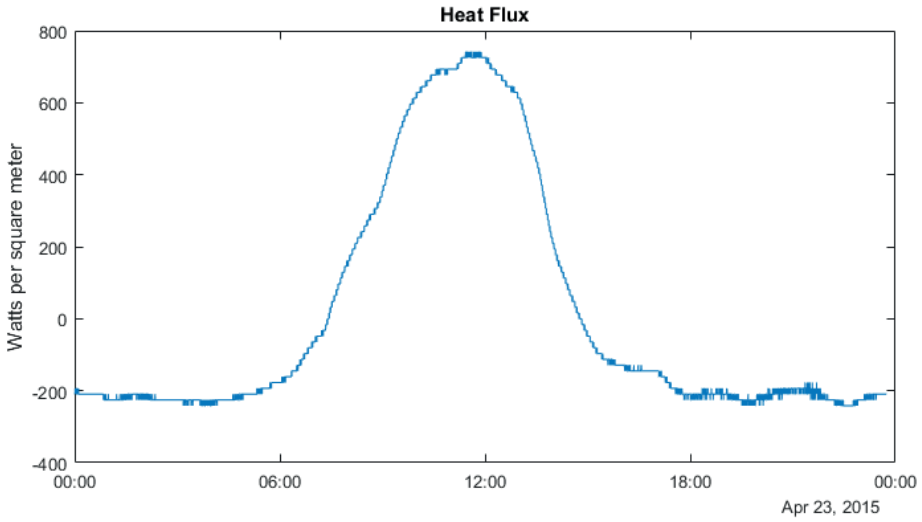


**Figure 29.** Heat flux data for 23rd of April 2015.

Figure 29 shows the net heat flux data on the asphalt surface for the same day. It should be noted that the envelope of the heat flux graph follows the pyranometer graph envelope with a time shift. This is caused by the fact that the heat transfer starts after the surface builds up some temperature as a result of solar irradiation. Similarly the surface starts to dissipate heat back after a certain time shift when the solar power decreases. It is obvious that the heating and cooling of the surface takes some time.

One important thing to note here is that the heat flux can have negative values. Negative flux means the heat is dissipating back into the atmosphere while the asphalt surface cools down.

The peak value of heat flux of the given day is $\approx$700 w/m$^2$. However, when the values are averaged over the entire day the mean value is calculated as 14 w/m$^2$ because of the negative values during the night. The constant loss during the night causes the surface temperature to drop. According to Davies and Davies (2010), this effect is called Radiative Cooling. If the sun would suddenly disappear, the earth temperature would exponentially approach to the 0 K limit in the darkness of the space.

The average night time heat loss for the given day is approximated as a constant value because for one day period the change between two consequent days is almost

zero and can be neglected. This constant value is calculated by using 200 samples an hour before and after the midnight. For the chosen day above, average night time heat loss value is 130 w/m$^2$.

According to the measurement values the average absorption ratio $\sigma$ for the given day is calculated as follows. If we denote the average heat flux as $\Phi$ and the average pyranometer power as $\lambda$:

$$\sigma = \frac{\Phi}{\lambda} \tag{4.9}$$

This formula applied for the given day results in:

$$\sigma = \frac{14 \text{ w/m}^2}{230 \text{ w/m}^2} = 5.9\% \tag{4.10}$$

The result for the given day is not surprising since the April in Finland is the period just after the snow melts. So the ground is still cool and it is heating up and by absorbing the solar energy.

In addition to that, it is possible to calculate the ideal harvesting case where the night time losses are totally eliminated and the positive heat flow is harvested ideally.

If the positive part of the heat flow is integrated, the optimum absorption rate can be calculated as:

$$\sigma_{\text{p}} = \frac{139 \text{ w/m}^2}{230 \text{ w/m}^2} \approx 60\% \tag{4.11}$$

The analysis on this example day explains the energy exchange model between the solar irradiation the and asphalt surface.

### 4.4.2 Soil Temperature Model

The heat flow and the resultant energy transfer occurring on the asphalt surface causes the temperatures in deeper soil layers to change. In this part, we explain the scientific model built for our soil temperature calculations within the first 0.5 m depth of the soil.

From the physics we know that the temperature change $\Delta t$ is:

$$\Delta t = \frac{Q}{m \cdot c} \tag{4.12}$$

where Q denotes the energy, m is the mass and c is the specific heat.

The energy Q can be easily obtained by using the average heat flux $\Phi$. For any given day the Q can be calculated by applying the formula:

$$Q = \Phi \cdot A \cdot t \tag{4.13}$$

Here the A is the area and t denotes the time. For a daily analysis, unit area of 1 $m^2$ and the number of seconds in a day is applied.

Next, in equation 4.12 calculating m is also straightforward since the volume V and the soil bulk density d is known:

$$m = V \cdot d \tag{4.14}$$

The last term in equation 4.12 is the specific heat of the soil.

According to European Environment Agency EEA (2012), the specific heat capacities for dry and wet soils are calculated as follows.

For dry soil:

$$c_s = 1.64 \cdot t_s + 704 \tag{4.15}$$

where $t_s$ is the soil temperature. For simplicity the research team has used $t_s$ value as $5°$C.

For wet soil:

$$c = \frac{100 \cdot c_s + 4190 \cdot w}{100 + w} \tag{4.16}$$

In the formula above, the $w$ represents the water mass percentage in the soil. According to European Environment Agency (EEA) the value of the $w$ is approximately 25 in the area of measurements.

# 5 RESULTS

In this section the results from each research case is represented.

## 5.1 Camera Integration to Wireless Sensor Node

Using the new hardware board presented in previous sections, images were successfully captured. Developed image processing techniques for wireless sensor devices were applied. The application of monochrome transformation algorithm for a sample image is represented in Figure 30.

**Figure 30.** Monochrome image transformation.

Although a simplification was applied to avoid floating point multiplication, the results were satisfactory and posed no challenge in applying further image processing methods.

Gradient calculations are applied on top of monochrome images. As described previously, the square root calculations for traditional image processing methods were replaced by a new algorithm.

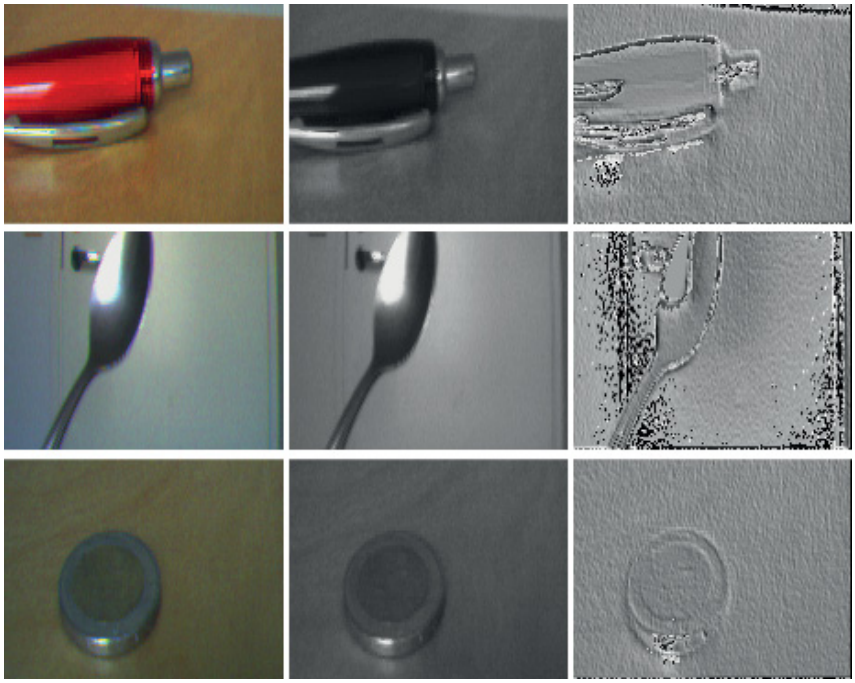

**Figure 31.** Gradient calculation method applied.

It would be good to emphasize that all those operations were performed inside the UWASA Node and the .bmp file was also generated inside the node. A 3 x 3 two dimensional convolution kernel was applied both horizontally and vertically. Then the iterative Babylonian square root calculation method was applied four times for every pixel. Here it is worth mentioning how much computational power would be needed for every pixel even if the hardware was capable of square root calculations. Although this was not benchmarked, the traditional method would provide more accurate result but it would require much more computing power in return.

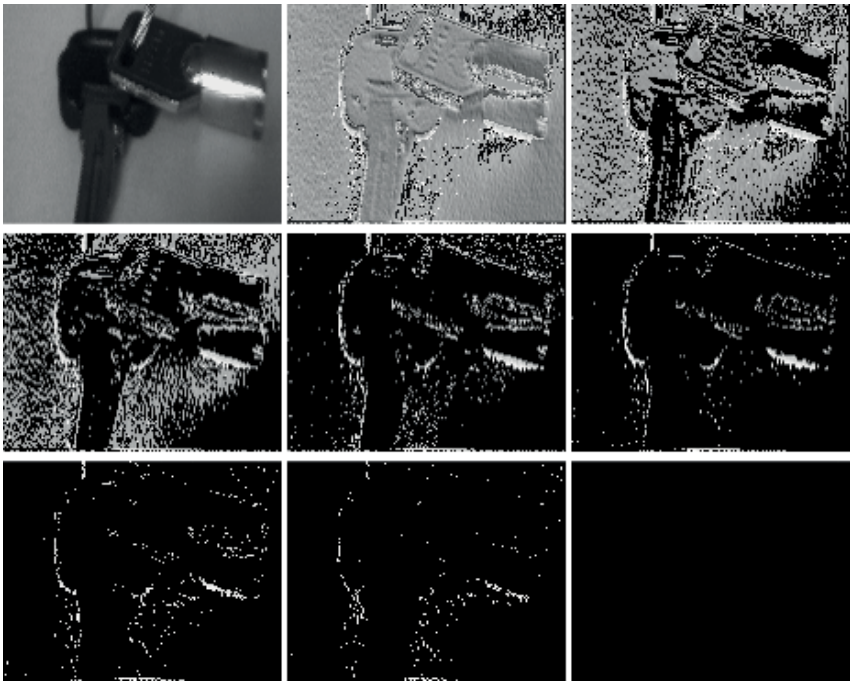

**Figure 32.** Edge detection method applied with different levels of filtering.

Figure 32 shows results for different levels of edge detection filters varying from none to max. In order to recognize the shapes, advanced methods operate on edge detected images. In the depicted experiment, filtering level of 5 (6th sample) seems to achieve the best result.

Since in this research the focus is on wireless sensor networks, the transmission requirements were also analyzed. Depending on their size, images are formed of high amount of data. The author proposed that only the coordinates of the white pixels could be transmitted after the edge detection algorithm. This results high amount of savings in bandwidth usage. It is possible to compare the amount of transmission size for every case depicted previously in Figure 32.

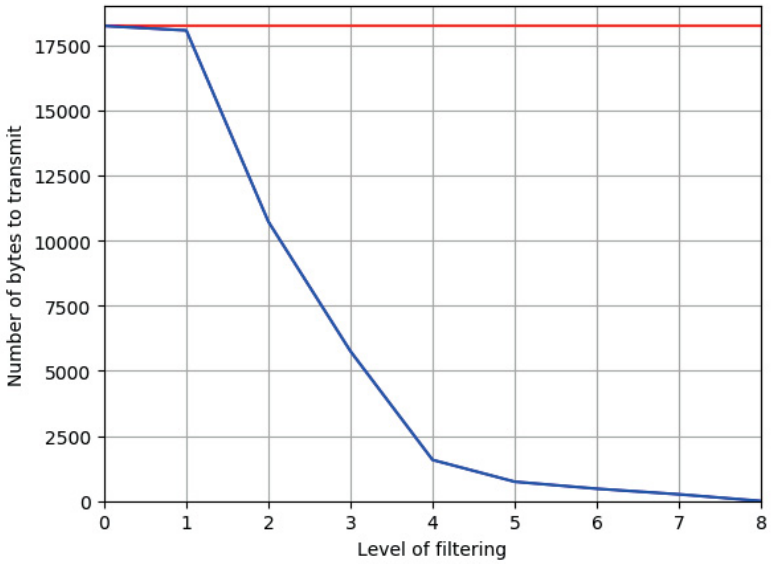


**Figure 33.** Number of bytes to transmit for each filtering level.

Figure 33 is very important in terms of network usage because in wireless networks every transmitted byte costs battery lifetime. Since the best edge detected case seemed to be achieved by applying level 5 filtering, it is worth mentioning that the transmission would require only 740 bytes to transmit instead of 18240 bytes for whole image. The transmission size in this case is reduced down to 4%.

## 5.2 Seed Flow Monitoring in Wireless Sensor Networks

There are two important points to mention about the results of seed flow monitoring case. First one is related to detection of seeds and the second point is about battery lifetime.

### 5.2.1 Detection Results

During the seed flow experiments the research group decided to keep the ADC module always operational for testing purposes. Normally the seed counting is based on comparator interrupts to save the battery; but ADC outputs provide better information for testing purposes.

In the following graph, ADC was configured to measure 500 samples per second and data was captured for 30 seconds.

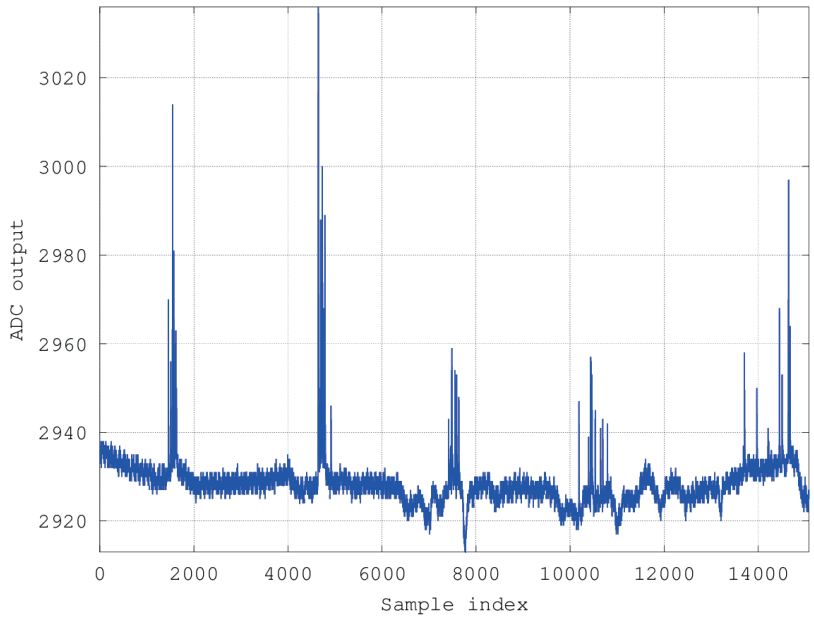


**Figure 34.** ADC output for 30 seconds sampled at 500 Hz.

15000 samples were taken in total. Exactly 50 seeds were dropped in 5 bursts and each burst contained precisely 10 seeds. The voltage spikes generated by the bursts are clearly distinguishable.

Figure 35 shows a closer look at the 4th burst.

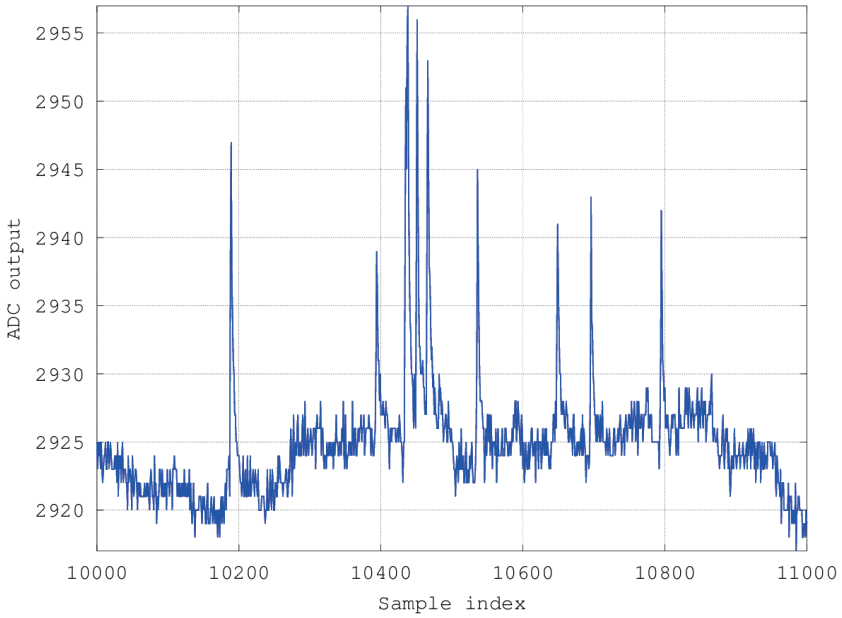


**Figure 35.** A closer look at the samples from 10000 to 11000.

In Figure 35 it is possible to count every seed dropped. This graph shows only 9 peaks instead of 10, indicating that there was a simultaneous fall.

It is possible to zoom in even more and take a closer look at each peak. By determining the width of the peaks it is possible to calculate the duration of a single seed fall.

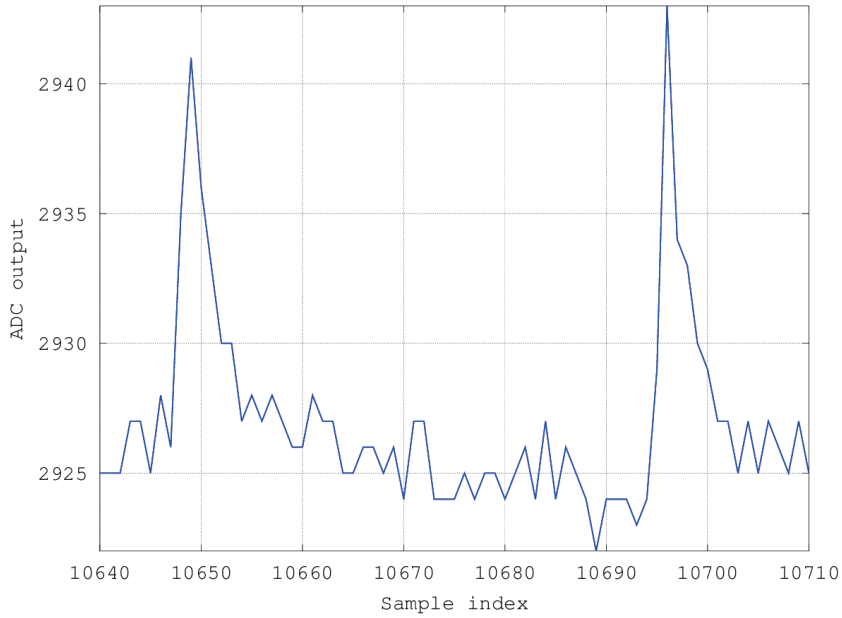


**Figure 36.** Only two spikes are visualized.

The width of the spikes corresponds to seed's falling duration. Here the width of a falling event takes 10 samples, meaning the fall duration is 20 ms.

In comparator mode when the seed is passing through the light based system, the SURFbutton node receives an interrupt and goes back to sleep after 2ms. This is about 10% of the time until the seed passes the light detection system.

In overall the seed flow detection system provided satisfactory results. The experiments were done based on realistic seeding rates and the measurements were successful.

### 5.2.2 Power Usage Results

SURFbutton devices operate using a coin sized battery. Those batteries are rated at 500 mAh. The power consumption tests showed that if the seed drop rate is assumed to be 100 seeds per second, the average current consumption was 303.45 $\mu$A. In that case the lifetime of a SURFbutton would be:

$$\frac{500\,mAh}{303.45\,\mu A} = 1648\,hours = 69\,days \tag{5.1}$$

The power consumption test results are also satisfactory because the seeding season takes about one or two weeks.

## 5.3 Localization Services for Online Common Operational Picture and Situation Awareness

Wireless sensor node distribution capability has been integrated to the mobile robot. Thus, the robot is able to deploy the sensor nodes to critical points inside the building. The node deployment is controlled over the ICE server. Whenever a node is dropped, the information is published to the ICE server instantly with a timestamp.

A mobile robot features many benefits in emergency situation; most importantly, it can be deployed to gather information about an unknown situation without risking human lives. In this research work the robot is in central role of creating a common frame of reference for the system and is used as a scout. The robot builds a metric map of the environment while exploring and localizes itself against the same map. In addition, the robot deploys static nodes into known locations.

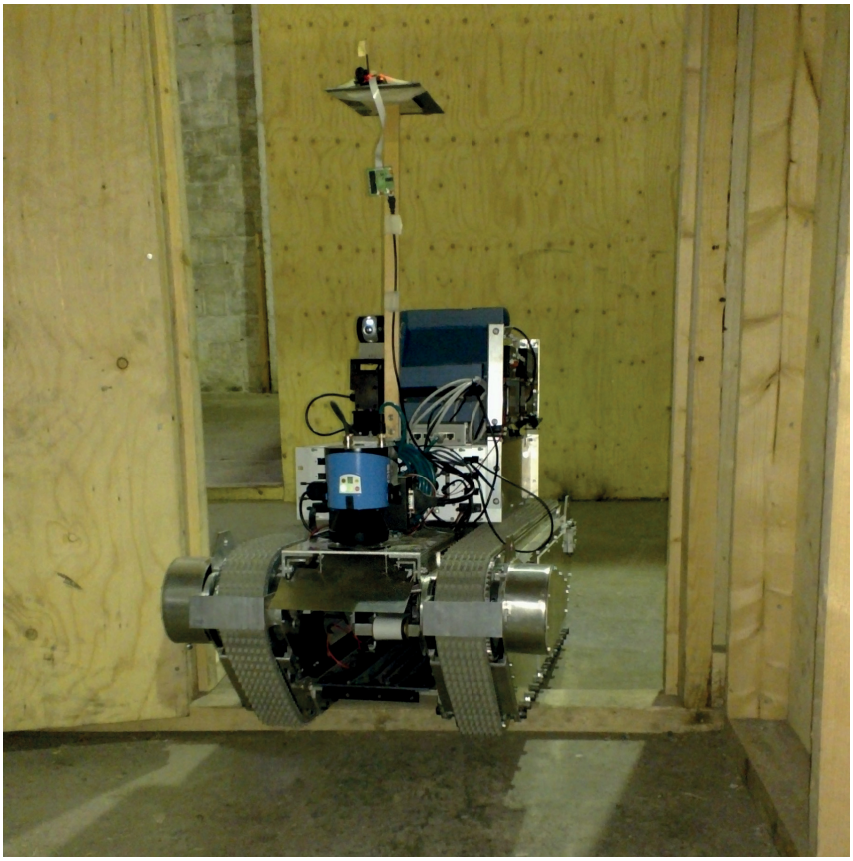

**Figure 37.** Mobile robot distributes the wireless sensor nodes.

The mobile robot system is illustrated in Figure 37. The robot is a tracked platform, weighting approximately 100kg and carries along 100 Ah of energy as well as sensors and computation power. In this research we use a laser range finder for creating the map and a camera with pan-tilt unit for providing feed back for the operator. In addition, the robot is equipped with a communication subsystem which enables the communication with the robot practically in all environments without need for site-specific infrastructures.

Finally, the robot has a wireless sensor node distribution system installed inside of it. An operator can deploy the wireless sensors into strategic places in the building. The dropped nodes are location labeled where the robot drops them.

The footage of taken by Finnish Combat Camera Team (2013) for localization methods are available online for viewers.

## 5.4 Heat Flux Measurements Under the Asphalt in Cold Climate Region

The proposed models for both the surface heat flow and the soil temperature measurements have provided accurate and reliable results. Theoretical calculations and energy transfer models were compatible with practical results.

The surface heat flow model can be extended any number of days and the software generates a report about the important parameters.

The captured data contained millions of samples spanning over two years. Of course it is not possible to represent and discuss all the data in this thesis. But to visualize and analyze, some results from summer and winter days are presented in this section.

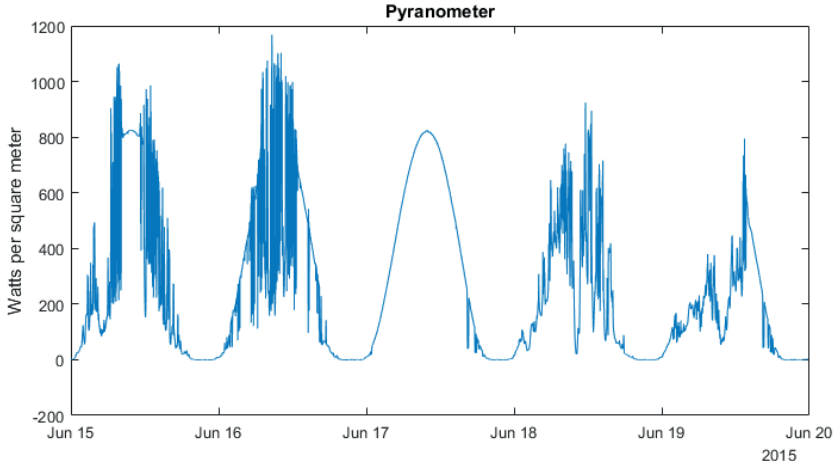


**Figure 38.** Pyranometer data between 15-20 June 2015 (Summer).

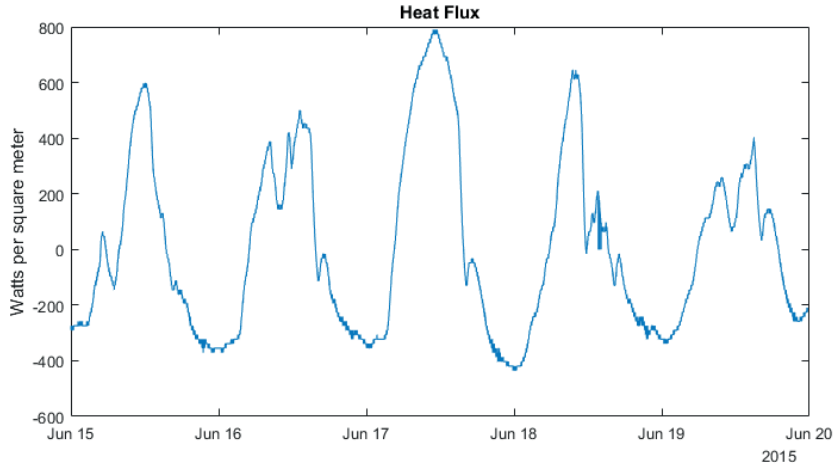


**Figure 39.** Heat flux data between 15-20 June 2015 (Summer).

**Table 4.** Generated Software Report for Summer.

| **Definition** | **Calculation** |
|---|---|
| Average Pyranometer Power | 260 w/m$^2$ |
| Average Net Heat Flux $\phi$ | 8.4 w/m$^2$ |
| Average Night Time Loss | -320 w/m$^2$ |
| Absorption Ratio | 3.3% |
| Temperature change within 0.5 m surface depth | 0.21 °C |

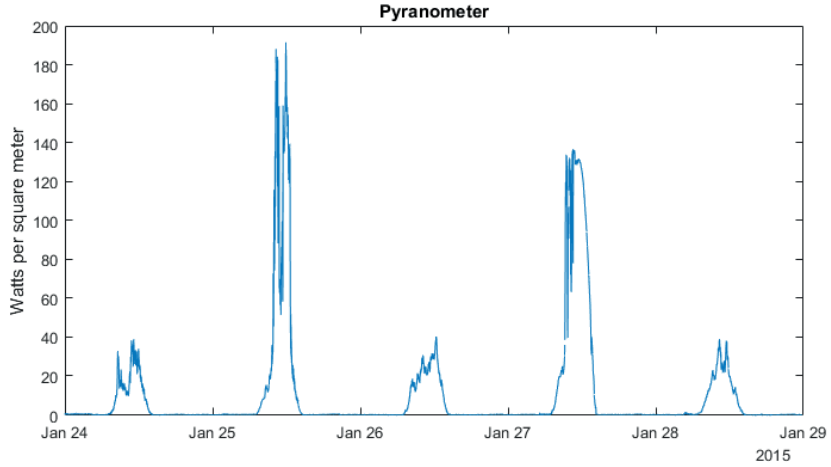


**Figure 40.** Pyranometer data between 24-29 January 2015 (Winter).

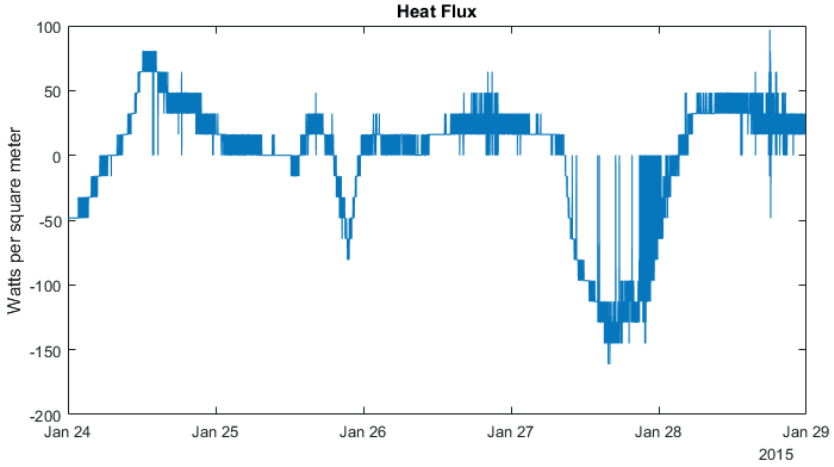


**Figure 41.** Heat flux data between 24-29 January 2015 (Winter).

**Table 5.** Generated Software Report for Winter.

| **Definition** | **Calculation** |
|---|---|
| Average Pyranometer Power | 11 w/m$^2$ |
| Average Net Heat Flux $\phi$ | -1.9 w/m$^2$ |
| Average Night Time Loss | -12.9 w/m$^2$ |
| Absorption Ratio | -18% |
| Temperature change within 0.5 m surface depth | 0.00 °C |

From these results it can be concluded that the pyranometer data and heat flux data

have very similar envelopes. This shows that the main source of the surface heat transfers is the solar power.

Considering the summer measurements, it is clear that heat flux levels follow the pyranometer data by a shift of few hours. This shifting effect is more noticeable by comparing the first and last portions of the graphs. When the solar power arrives to the earth the surface temperature needs to rise first, before transferring the heat below. Same idea applies to cooling as well.

Winter measurement values for both pyranometer and heat flux are much smaller in comparison to summer. One important thing to mention here is that during the winter the ground is covered by a thick layer of ice and snow. Although the solar power sees a peak of 150 w/m$^2$ the heat flux level is very low. There is a good snow isolation and heat transfer is minimal.

The measured results are so accurate with regards to both amplitude and timestamps that one can easily notice the long days in summer and short days in winter. This is due to the northern latitudes of Finland. There is a huge gap between summer and winter daytime lengths. In summer there is sunlight for almost the entire day whereas in winter the sunlight rays carry little energy and the daytime lasts for few hours.

By doing additional analysis not covered here, but presented in Table 6, the software reports for autumn days have provided negative average heat flux. This result is expected because during the autumn the earth is in cooling process.

**Table 6.** Analysis for 5 days from each season.

| | **Autumn** | **Winter** | **Spring** | **Summer** |
|---|---|---|---|---|
| **Pyranometer Power (w/m$^2$)** | 68 | 11 | 225 | 260 |
| **Heat Flux (w/m$^2$)** | -13.4 | -1.9 | 40.6 | 8.4 |
| **Average Night Loss (w/m$^2$)** | -126.05 | -12.99 | -218.06 | -320.29 |
| **$\Delta$t at 0.5 m during 5 days (K)** | -0.31 | 0.00 | 0.94 | 0.21 |
| **Absorption Ratio (%)** | -19.4 | -18 | 18 | 3.3 |

# 6 DISCUSSION AND CONCLUSION

Wireless sensor networks today has wide variety of applications. During the doctoral studies and research applications; many aspects, benefits and capabilities of wireless technologies were investigated. Real life applications in agriculture, military and earth sciences were developed and valuable information was collected and analyzed using scientific methods.

Camera integration to wireless devices was a challenging task and this was known beforehand. However the possibilities were discovered new methods were introduced for more efficient computing as well as less resource hungry transmission methods were discovered.

In agricultural application, the practical problems defined by the industry were addressed and it was shown how the wireless sensors network could be utilized in precise farming. It became clear that real time measurement and monitoring systems open new possibilities for improvements in future farming. Wireless data transmission possibility between the tractor and the agricultural implements allow the future farming systems to be installed without cable connection, thus reducing the farmer's effort to attach and detach the machinery. Another benefit of the real time measuring and monitoring systems is that the farmer becomes aware of the problem immediately and can take necessary action on time. In case the farmer would not be aware of the failure and continued on faulty seeding, this would cause some areas of the field to be empty during harvest.

Device free localization by distributing the wireless sensor networks in the urban crisis area helps the law enforcement units to get a clearer picture of the situation in a shorter time. Satellite images and unmanned aerial vehicles pose limitations when the important events take place indoors. The radio signals of wireless devices are able to penetrate walls so that the movements inside the building can be detected. This work contributes to urban safety and security by wireless sensor network deployment.

Usage of wireless sensor networks in earth sciences help reduce the installations costs and even in some cases allows for such installations that would not be possible using cable based systems. In the case represented, heat measurement platform had to be located in the university parking yard. The Linux PC that collects and logs the data was located approximately 100 meters away. Cable based solution in this case would be very costly because the cables would possibly be needed to laid underground. Apart from the advantages of wireless sensor platforms, many important findings were discovered and new ideas were developed for building a new theory about the energy exchange mechanism between the sun, earth's surface and deeper layers. The model was introduced and verified with practical results. Quantitative research methods and obtained data allowed the research group to benchmark

physical properties of the soil and environmental factors in Finland.

In summary, the research applications covered in this thesis demonstrated the benefits of wireless sensor networks, their capabilities and new methods.

Starting from analytical studies and getting acquainted with wireless sensor technologies, it has been a long and a rewarding journey. Throughout the doctoral studies it has been an exciting and instructive experience to be guided by industrial experts and scientists who brought the research and real applications together in various projects. During the studies there has been a chance to attend the lectures and share ideas with the developers of important communication standards such as the Constrained Application Protocol (CoAP) and the (IPv6 over Low-Power Wireless Personal Area Networks) 6LoWPAN.

Collaboration with experts from military, agricultural and earth sciences made it possible to understand the challenges and requirements of wireless sensor network deployments. Fulfilling these requirements always involved pushing the limits from technological point of view. Since the technology is evolving so rapidly, the chosen equipment and materials had to be state-of-art devices. In wireless technologies there has seen so rapid advancements that during the research process, always better electronic components, better software protocols and chemical technologies like Ferroelectric Random Access Memory (FRAM) became commercially available.

As conclusion, summarizing the scientific contributions for each research case; in vision sensor integration, low power consuming algorithms were developed for image processing and transmission. Transmission is very power consuming tasks in wireless sensor networks so this research introduces novelties in computation and also in networking. Seed flow monitoring case has introduced real-time monitoring systems for precise farming and better soil usage efficiency. Localization methods using wireless sensor networks allowed defining new ways to obtain information about indoors in emergency cases. In earth sciences, new mathematical models were built for understanding and studying the energy harvesting possibilities. Using wireless sensor technologies here played a key role in data acquisition and analysis.

In future, it seems that wireless sensor networks will be used more in a form of IoT devices. The development of those devices started almost two decades ago and nowadays they are available in multiple forms in various areas such as medical, transportation, agricultural, energy, and environmental monitoring.

# 7 SUMMARIES OF THE ARTICLES

## I. Camera Integration to Wireless Sensor Node

UWASA Node is a wireless sensor platform developed by researchers in University of Vaasa. It is a generic platform that contains a power module and a master module. Additional slave modules can be added on top of the hardware in a stacked manner. This allows application specific customization without modifying the core hardware.

In this research a new hardware interface was developed for adding vision capabilities along with image processing methods to wireless sensor networks. The hardware was built and tested, then software was developed for capturing and processing images.

Low computational power of the embedded devices required more efficient image processing methods. These algorithms were developed and the results have been satisfactory. Furthermore, image compression and efficient transmission methods were developed adding more scientific novelties.

## II. Seed Flow Monitoring in Wireless Sensor Networks

A more efficient seeding leads to better harvesting results in agriculture. The requirements of this research was defined by the funding industrial partner in their seed drill products.

While operating in humid soils, the seeding pipes often gets stuck by mud during the tractor's maneuvers. In that situation the driver may not realize that one or more pipes becomes inoperational. This problem results in non-germinated rows in the field and finally causing less efficient farming.

In order to overcome this problem the research team introduced a seed flow monitoring system that is able to measure the seed flow rates in each pipe of the implement. Usage of wireless technologies was necessary due to rotating machinery parts and the ease of implement's attachment to the tractor. An LCD screen was used to display the flow rates of each pipe to the driver in real-time. This allows the seeding problems to be identified immediately and necessary actions can be taken as soon as possible.

## III. Localization Services for Online Common Operational Picture and Situation Awareness

In case of urban crisis such as school shootings, kidnappings, robberies, fire, and terrorist activities; the law enforcement units need better situational awareness to plan and execute the operation in a limited time. The usage of Unmanned Aerial Vehicle (UAV)s or satellite images provide limited information about the current situation indoors. In such cases the warfare environment is highly dynamic so the common operational picture needs to be built and updated in real-time, and shared with friendly forces.

This research focuses of possibility of device free localization methods using the radio signals of wireless sensor nodes. These sensor nodes are to be dropped by a mobile robot in certain locations and the position with a timestamp is published through all network assets. Based on the signal strength measurements from each node to every other node, it is possible to locate and track the movements behind the walls.

A node distribution mechanism was developed and installed to the mobile robot that is equipped with laser rangefinder and a camera to get better information of indoors without risking any more human lives. The robot operator could use a software to issue commands for dropping a wireless sensor node at any moment.

## IV. Heat Flux Measurements Under the Asphalt in Cold Climate Region

During summer days the sunlight is so strong that the asphalt layer temperatures rise dramatically. This research aims to measure and analyze the effects of solar power on the asphalt surface and temperature changes in deeper layers of the soil.

The research team decided to measure three physical quantities to model and explain the heat exchange mechanism between the sun, the asphalt surface and deeper layers of the earth. A pyranometer was used to directly measure the solar power magnitude arriving to the earth. Second data source was the heat flux plate buried about 5 cm under the asphalt surface. This sensor measures the heat flowing in both directions to or from the earth's surface. The relation between the solar power and the heat flux was used to analyze how much of the incoming sunlight is absorbed and transferred to deeper layers. The third source of measurements was the distributed temperature sensing device. This device uses laser beam that travels through the optical fiber cable and provides the soil temperatures at various depths down to 10 meters.

Wireless sensor platforms were used to capture those physical quantities for nearly a period of two years. Based on those findings and laws of physics, the research team has modeled the heat exchange mechanism for both the surface layers and deep layers using a mathematical software. The surface model was used to explain the absorption rates and the amount of heat exchange for any given time period. The soil temperature model was used to measure the longer term effects of the heat transfers in deeper layers.

This research has been very successful utilization of wireless sensor networks in earth sciences. The measurements were very accurate and consistent with the meteorological events.

# REFERENCES

Adler, R. J. (1990). *An introduction to continuity, extremes, and related topics for general gaussian processes* (Vol. 12). Institute of Mathematical Statistics Lecture Notes-Monograph.

Akyildiz, I., et al. (2002). A survey on sensor networks. *Communications Magazine, IEEE*, *40*, 102 - 114.

Allen, A., Milenic, D., & Sikora, P. (2003). Shallow gravel aquifers and the urban 'heat island' effect: A source of low enthalpy geothermal energy. *Geothermics*, *32*, 569-578.

Björkbom, M., Timonen, J., Yiğitler, H., Kaltiokallio, O., García, J. M. V., Myrsky, M., ... Koivo, H. N. (2013). Localization services for online common operational picture and situation awareness. *IEEE Access*, *1*, 742-757.

Brogowski, Z., Kwasowski, W., & Madyniak, R. (2014). Calculating particle density, bulk density, and total porosity of soil based on its texture. *Soil Science Annual*, *65*.

Çuhac, C., Mäkiranta, A., Välisuo, P., & Hiltunen, E. (2019). Heat flux measurements under the asphalt in cold climate region. *Applied Energy*.

Çuhac, C., Virrankoski, R., Hänninen, P., & Elmusrati, M. (2012). Seed flow monitoring in wireless sensor networks. *Aalto University Workshop on Wireless Sensor Systems (WoWSS)*.

Çuhac, C., Yigitler, H., Virrankoski, R., & Elmusrati, M. (2010). Camera integration to wireless sensor node. *Aalto University Workshop on Wireless Sensor Systems (WoWSS)*.

Cramér, H. (1961). On the structure of purely non-deterministic stochastic processes. *Arkiv för Matematik*, *4*, 249–266 (1961).

Davies, J., & Davies, D. R. (2010). Earth's surface heat flux. *Solid Earth*, *1*, 5-24.

Dehner, U., Müller, U., & Schneider, J. (2007). Erstellung von planungsgrundlagen für die nutzung von erdwärmekollektoren. *Landesamt für Bergbau, Energie und Geologie*, *5*.

Dellajustina, F., et al. (2014). The hidden geometry of the babylonian square root

method. *Applied Mathematics*, *05*, 2982-2987.

Diamond, S. M., & Ceruti, M. G. (2007). Application of wireless sensor network to military information integration. *Industrial Informatics*, *1*(322), 317.

E. Demarsh, L., & J. Giorgianni, E. (1989). Color science for imaging systems. *Physics Today - PHYS TODAY*, *42*, 44-52.

EEA. (2012). *Global surface soil moisture content based on remote sensing data.* Retrieved from https://www.eea.europa.eu/data-and-maps/figures/global-surface-soil-moisture-content

Finnish Combat Camera Team. (2013). *Wism ii project.* Retrieved from http://www.youtube.com/watch?v=9v1fFIHRWGE

Florides, G., & Kalogirou, S. (2007). Ground heat exchangers—a review of systems, models and applications. *Renewable Energy*, *32*(15), 2461 - 2478.

Fowler, D., & Robson, E. (1998). Square root approximations in old babylonian mathematics: Ybc 7289 in context. *Historia Mathematica*, *25*(4), 366 - 378.

FreeRTOS. (2018). *Freertos - market leading rtos (real time operating system) for embedded systems with internet of things extensions.* Retrieved from www.freertos.org

Gomes, R., et al. (2019). Adaptive and beacon-based multi-channel protocol for industrial wireless sensor networks. *Journal of Network and Computer Applications*, *132*, 22 - 39.

Hawkins, S. E., & Ess, D. R. (2012). *Grain drill metering systems and the need for calibration.* Retrieved from www.extension.purdue.edu/extmedia/ABE/ABE-126-W.pdf

He, T., Krishnamurthy, S., Luo, L., Yan, T., Gu, L., Stoleru, R., … Krogh, B. (2006). Vigilnet: An integrated sensor network system for energy-efficient surveillance. *ACM Transactions on Sensor Networks*, *2*.

Hida, T., & Hitsuda, M. (1993). *Gaussian processes* (Vol. 120). Translations of Mathematical Monographs, AMS, Providence.

Hunt, G. A. (1951). Random fourier transforms. *Trans. Amer. Math. Soc.*, *71*, 38-69.

Ibragimov, I. A., & Rozanov, Y. A. (1970). *Gaussian random processes*. Nauka,

Moscow (Russian). English transl. Springer-Verlag, New York.

Jung, S. J., et al. (2013). Wireless machine-to-machine healthcare solution using android mobile devices in global networks. *Sensors Journal, IEEE*, *13*, 1419-1424.

Junkkari. (2019). *Simulta 2500 nl.* Retrieved from https://www.junkkari.fi/web/en/simulta-2500-nl

Kahane, J.-P. (1985). *Some random series of functions processes*. Cambridge Univ. Press, Cambridge.

Kaltiokallio, O., et al. (2013). *A Multi-Scale Spatial Model for RSS-based Device-Free Localization.* Retrieved from http://arxiv.org/abs/1302.5914

Kanopoulos, N., et al. (1988). Design of an image edge detection filter using the sobel operator. *IEEE Journal of Solid-State Circuits*, *23*(2), 358-367.

Lamperti, J. W. (1962). Semi-stable stochastic processes. *Trans. Amer. Math. Soc.*, *104*, 62-78.

Li, C., Shang, J., & Cao, Y. (2010). Discussion on energy-saving taking urban heat island effect into account. In *2010 international conference on power system technology* (p. 1-3).

Long, T. T. (1968). Représentations canoniques des processus gaussiens. *Annales de l'I.H.P. Probabilités et statistiques*, *4*(3), 179-191.

Makhdoom, I., et al. (2019). Blockchain's adoption in iot: The challenges, and a way forward. *Journal of Network and Computer Applications*, *125*, 251 - 279.

Mallick, R. B., Chen, B.-L., & Bhowmick, S. (2009). Harvesting energy from asphalt pavements and reducing the heat island effect. *International Journal of Sustainable Engineering*, *2*(3), 214-228. https://doi.org/10.1080/19397030903121950

Mayocchi, C., & Bristow, K. (1995). Soil surface heat flux: Some general questions and comments on measurements. *Agricultural and Forest Meteorology*, *75*, 43-50.

Palomäki, H., Hööpakka, H., & Çuhac, C. (2012). Wireless seed drill monitoring system. In *11th international symposium on ambient intelligence and embedded systems(AmiES-2012).* Espoo, Finland.

Park, C. (1981). Representations of gaussian processes by wiener processes. *Pacific J. Math.*, *94*(2), 407–415.

Santamouris, M. (2003). *Solar thermal technologies for buildings - a state of the art*. Park Square, Milton Park, Abingdon, Oxon OX14 4RN United Kingdom: James Ltd.

Sayde, C., Gregory, C., Rodriguez, M., Tufillaro, N., Tyler, S., Giesen, N., ... Selker, J. (2010). Feasibility of soil moisture monitoring with heated fiber optics. *Water Resources Research*, *46*(6).

Sensornet. (2007). Oryx dts user manual v4 [Computer software manual].

Sensornet. (2017). Distributed temperature sensing system user manual [Computer software manual].

Suomi, J., & Käyhkö, J. (2012). The impact of environmental factors on urban temperature variability in the coastal city of turku, sw finland. *International Journal of Climatology*, *32*(3), 451–463. https://doi.org/10.1002/joc.2277

Thulasiraman, P., et al. (2019). Countering passive cyber attacks against sink nodes in tactical sensor networks using reactive route obfuscation. *Journal of Network and Computer Applications*, *132*, 10 - 21.

Ukil, A., Braendle, H., & Krippner, P. (2012). Distributed temperature sensing: Review of technology and applications. *IEEE Sensors Journal*, *12*(5), 885-892.

Virrankoski, R. (2013). *Wireless sensor systems in indoor situation modeling ii* (No. 188).

Wang, N., Zhang, N., & Wang, M. (2006). Wireless sensors in agriculture and food industry - recent development and future perspective. *Computers and electronics in agriculture*, *50*, 1-14.

Wikipedia. (2018). *Wireless sensor networks.* Retrieved from https://upload .wikimedia.org/wikipedia/commons/2/21/WSN.svg

Xu, Q., & Solaimanian, M. (2010). Modeling temperature distribution and thermal property of asphalt concrete for laboratory testing applications. *Construction and Building Materials*, *24*, 487–497.

Yiğitler, H., et al. (2010). Stackable wirless sensor and actuator network platform for wireless automation: the UWASA Node. In *Aalto university workshop on wireless sensor systems.* Espoo, Finland.

Zagan, I., et al. (2019). Hardware rtos: Custom scheduler implementation based on multiple pipeline registers and mips32 architecture. *Electronics*, *8*, 211.

Zhu, K., Blum, P., Ferguson, G., Balke, K., & Bayer, P. (2011). The geothermal potential of urban heat islands. *Environ. Res. Lett.*, *6*(019501).

# Camera Integration to Wireless Sensor Node

Caner Çuhac, Huseyin Yigitler, Reino Virrankoski, and Mohammed S. Elmusrati

University of Vaasa, Department of Computer Science,
Communications and Systems Engineering Group
P.O. Box 700, FI-65101 Vaasa, Finland
caner.cuhac@student.uwasa.fi, {husali, reino.virrankoski, mohammed.elmusrati}@uwasa.fi

***Abstract*— A wireless vision sensor, which is capable of processing vision data, has great potential to be utilized in applications like swarm robotics, indoor situation monitoring and modelling. Although limited resource nature of the wireless sensor network nodes prohibit substantial utilization of vision sensors, stackable design of the UWASA Node allows development of a wireless vision sensor that is capable of processing image data, acquired by the camera board of the CMUcam3. In this work, we are introducing a wireless vision sensor hardware based on the UWASA Node.**

***Index Terms*— Visual Data Processing, Visual Feature Extraction, Wireless Vision Sensor Node.**

## I. Introduction

Vision sensor is an essential part of some robotics, control and data fusion applications. A wireless vision sensor, which is capable of processing vision data, has great potential to be utilized in applications like swarm robotics, indoor situation monitoring and modelling. The main aim of this work is to develop a vision sensor board for the UWASA Node.

Wireless Sensor and Actuator Networks (WSANs) provide means to intelligently acquire and change the state of the physical world. These networks are composed of low cost, low power, short distance and multifunctional sensor nodes, [1]. Many wireless sensor platforms which are developed so far have shortages in transmission capacity, power consumption, data processing or system adaption and compatibility. These shortages yield development of different platforms for different applications, causing long and uneven development and adaptation periods, [2]. Aiming to be a generic wireless sensor platform, the UWASA Node has been developed within the context of GENSEN project [2] by researchers in University of Vaasa. The UWASA Node is designed to adopt itself to application demands by providing means of modularity via relatively simple slave modules.

The modular/stackable nature of the UWASA Node permits addition of more resources to the node, allowing possibility of effective development of wireless vision sensors. Moreover, unique features of this architecture allow accessing and processing vision data in the node, while still advertising meaningful data over the network. Designing a slave vision module for the UWASA Node is the main goal of this work.

There are already developed camera platforms with low power microcontroller interfaces. CMUcam3 [3] is one of those platforms which has a publicly available software. Additionally, it uses a microcontroller which belongs to the same family as the Main Controller of the UWASA Node. In this design, the camera board of the CMUcam3 will be used as vision sensor. The slave module that will be developed will reflect all of the hardware related features of CMUcam3, so depending on the application requirements, it will be possible to switch between different camera boards having different specifications.

Some applications may need pan-tilt movement of the camera, registration of inertial information on the images, or accurately synchronized operation among the network entities. These kind of applications are in-directly supported by the proposed hardware due to stackable nature of the UWASA Node. Instead of developing different slave boards to add support for those applications, pan-tilt servo motor interfaces is added to the targeted hardware module.

The resource limited nature of wireless sensor nodes has led to development of wireless vision sensors focused on image acquisition and direct transmission of those images to a central computer while maintaining low power operation [4]. Since wireless sensor nodes usually have very limited computational power and low transmission bandwidth, either frame rate is very low or they perform very basic operations on visual data like line tracking [5].

In this work the scope is restricted to developing the basic camera node hardware, developing computer vision methods up to a reasonable level, testing the feasibility of in-node image processing, and adding pan-tilt camera rotation abilities to camera board.

The paper is organized as follows: Section II defines the problems and challenges related to vision sensing on wireless sensor nodes. Section III discusses about advantages of solving those problems by using UWASA Node and about the structure of the offered design followed by conclusion in Section IV.

This work is supported in part by the Finnish Funding Agency for Technology and Innovation (TEKES), and is developed as a part of the GENSEN project.

## II. Problem Definition

### *A. Amount of Data*

Acquiring vision data requires handling large amount of data, while consuming relatively high acquisition energy. Although those factors contradict with the low power definition of the wireless sensor node operation, for some applications it is inevitable to use vision sensors. The low range – low bandwidth nature of wireless communication restricts the amount of information that can be transferred between the network nodes [6]. This restriction requires preliminary processing of image data to extract meaningful information before any transmission. However, before any processing the acquired vision data should be calibrated to minimize the effects of non-ideal behaviour of lenses, vision sensors etc. Therefore, such a node should be able to calibrate and process acquired data. In this work, we are dealing with optimum utilization of vision sensor on limited resourced wireless sensor nodes.

### *B. A-synchronization of Vision Data*

Continuous output of the camera should be handled in such a way that calibration and processing have to be performed over whole frame image data. Hence, the output of vision sensor should be buffered so that processing unit can perform its tasks synchronized in terms of frames, not pixels. Moreover, a frame usually consists of large data chunks. Consequently most of the small embedded processors should be supported by extra memory units to allow frame-wise processing [5].

### *C. Application Specifications*

Another problem is to determine computational power requirements of computer vision algorithms that will run on the node. The feasibility of each algorithm should be analysed to determine the reasonable level of in-node processing to fulfil application demands. This requires a decision on the trade-off between data processing and power consumption, if the method requirements can be fulfilled by limited resources of the node.

It should be noted that the low-bandwidth wireless link imposes additional positive demand on processing level. The node should be able to perform at least some of the computer vision methods like feature extraction, scaling, compression, which increases power consumption. This trade-off requires carefully engineered design of node software that meets the application demands on information exchange level and node lifetime [5].

## III. Design Details

### *A. UWASA Node*

UWASA Nodes are modular – stackable wireless sensor platforms in small dimensions, providing relatively high process power while maintaining low power consumption. UWASA Node's modular-stackable structure allows extendibility of the node without primary change in the design. Hardware model of the node is shown in Figure 1.

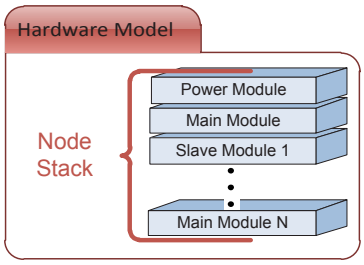


Figure 1: Hardware Model of the UWASA Node

The hardware structure has two essential parts: Power Module and Main Module.

Power module consists of a Li-Ion battery providing 3.7 V DC voltage. Power module has many hardware and software related specifications to utilize efficient power management. Main module has two main parts: Main controller and RF controller. Main controller is ARM7TDMI-S 32-bit LPC2378 processor which operates up to 72 MHz. RF controller TI CC2431 System on Chip (SoC) has integrated RF transceiver and 8051 8-bit CPU units on the chip. RF controller supports IEEE 802.15.4 MAC hardware and RF power on/off features.

### *B. Vision Sensor Interface*

In this work, a slave module will be designed as an interface of the main module to the vision sensor. The logical control of all main hardware components on slave module will be performed by External Memory Controller Interface (EMC) and a few General Purpose I/O (GPIO) pins. Figure 2 shows the hardware components of the slave module and relations between them. A GPIO pin will control data traffic direction, while EMC is responsible for data exchange between the memory peripherals (FIFO, SRAM and processor). The camera is configured via Serial Camera Control Bus (SCCB).

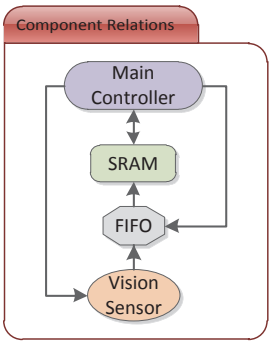


Figure 2: Hardware components and their relations

The data acquired from the vision sensor will pass to the designed slave module. The very first action on the vision data is to store it in a First-In/First-Out (FIFO) buffer IC to enable frame level processing. The chunk of data in the FIFO buffer is transferred to the internal memory bus of the processing unit using EMC of the main controller of UWASA Node. EMC is utilized for glue-less data transfer from FIFO to an external

Static Random Access Memory (SRAM). Since EMC maps internal memory bus of processor to I/O pins, SRAM connected to EMC can be read or written by a single instruction, and can be considered as internal memory of the processor. Selected SRAM capacity for this interface is 1 MB and has very short access time (12 ns). Access time is extremely important factor because in vision data processing speed is crucial. Another benefit of EMC is that its access time is configurable to relatively precise time resolution, which improves process rate efficiency when interfacing external memory devices with different access times.

The designed hardware architecture that allows glue-less frame data transfer from FIFO to SRAM is shown in Figure 3. The EMC (EMIF) of the processor is responsible for providing address information to SRAM, while enabling the data direction from FIFO to SRAM. Since the timing requirements of both FIFO and SRAM are selected to enable this operation, one byte of frame data is transferred with single instruction of the processor.

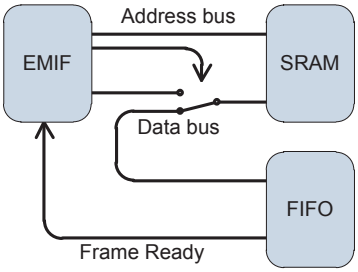


Figure 3: Transferring frame data from FIFO to SRAM.

Another important feature of the architecture is its ability to adopt itself to glue-less SRAM access. This option is shown in Figure 4. Since the EMC is a mapping of internal memory bus of the processor to I/O port, the frame data transferred to SRAM is ready for processing.

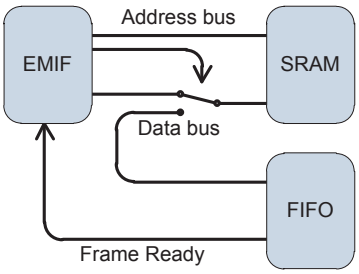


Figure 4: Accessing the SRAM content.

### C. *Development Stages*

The proposed hardware module will also contain Secure Digital (SD) memory card, and Full Speed USB 2.0 interfaces. The SD card will provide permanent storage of raw, and/or processed image data for debugging and logging purposes. The USB interface will allow step by step computer vision library development. In other words, at the very beginning of the algorithm development stage, the whole method will run on the development PC. After verifying the functional operation, the sub-parts of the algorithms will be ported to the node. This method of algorithm development will allow us to identify the parts of algorithm which need to be optimized with respect to efficiency of generated code, or will prove that it is impossible to implement that algorithm on the node.

### D. *Vision Sensor*

The vision sensor which is used in preliminary design has a maximum resolution of 352 x 288 pixels and provides up to 60 fps or any lower fps value. It can be configured to work in 8-bit RGB, YCrCb and HSV colour space modes. It is not a sophisticated vision sensor but since this work is focused on limited image processing, it is enough to prove the concept. It is the same vision sensor used in the CMUcam3, as shown in Figure 5.

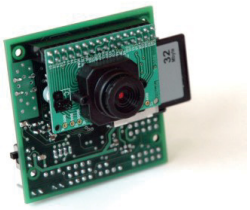

Figure 5: CMUcam3 (In this design only the vision sensor board will be used) (CMUcam3: Open Source Programmable Embedded Color Vision Platform)

### E. *Extendibility Support*

The proposed hardware architecture does not provide intrinsic extendibility support, except the options provided by the UWASA Node. Since the UWASA Node provides necessary means to extend its features by adding additional slave modules, it is possible to develop another slave module that contains high process power DSP and larger memory.

On the other hand, since the camera board is a separate board, it is possible to design another vision sensor board that contains a better imaging sensor.

## IV. Conclusion

The proposed architecture was designed as proof of concept of effectiveness of the UWASA Node architecture as wireless vision sensor. It aims to be a simple solution for low-power, low-cost wireless vision sensor having basic image processing and feature extraction functionality. The proposed hardware aims to provide basic interfaces for aiding the porting of computer vision methods, via SD card and USB interfaces. Moreover, it also contains servo motor connection capability to support pan-tilt motion of the vision sensor board. Other advantages of this designed interface is easy extendibility in the terms of better quality vision acquisition and higher process power via simple modifications on hardware.

## REFERENCES

[1] I. F. Akyildiz, W. Su, Y. Sankarasubramaniam, and E. Cayirci, "Wireless sensor networks: a survey," *Computer Networks*, vol. 38, no. 4, pp. 393-422, 2002.

[2] Reino Virrankoski and S Keskinen, "GENSEN: A Novel Combination of Product, Application and Technology Platform Development in the Context of Wireless Automation," in *Proceedings of the 14th International Conference on Productivity & Quality Research (ICPQR 2009)*, Alexandria, Egypt, 2009.

[3] CMUcam3: Open Source Programmable Embedded Color Vision Platform. [Online]. www.cmucam.org

[4] M. Casares, M.C. Vuran, and S. Velipasalar, "Design of a Wireless Vision Sensor for object tracking in Wireless Vision Sensor Networks," in *Distributed Smart Cameras, 2008. ICDSC 2008. Second ACM/IEEE International Conference on*, 2008, pp. 1--9.

[5] C.H. Zhiyong, L.Y. Pan, Z. Zeng, and M.Q.H. Meng, "A novel FPGA-based wireless vision sensor node," in *Automation and Logistics, 2009. ICAL'09. IEEE International Conference on*, 2009, pp. 841--846.

[6] C. Wu, H. Aghajan, and R. Kleihorst, "Real-time human posture reconstruction in wireless smart camera networks," in *Proceedings of the 7th international conference on Information processing in sensor networks*, 2008, pp. 321--331.

# Seed Flow Monitoring in Wireless Sensor Networks

Caner Çuhac, Reino Virrankoski, Petri Häninen and Mohammed Elmusrati
University of Vaasa
Department of Computer Science
Communications and Systems Engineering Group
P.O.Box 700, FI-65101 Vaasa, Finland
{caner.cuhac, reino.virrankoski, petri.haninen mohammed.elmusrati}@uwasa.fi
Hermanni Hööpakka and Heikki Palomäki
Seinäjoki University of Applied Sciences
School of Technology
P.O Box 412, FI-60101 Seinäjoki, Finland
{heikki.palomaki, hermanni.hoopakka}@seamk.fi

***Abstract*—In agricultural fields better seeding leads to better results during the harvest. There are some practical problems related to seeding process caused by the environmental conditions. For instance, occasionally damp soil gets stuck at the end of the seeding pipes of the implement, which prevents the seed from reaching the ground. In addition to that, after the crops start growing, some farmers experience that there were actually no seed flow in some of the pipes. In such cases, it would be beneficial to notify the driver about the problem immediately. In order to solve these sort of problems, this work introduces a real time wireless seed flow monitoring system for seed drill implements. Besides all these, monitoring the seed flow rate in each pipe and providing the measurements to the tractor operator in real time would help optimizing the seeding costs and increasing the efficiency of soil usage. The number of seeds per square meter can be obtained by using the seed counting information. This information combined with germination rate can be utilized in precise farming.**

## I. Introduction

During the seeding season of the agricultural fields, it is important to decide the amount of the seeds to spread per certain area in order to achieve the best efficiency in harvesting. Although the target numbers may be clear, there are some practical problems which may occur during the seeding process. For instance, the seeding mechanism may get blocked by humid soil, preventing the seeds from reaching the ground; or for some reason, the mechanism may not be dropping the seeds to the pipe [1]. In such cases, it would be beneficial to have a monitoring system to generate warnings to the driver. Moreover, uniform distribution yields the soil sources to be equally shared between the crops.

In order to verify that the seeds are flowing at the desired level, a real time monitoring system is needed. Cabled systems are not always the best solutions in industrial environments because of the cabling complexity and costs [2], while there are alternative wireless technologies providing the equal functionality. This logic applies to agricultural environments as well. Due to recent advances in wireless automation systems, vehicle guidance and machinery management in agriculture sector are drifting to wireless technologies [3].

University of Vaasa and Seinäjoki University of Applied Sciences have been researching a wireless monitoring system to be integrated on seed drill implements. The monitoring system consists of two wireless subsystems: The measurement level SURFbuttons and the control level UWASA nodes. On the implement side, there are SURFbuttons located on each pipe. These buttons measure the seed flow rate and send their data to a sink SURFbutton. The sink SURFbutton has a wired bridge to a UWASA Node which is used for collecting and passing the measurements. On the tractor side, there is another UWASA Node that receives the data coming from the UWASA Node located implement side. After the reception and a simple data processing, it displays the flow rate by employing graphics on an LCD screen located on the driver's panel. During the operation, in case any problem occurs at a specific pipe, the indicator of that pipe turns to red to attract the driver's attention.

The seed flow measurement is realized by using Light Emitting Diodes (LED) and Light Dependent Resistors (LDR) located on every pipe. Since both the wireless nodes and the LEDs are powered by batteries, the power consumption is analyzed for different operational cases.

## II. Design Considerations

Grain seeds come in various sizes depending on the type of the crop. Although the grains which are widely sown in Ostrobohnia region such as rye, wheat, barley and oat have somehow similar sizes [4]; this research aims to provide a monitoring solution which can be operate on any type of grain, including corn.

As a consequence of relatively small and various grain sizes, currently available high frequency ultrasonic measurement sensors were found inadequate to be used in the seed monitoring system. Another option would be microwave sensors but the electromagnetic characteristics of the grains are not good for such option and their price compared to the price of the seed drill is too high. Apart from that, there would be interference between adjacent pipes for both ultrasonic and microwave sensor types. In addition to those types, proximity

sensors were considered as well, but commercially available proximity sensors would not operate on such small surfaces like grain, since they require a flat surface to reflect their pulses.

Eventually some early tests have shown that using infrared LEDs and LDRs is a suitable option for detecting the seeds. One apprehension had been the dust generated by a falling grain, but this was overcome by placing the LEDs and LDRs in suitable locations on the pipe as seen on Figure 1. Another issue was the daylight interference on the LDRs but this was overcome by covering the pipe with opaque material.

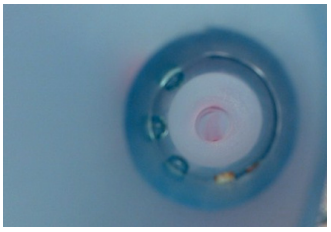

Figure 1. LEDs and LDRs are located inside the pipe.

Since the LEDs would consume much more power than the rest of the wireless network devices in the system, it would be beneficial to seek for alternative energy harvesting solutions in the future. As for now, the research group has decided to keep the existing measurement solution for the first experiments.

## III. System Structure

The system is designed to be integrated partially on the tractor side and partially on the implement side. The structure of the entire system is represented in Figure 2.

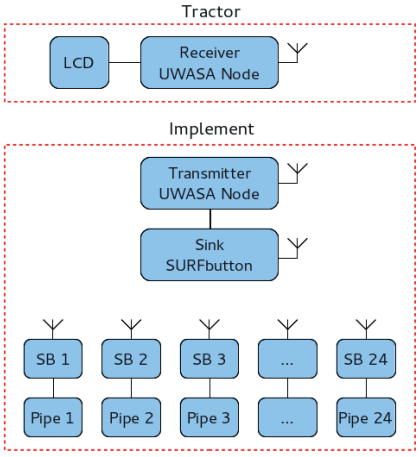


Figure 2. Structure of the system.

The tractor side consists of a receiver UWASA Node and an LCD screen which displays the seed flow rate in real time, based on the data coming from the implement. On the implement side, there are SURFbuttons on located on each seeding pipe. These buttons supply power to measurement LEDs which are emitting infrared light inside the pipe. On the opposite side of the LEDs there are LDRs continuosly receiving the infrared light. When a grain falls down through the pipe, it blocks the light path and the resistance of LDR changes. This creates spikes on the voltage level of the comparator peripheral of the SURFbutton. At that point the SURFbutton had been keeping itself in sleep mode until a grain had fallen. Comparator interrupt causes the SURFbutton to wakeup from the sleep mode, so that it can increment a counter value, and go back to sleep mode again. This wake up and increment process repeats for multiple times, and after a certain period of time, each SURFbutton wakes itself up to transmit its counter value to the sink button, and resets the counter. The transmission process only takes about 2ms. After the measurements are collected by the sink button, they are passed to transmitter UWASA Node over the SPI bridge. The transmitter UWASA Node puts the data into a packet and transmits it to the receiver UWASA Node which is located inside the tractor panel. Receiver UWASA Node then parses the packet and updates the LCD display with new values every second. This process goes on as long as the seeding process continues. The LCD display can be seen on Figure 3.

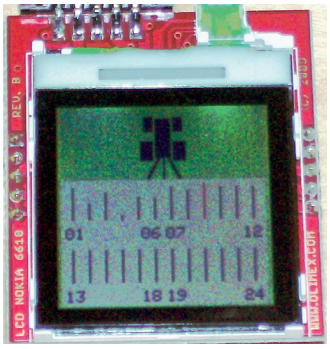


Figure 3. LCD displays the flow rates in real time.

The display shows lines numbered from 1 up to the total number of the pipes in the implement. The length of each line corresponds to the current flow rate on that pipe. In case a problem like a stuck pipe is detected, the line color turns to red (as can be seen on 9th pipe) to indicate a warning to the driver.

## IV. Test Results

Two series of tests were performed in laboratory environment. The purpose of the first series was to monitor and log the raw data output of the measuring SURFbutton's ADC.

The second series were carried out to measure the power consumption under different circumstances.

### *A. Monitoring and Logging Raw Data*

In this part of the tests, instead of using the comparator interrupts, samples were gathered continuously at a rate of 500Hz, making it possible to capture the data while there is no seed flow. The Figure 4 is composed of 15000 samples and it represents data collected over exactly 30s. In this test a total number of 50 seeds were dropped down through the pipe in 5 groups, and each group consists of 10 seeds. It can be seen from Figure 4 that the seed flow generates detectable voltage spikes on the ADC output.

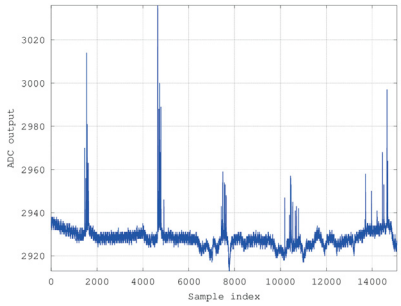


Figure 4. Graph of the raw data captured over 30s.

Figure 5 was generated by zooming in on the samples from 10000 to 11000 of the Figure 4. It can be seen that every seed generates detectable voltage spikes on the output.

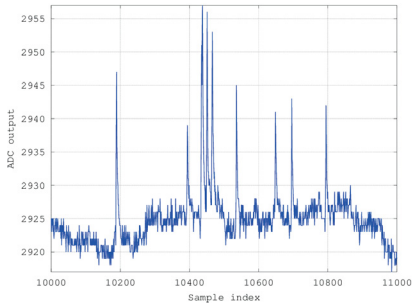


Figure 5. A closer look to the graph. Each falling seed creates voltage spikes.

Figure 5 shows only 9 peaks though there have been 10 grain seeds falling during that time. The reason here is that some of the seeds had been falling almost simultaneously, overlapping with each other. Some advanced signal processing is needed to be able to count the seeds in such cases. So far Fourier analysis, wavelets and some other peak detection methods have been applied on the data, and the seed counting algorithm development is on progress. Some preliminary results are presented in Figure 6, where two overlapping seeds are detected from the processed data and indicated by the Boolean values.

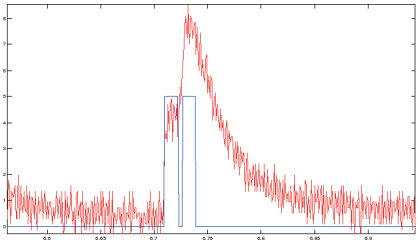

Figure 6. Two overlapping seeds are detected from the processed data and indicated by the Boolean values.

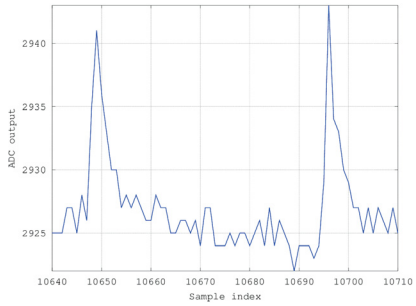


Figure 7. Two spikes seen on the graph. Each falling seed approximately corresponds to 10 samples.

Zooming more on the samples from 10640 to 10710, two spikes can be seen in more detail in Figure 7. Since the sample rate is 500Hz, this figure gives an idea about the travelling time of a seed while it is passing between the LEDs and LDR. The width of each spike can be considered 10 samples and that corresponds to 5ms in time. One interesting fact to point out here is that, rising edges of these spikes cause an interrupt on the microcontroller, and microcontoller again goes to sleep within 2 ms, which is shorter than duration of a voltage spike.

### *B. Power Consumption*

The second series of the tests consists of power measurements on a seed drill machine prototype. The purpose of the analysis is to find out the power consumption of the SURFbuttons located on the pipes while they are operating under different conditions. Power consumption values are represented in terms of current consumption at 3V.

Power consumption of a measuring SURFbutton can be divided into three separate components. One of them is the transmission power. The test results have proven that the average value of the current drawn from the battery for periodic

transmissions is 0.45$\mu$A. Handling the comparator interrupts is another power consuming operation. The SURFbutton keeps itself in sleep mode until a voltage spike is detected. After waking up, handling the ISR and going back to sleep takes 2ms in total. During that time the microcontroller consumes 1.5mA. Time average of the current consumption in this case, depends on the number of interrupts in given time. For that reason, multiple measurements were performed at different seed flow rates. The last and the main power consuming issue is to keep the infrared LEDs on. This introduces a current consumption of 29.3mA continuously, although there are neither transmission nor comparator interrupts.

In order to verify those separate measurements, seed feeding mechanism of the seed drill was loaded with rye, and rotated at constant speeds. Power consumption has been monitored and the calculations have been verified. The following table summarizes the power consumption in different situations.

TABLE I
POWER CONSUMPTIONS IN DIFFERENT TEST CASES

| Test Case | Current Consumption |
|---|---|
| Only transmission | 3.45$\mu$A (10.35$\mu$W) |
| 100 seed/s, LEDs off (interrupts simulated) | 303.45$\mu$A (910.35$\mu$W) |
| No seed flow, LEDs on | 29.3mA (87.9mW) |
| Slow seed flow, LEDs on | 29.6mA (88.8mW) |
| Fast seed flow, LEDs on | 30.8mA (92.4mW) |

First case is independent from the seed flow rate so it was measured directly from the device. In the second case, a 100Hz square wave signal was applied to the comparator input to simulate exactly 100 seed/s. The remaining tests were practiced on the seed drill prototype. In the third case the current consumption was recorded as 29.3mA while the seed feeding axle was still. Then it was rotated at a speed of 0.3rpm to experiment a slow seed flow. In this case, the microcontroller frequently wakes up, handles the ISR, and goes back to sleep mode. Lastly the axle was rotated at 1rpm to perform the fast flow experiment where the microcontroller receives so many interrupts that it almost never goes to sleep mode.

### C. Battery Lifetime

Based on the test results it is possible to estimate a lifetime for the measurement part of the seed flow monitoring system. SURFbuttons are relatively small devices compared to AAA sized batteries, thus they operate mainly on cell sized batteries. As for 2012, commercially available cell sized batteries offer 500mAh of charge. Considering these values the system would continuously operate for:

$$\frac{500mAh}{30mA} = 16.7\ hours \tag{1}$$

In case there would be an external source to power the LEDs so that SURFbutton battery only needs to handle the power supply for communication and computation, the system would last for:

$$\frac{500mAh}{303.45\mu A} = 1648h = 69\ days \tag{2}$$

of active operation.

These results show how significantly the lifetime would extend in case the energy harvesting solutions would be applied.

## V. CONCLUSION AND FUTURE WORK

Using the wireless sensor networks in agriculture sector, many problems which are still unsolved just because of the cabling requirements can be reconsidered and new solutions may be introduced.

This research proves that using the wireless sensor networks it is possible to monitor the seed flow in real time. Using only the cabled systems in this case would be inappropriate since there would be much more wires around mechanical structures.

Power measurements have shown that the operation duration is feasible, but the energy harvesting solutions would significantly increase the lifetime of the system. In case the LEDs would be powered by an energy harvesting device, the system would operate much more than a seeding season.

Further systematic data analysis are able to provide information about the number of the seeds dropped per square meter. In future this work may be extended so that the seed flow rates can be logged to a non-volatile memory, including location and timestamp to keep statistics.

## REFERENCES

[1] S. E. Hawkins and D. R. Ess. (2012) Grain drill metering systems and the need for calibration. [Online]. Available: www.extension.purdue.edu/extmedia/ABE/ABE-126-W.pdf

[2] H. Yiğitler, R. Virrankoski, and M. S. Elmusrati, "Stackable wirless sensor and actuator network platform for wireless automation: the UWASA Node," in *Aalto University Workshop on Wireless Sensor Systems*, Espoo, Finland, Nov. 2010.

[3] N. Wang, N. Zhang, and M. Wang, "Wireless sensors in agriculture and food industry - recent development and future perspective," *Computers and electronics in agriculture*, vol. 50, pp. 1–14, Jan. 2006.

[4] H. Palomäki, H. Hööpakka, and C. Çuhac, "Wireless seed drill monitoring system," in *11th International Symposium on Ambient Intelligence and Embedded Systems(AmiES-2012)*, Espoo, Finland, 2012.

IEEE Access
practical innovations : open solutions

Received September 9, 2013, accepted October 8, 2013, date of publication October 25, 2013, date of current version November 1, 2013.

*Digital Object Identifier 10.1109/ACCESS.2013.2287302*

# Localization Services for Online Common Operational Picture and Situation Awareness

**MIKAEL BJÖRKBOM[1], JUSSI TIMONEN[3], HÜSEYIN YIĞITLER[1], OSSI KALTIOKALLIO[1], JOSÉ M. VALLET[1] GARCÍA, MATTHIEU MYRSKY[1], JARI SAARINEN[1], MARKO KORKALAINEN[4], CANER ÇUHAC[2], RIKU JÄNTTI[1], REINO VIRRANKOSKI[2], JOUKO VANKKA[3], AND HEIKKI N. KOIVO[1]**

[1]School of Electrical Engineering, Aalto University, Aalto FI-00076, Finland
[2]Department of Computer Science, University of Vaasa, Vaasa 65200, Finland
[3]Department of Military Technology, National Defence University, Helsinki 00870, Finland
[4]VTT Technical Research Centre of Finland, Espoo 02044, Finland

Corresponding author: M. Björkbom (mikael.bjorkbom@aalto.fi)

**ABSTRACT** Many operations, be they military, police, rescue, or other field operations, require localization services and online situation awareness to make them effective. Questions such as how many people are inside a building and their locations are essential. In this paper, an online localization and situation awareness system is presented, called Mobile Urban Situation Awareness System (MUSAS), for gathering and maintaining localization information, to form a common operational picture. The MUSAS provides multiple localization services, as well as visualization of other sensor data, in a common frame of reference. The information and common operational picture of the system is conveyed to all parties involved in the operation, the field team, and people in the command post. In this paper, a general system architecture for enabling localization based situation awareness is designed and the MUSAS system solution is presented. The developed subsystem components and forming of the common operational picture are summarized, and the future potential of the system for various scenarios is discussed. In the demonstration, the MUSAS is deployed to an unknown building, in an ad hoc fashion, to provide situation awareness in an urban indoor military operation.

**INDEX TERMS** Localization, mapping, networks, situation awareness.

## I. INTRODUCTION

Urban situation awareness and especially localization information is important in many applications. Operations, such as search-and-rescue, military operations, urban combat, hostage situations, emergency situations, indoor fire, or earthquake damaged buildings, rely on localization information, as the map of the environment and location of targets in a possible unknown area is needed. Combining information from several subsystems is a key aspect in these perilous applications. Knowing where things are and combining several sources of information, enables context aware data gathering, analysis and decisions, and aid in situation awareness.

In this paper, a novel solution is presented, called Mobile Urban Situation Awareness System (MUSAS), which is an integrated system that provides localization services of several types to enable situation awareness with focus on an urban environment. The target use of the proposed MUSAS is an operation in an urban environment where locations of own field team members, persons and objects are of key importance. The operation environment is typically partly unknown, which require mapping and localization of objects.

A general use case scenario for the MUSAS is an operation in an urban environment as shown in Fig. 1. A field team performs some task based on the instructions from the mission leader and upper echelon. A common operational picture (COP) [1] of the situation is formed, by the COP server and the MUSAS operator managing the system, using data from several subsystems deployed in the field. The COP is relayed to all the parties involved: the field team, mission leader, and upper echelon, to assist them in performing their tasks. Field team members have a hand-held device for interfacing with the COP. The COP contains information of locations of objects and targets of the task, typically humans, overlaid on a map of the environment, to assist in situation awareness.

  

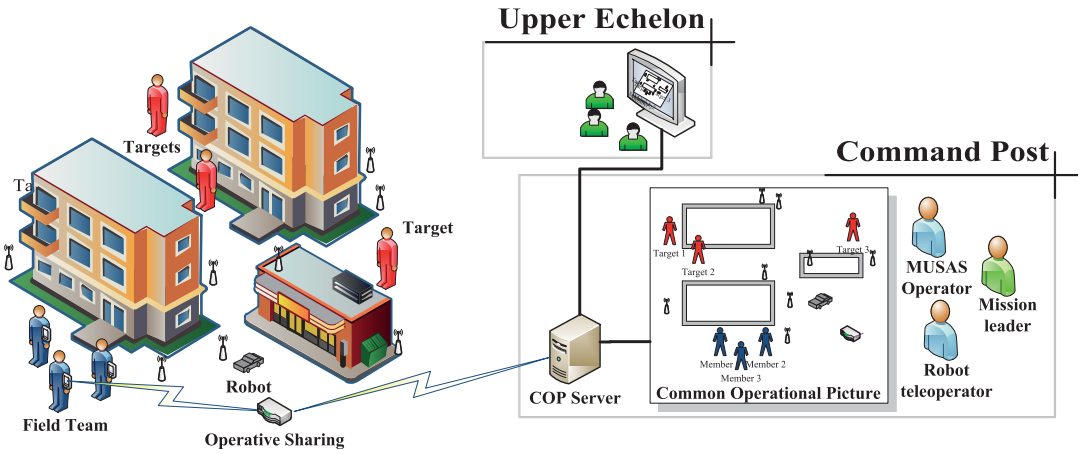


**FIGURE 1.** General use case example for the MUSAS and entities involved.

### A. OBJECTIVES AND CONTRIBUTIONS

A key contribution of the MUSAS is providing a system for online localization based situation awareness using multiple localization and mapping methods. Compared to other similar systems, the MUSAS does not assume or rely on anything of the target environment. The MUSAS builds up its own infrastructure using Wireless Sensor Network (WSN) and Wireless Local Area Network (WLAN) technologies. It maps the unknown area and updates the knowledge as entities are localized. Location information of moving targets is tracked and updated to the COP model and all users. The system can operate both outdoors and indoors and has through wall observation capabilities.

The contributions of this work include describing the general design of an online system for producing and integrating information for a common operational picture, based on mapping an unknown environment and appending several localization information sources. A survey of existing solutions and relevant technologies are done. The subsystems are presented, including their technical details and relevant literature. An implementation is presented and the experiences from a test demonstration are discussed. Other issues related to situation awareness, such as data associating and clustering, object recognition and feature extraction, target identification and tracking, and prediction, are not considered.

In this section, the objectives of the MUSAS, related situation awareness solutions, and the contributions of this paper are described. In Section II, a general system description of a localization based situation awareness system is done, and feasible localization solutions suitable for the use case scenario are identified. The proposed MUSAS architecture and an overview of the implementation are presented in the following sections. In Section III, the robot system is described, including mapping an unknown area using simultaneous localization and mapping (SLAM) by the robot. In Section IV, the localization subsystems are described in more detail with the information they produce for making the COP. Wireless sensor node localization is treated in Section IV-A. Object localization has also been implemented, both for cooperating objects or persons, in Section IV-B, and for non-cooperating persons. For the non-cooperating case, radio tomography can be used, as presented in Section IV-C. In Section V the experiences from a test deployment and the use of the MUSAS in urban combat situations is described. Finally a short conclusion is given with some notes on the use of such systems in other scenarios. A technical report of the system with more detailed information on the implementation can be found in [2].

### B. COMMON OPERATIONAL PICTURE

According to [3], situation awareness consists of several levels. The first level is perception or sensing. In the second level, comprehension is built from the observed data, as meaning is assigned to each piece of information and the relations between the components are inferred. In the third level, the situation implications are projected or predicted into the future. In this work only the first two levels are considered, where data is gathered by several entities and fused to some comprehensible picture of the situation. The task of the user is then to decide actions or predict the future based on the produced situation picture.

A common operational picture displays all gathered and combined data from several sources in a single presentation to the user [4]. The information is merged into a common frame of reference and visualized on a screen from where it is easy to comprehend the current situation. The main task of COP systems is thus to bring together data from different subsystems and present that into an overview for enabling situation awareness of a variety of users and different teams [1].

The early studies of COPs were carried out in the 1980's [4]. A major milestone is the development of a large group display to enable situation awareness in military command posts [3]. COPs have been successfully utilized in situations such as large scale natural disasters [5] and terrorist acts, where COPs have had a large impact on reducing human casualties.

A COP is often associated with geographical data, for instance in a combination with a Geographic Information System (GIS), as typical applications are tied to a possible large geographical area. Available maps, blue prints and floor plans can serve as a backdrop to pin the location based information to real-world coordinates and tie them to the environment.

### C. SITUATION AWARENESS

Most of the situation awareness literature concerns military cases. The Joint Vision document from 2001 [6], highlights the importance of information superiority throughout the battlefield. Situation awareness of individual soldiers is an important issue, and different armies around the world are developing their future soldier concepts. The target is to create a soldier, who is not only a warrior, but also an active information creator and consumer. The report [7], summarizes some different programs. For example, the Future Soldier program is an international endeavor, led by the USA, to create a soldier of the 2030 [8]. An example of a networked system of systems is the Future Combat Systems (FCS) which links 18 different systems into an operating entity [9].

The Common Operating Picture Software/Systems (COPSS) for emergency management is presented in [10]. This system supports a four dimensional COP and focuses on Shared Situation Awareness (SSA) and supports multiple information sources. Research on a Small Unit Operations Situations Awareness System (SUO SASS) is presented in [11], which has similar aspects as the MUSAS, in terms of ad hoc networks and location services focusing on soldiers. The use of commercial-off-the-shelf (COTS) products in tactical environments is studied in [12]. Especially, an implementation in Android environment, similar to the MUSAS, is studied in [13].

### D. SENSOR NETWORKS FOR EMERGENCY SITUATIONS

There are numerous wireless sensor network solutions envisioned for disaster and emergency situations where an infrastructure for data exchange is not readily available. In such scenarios, a WSN can be deployed in ad hoc fashion and provide the means for information exchange and other sensing purposes.

In disaster scenarios, scalable and heterogeneous network solutions for situation management are required. DistressNet [14] provides such a solution and it offers: ad hoc wireless architectures for communication, data exchange to improve situation awareness, and collaborative acoustic sensing for human detection. The system has also multiple solutions for localizing the nodes with the purpose of topology-aware routing and congestion control.

The VigilNet [15] system targets military surveillance, exploiting sensor networks to track targets in areas of interest. The authors consider the setup and operation requirements of the network. In addition, the importance of node localization is considered and Global Positioning System (GPS) is used to fulfill the task. VigilNet targets long term operation and thus energy constraints have an essential role in the system design. On the contrary, the system presented in this paper is deployed for short time intervals and therefore, energy consumption of the nodes does not have to be considered in the system design.

Diamond and Ceruti [16] discuss a military COP model and system architecture for modern warfare. The use of commercial and COTS wireless devices, the diverse sensing possibilities of the devices, and data fusion of different information are seen as effective ways to improve situational awareness for military purposes. Such augments in situational awareness enable new combat paradigms for modern warfare. In contrast to the hypothetical investigation of [16], an actual implementation is presented in this paper.

### E. MAPPING AND SEARCH-AND-RESCUE ROBOTICS

Reconnaissance and mapping of an unfamiliar area using a mobile robot, discussed in more detail in Section III, is indispensable, if it is unsafe for humans to enter. Mapping is needed to be able to navigate, operate, and localize the sensed information. The mapping of damaged buildings in an earthquake situation using both ground and aerial robots is presented by [17], where the mapping results of several robots are combined to produce a three dimensional map. Similar robots could be integrated in the MUSAS, with the addition of other subsystems, delivering various other information sources, such as localization of people and objects.

An EC project, Building Presence through Localization in Hybrid Telematic Systems (Pelote) [18], [19], studied the control of a human-robot team in a fire fighting scenario. The proposed solution consisted of a fire-fighter localization system [20], teleoperated robots [21] and an information fusion scheme to synthesize a common model from acquired data. One of the key contributions of the project was that it was experimentally shown that position information is critical in maintaining common situation awareness among the distributed team.

Similar to the MUSAS, Pelote emphasizes the importance of location based information. However, the MUSAS differs from Pelote in that it does not assume a priori information about the target environment. Furthermore, the MUSAS is built upon wireless sensor networks, which extend the range of applicable use case scenarios and enable new positioning possibilities, such as non-cooperative device free localization (DFL).

## II. SYSTEM ARCHITECTURE

The target of the MUSAS is to provide a common operational picture for the command post, to the field team and share it

with the upper echelon. This is accomplished by combining information from several different subsystems into a single view. In this section, the general system design and components of the implemented MUSAS is presented. This section is concluded by a description on how the COP information is distributed and presented to the user to aid in situation awareness.

### A. GENERAL SYSTEM OVERVIEW

A common operational picture is the visual representation of the up-to-date state of the operation. In this case, focusing on localization information of each entity. The COP includes, but is not limited to, the positions of targets and field team members, and the status of individual assets with respect to a common frame of reference, i.e. a map of the area.

To achieve a COP, information from several online localization systems, backdrop information, such as geographical data and operative information, must be integrated and distributed to all users, as summarized in Fig. 2. The COP server forms the COP model based on inputs provided by all subsystems, and it shares the resultant model with the upper echelon and with the field team using the operative sharing subsystem. The backdrop information subsystem provides basic information related to the operation and the environment. Based on the localization systems, online situation and localization information are formed, and updated the COP model to the current state of the situation. The operative sharing subsystem allows transferring and displaying the generated COP model to the field team, and conveying status updates from the field team to the COP server. Similarly, the upper echelon subsystem provides means for conveying the COP model to the command post, and delivers executive commands to the COP server.

### B. INFORMATION SHARING AND INTEGRATION

The COP model must support integration of data gathered from multiple sources. In the MUSAS, various types of information are provided by different subsystems such as mapping information from the robot, and position based content from the team member and target localization subsystems as shown in Fig. 2. Transferring information from

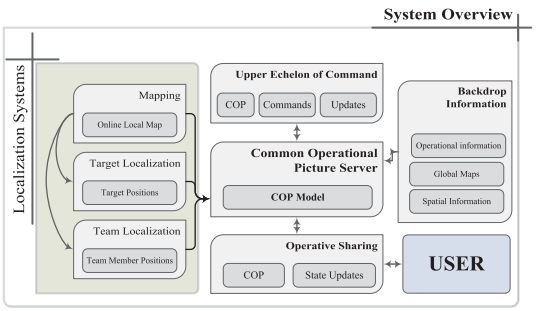


**FIGURE 2. General localization based common operational system overview.**

the individual subsystems to the COP server and sharing the up-to-date COP model with the upper echelon and users requires a sophisticated networking paradigm. The networking demands can be conveniently fulfilled by abstracting the network away and utilizing a distributed object system architecture. This solution abstracts the underlying technologies to independent functional entities and the integration of the subsystems is done by using a common data sharing framework.

Interactions among distributed object systems is generally enabled by utilizing object-oriented middleware, such as Common Object Request Broker Architecture (CORBA), Remote Method Invocation (RMI) [22] and Internet Communication Engine (ICE) [23]. Middleware, such as CORBA and ICE simplify the development of a distributed system. In addition, they allow independent development efforts of the subsystems, as they support multitudes of operating systems and programming languages.

Considering the diverse requirements of the MUSAS subsystems and the time constraints of data integration and sharing, ICE emerges as the best alternative. This particular middleware architecture is augmented by several services, including a publisher-subscriber topic based event distribution system called IceStorm. Using the IceStorm service, information exchange among the subsystems can be implemented as asynchronous event invocations in topic subscribers. The COP server and subsystems are thus interfaced by abstracted topics defined in and managed by IceStorm.

A fundamental need for a system supporting spatial situation awareness is a subsystem for binding the information from various sources to real world locations. Part of the integration process is associating and combining the position information from the individual localization subsystems to geographic information. Geographic layers, such as maps and blueprints, provide a global coordinate system for the various subsystems. Thus, the location information of the subsystems is inserted into the COP model and delivered to the users in conjunction with the geographic information.

Geographic Information System is one of the well-studied comprehensive solutions, which offers a closed infrastructure and a variety of functions for this purpose. GIS provides means to present the information in layers to aid visual cognition. Further, GIS offers a framework for integrating positioning information generated by the other localization subsystems. By using this framework, the COP server is able to increase the abstraction level of individual objects. The information of individual subsystems is not anymore an object with x- and y-coordinates that are bound to its local coordinate system. Rather, it has a location based on real world coordinates and a certain type, symbol and additional information provided by the COP model.

### C. SYSTEM TECHNOLOGIES AND OPERATION

The selected technologies for each subsystem in the MUSAS are depicted in Fig. 3, with brief motivation of the selections in this subsection. Further details are given in Section IV.

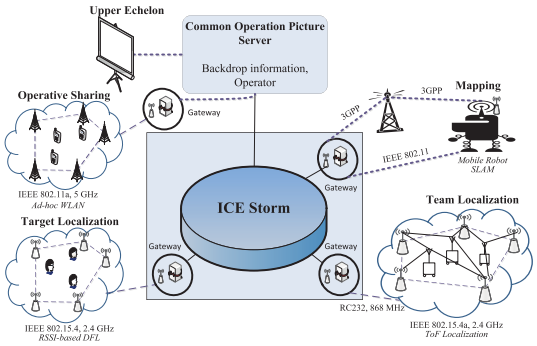


**FIGURE 3.** **The MUSAS system implementation and the utilized technologies.**

A common operational picture requires an accurate and up-to-date map of the operating environment, with a common notion of reference and direction. Since, in most of the considered scenarios, this knowledge is not available a priori, a mobile robot, which can generate the map while localizing itself is the most suitable solution among the alternatives, as demonstrated in Pelote [19]. Thus, in the MUSAS, a mobile robot, which is capable of simultaneous localization and mapping, is utilized to generate the map of the environment.

Wireless Sensor Networks can be successfully used to measure spatially distributed data, as a large number of nodes can be distributed in the area of interest. Therefore, an ad hoc WSN is a suitable solution employed in the MUSAS, where relying on existing infrastructure is not possible, due to several reasons, such as damaged and potentially unreliable existing systems.

The target and team localization subsystems aim at estimating the location of assets in the monitored environment. Despite the fact that both systems can be implemented based on visual or radar sensors, the limitations imposed by the cluttered environment and the cost, leverage radio based localization systems. Therefore, the proposed system is built on top of low-cost wireless networks.

An IEEE 802.15.4 network is employed for localizing non-cooperative targets using radio tomographic imaging [24], [25]. The IEEE 802.15.4 nodes are localized using the mobile robot to enable ad hoc deployment. The robot is connected by a versatile multi-radio gateway to support remote operation. For localizing team members, wearable sensors based on IEEE 802.15.4a, time of flight, and inertial sensors are used. To share the COP information to the users, an ad hoc IEEE 802.11a network is used. Gateways for each network are connected together with a wired local area Ethernet network and the ICEStorm publish-subscribe service is used to pass information to the COP server and the other subsystems.

The proposed solution is composed of different wireless communication technologies, some of which may operate on the same frequency band. Therefore, to not interfere with one another, the medium access of these technologies must either be synchronized, or they must be operated in non-overlapping frequencies. In the proposed system, the latter is mostly employed. Subsystem with overlapping frequencies, communicates in turns.

Many of the localization subsystems utilize location information from the other subsystems as depicted in Fig. 4. As an example, radio tomographic imaging requires that the location of the nodes are known. However, in most of the considered use-case scenarios, the node locations are not known a priori. One solution to this problem is to use the robot as a mobile beacon to locate other nodes of the network as described in Section IV-A. Another solution is to equip the robot with a node deployment system and distribute the nodes in desired positions as the robot explores the environment. It is to be noted that these two solutions are not complementary and can be used side by side. In the MUSAS, both options are utilized.

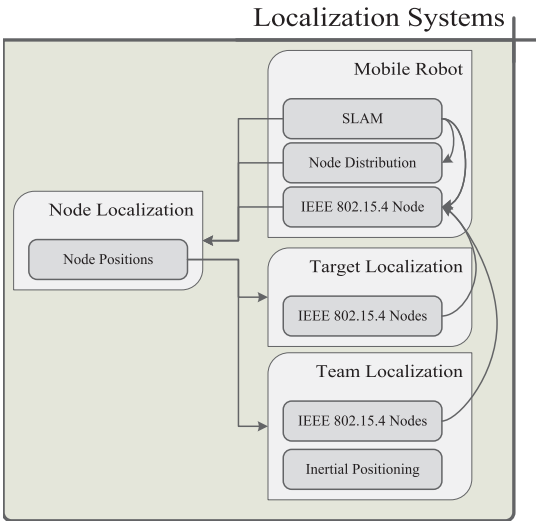


**FIGURE 4.** **Localization systems information flow.**

### *D. COMMON OPERATIONAL PICTURE SERVER*

The main task of the COP server is to produce the COP model, which includes all information that is significant for supporting situation awareness. The COP server encapsulates multiple functions, such as hosting relevant backdrop information, geographical information system, as well as publishing the formed COP. These entities are presented in Fig. 5, which is a detail view of the COP server block in Fig. 2. The COP server hosts also multiple services needed by the system, such as information sharing and operative sharing services. A command and control application is running as a front end application for the COP server, which provides a user interface for the command post operator.

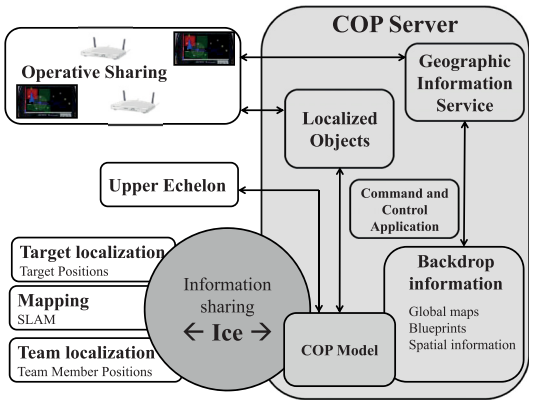


**FIGURE 5.** COP server framework.

### E. PRESENTATION

The COP is presented to the mission leader and upper echelon on a large group display, whereas the field team members are shown a scaled down version in a hand-held device. In either case, a user can zoom in and inspect detailed information associated with a region or object of interest.

The COP presented to the mission leader and the MUSAS operator is shown in Fig. 6. In the depicted scenario, the robot is heading forward in a corridor of an unknown building, simultaneously updating a SLAM generated map. The MUSAS operator identifies the blueprint of the environment and marks it appropriately. The color of the rooms can be changed according to the situation. Additionally, rooms, objects and events can be marked with appropriate NATO APP6B symbols and other polygon shapes, all referencing to local coordinates or real world coordinates (MGRS, WGS84). It is also possible to display the map partially transparent on top of a satellite map, to match it with the surroundings. This mode reveals shapes of the terrain and different targets such as monuments hidden in a forest, improving the situational perception.

The mobile application for the field team members, shown in Fig. 7, is created on an Android platform. Android is chosen because it allows easy deployment on new devices using the same operating system, and makes it possible to use a wide range of COTS products. The application is designed to be as simple as possible for a field team member to perceive the current operational picture. The hand-held application contains only a selected set of features which are presented in Table 1. Common use cases are moving the map, zooming the map, and adding a new object. Every feature is available by using only one hand, including opening the carrying pouch, where it is attached on the torso of the field team member.

### F. OPERATIVE SHARING

Sharing the COP information to hand-helds of the field team members is accomplished by using a mobile IEEE 802.11a (WLAN) based ad hoc capable, battery powered, access point network. The network, depicted in Fig. 8(a) and Fig. 3, enables flexible deployment and independence from external infrastructure. No special configuration is needed for the network and it acts as a normal WLAN network for the hand-held devices. The access point, pictured in Fig. 8(b), can automatically connect and join to the existing network access points in the field. When deploying the system, it can be placed anywhere, because it is battery driven. Furthermore,

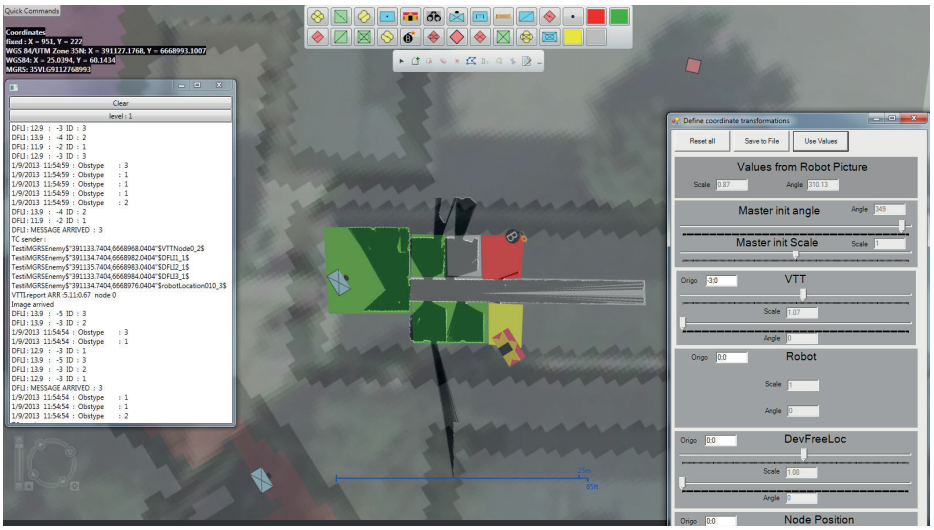


**FIGURE 6.** Command and control server application user interface.

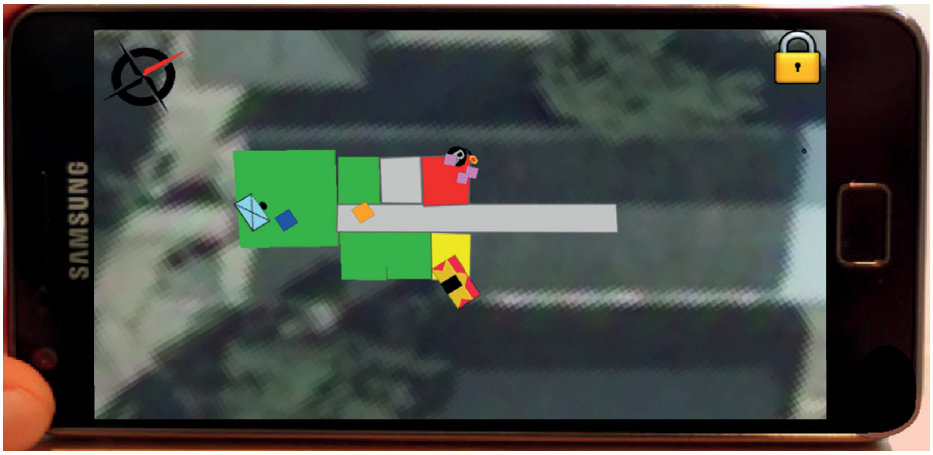


**FIGURE 7.** Hand-held device graphical user interface for assisting in situation awareness of field team members.

to expand the coverage, existing access points can be moved or new access points can be added.

## III. ONLINE INFORMATION ACQUISITION USING A MOBILE ROBOT

To operate in an unknown environment, reconnaissance to collect data and map the area is necessary. The map information, discovered objects, and other information are localized to the local map coordinates and further to global coordinates. For mapping and reconnaissance purposes, the MUSAS uses a mobile robot with SLAM capabilities. In this section, a short description of the mobile robot system is presented. The system components required for control, and how the location information provided by the robot is used in the system, is described.

### A. OVERVIEW

A mobile robot features many benefits in the use cases of the MUSAS. Most importantly, it can be deployed to gather information about an unknown situation without risking human lives and the robot is in a central role in creating a common frame of reference for the system.

The remote-controlled robot, shown in Fig. 9, is used as an exploring scout. The robot builds a metric map of the environment while localizing itself against the map. The robot is a tracked platform, weighting approximately 100kg and carries along 100Ah of energy as well as sensors and sufficient computation power. Further details about the robotic system can be found in [26]. In the MUSAS, a laser range finder and dead reckoning for creating the map are used. A camera with a pan-tilt-unit is provided for the teleoperator. In addition, the robot is equipped with a communication subsystem, which enables communication with the robot practically in all environments, without the need for an existing infrastructure.

To build up the localization and sensing infrastructure, treated in Section IV, the teleoperator can deploy wireless sensors into strategic places in the environment, using a wireless sensor node distribution subsystem integrated to the robot. The node deployment is controlled over ICEStorm. Whenever a node is deployed, the information, including the known location of the deployed node, is published to ICEStorm with a timestamp. Further, the robot communicates with the rest of the wireless network, and localizes nodes with unknown positions, deployed by other means, as explained in Section IV-A.

### B. COMMUNICATION AND CONTROL

The robot is controlled by teleoperating from the command post. The laser range finder data, the image from the camera, the calculated position and the constructed map of the area is sent to the teleoperation station display shown in Fig. 10. The calculated position of the robot and the constructed map is distributed from the teleoperation station to the COP server by using ICE, as shown in Fig. 3.

As a communication link between the robot and the teleoperation station, two multi-interface routers are used. The routers are especially designed for critical applications where broadband and reliable connectivity and largest possible coverage is needed. They have multiple different kinds of radio terminals, such as 3G HSPA, CDMA450/2000, WiMAX, Wi-Fi, LTE, Flash-OFDM, TETRA (Trans-European Trunked Radio, a radio specifically designed for use by government agencies and emergency services) or satellite, which can be used depending on the situation. The router monitors continuously all installed Wide Area Network (WAN) radios and switches to another radio if one fails or the quality of service is below a user specified threshold. In addition, the routers support virtual private networking, which enables secure and seamless connection, independent of the used radio technology.

**TABLE 1.** Hand-held device functions.

| Feature | Options |
|---|---|
| Map | Satellite or Raster |
| User views | Targets, team members, events, rooms (with colors), and compass |
| Marking objects | Event, Hostile, Unknown, Neutral |
| Gestures | Pinch - Zoom map Pinch + Rotate - Rotate map Short press - North up Long press - Select satellite or raster map |
| Compass | Displays North |

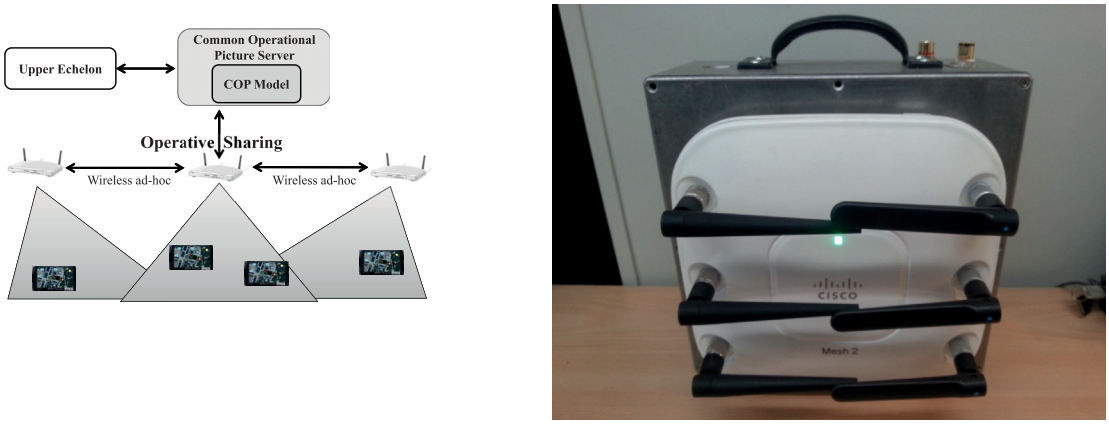


**FIGURE 8.** Operative Sharing (a) connecting the COP server and the field team member hand-helds using an ad hoc WLAN. (b) WLAN access point with batteries.

As a communication architecture, GIMnet [27], [28], which is a service-based communication middleware for distributed robotic applications, is used. From an application point-of-view, GIMnet provides a virtual private network where all participating nodes may communicate point-to-point using simple name designators for addressing. Using the multi-interface routers and the communication architecture, the system provides the possibility to seamlessly control the robot from virtually any remote location. The setup is mostly the same as in [29].

### C. SIMULTANEOUS MAPPING AND TRACKING

Simultaneous localization and mapping, is a well-studied field, and there are several approaches for solving it [30]–[32]. Here, the requirements are to map an arbitrary environment in real time, without changing the frame-of-reference during mapping. Because of these requirements, the problem is approached using a grid-based mapping and tracking (or Maximum Likelihood SLAM) method. The approach incrementally builds an occupancy grid through two steps: 1) Tracking, which maximizes the observation likelihood given the map, and 2) mapping, which fuses the observation with the map into the pose provided by the tracking step. This approach does not employ a loop-closing mechanism, and therefore is referred to as mapping and tracking, in order to distinguish it from a full SLAM solution.

**FIGURE 9.** The mobile robot unit used for exploring, mapping and node localization in the MUSAS.

The mapping step is a trivial occupancy update step using known pose and laser scanner data with a line model [33]. The tracking step uses a globally optimal search algorithm introduced in [34] for finding the best pose in the map. The search algorithm branches the pose space, with an objective to minimize the point distance to occupied map cells. The solution is bound by using an efficient approximation of the upper and lower bounds of the objective. The algorithm has

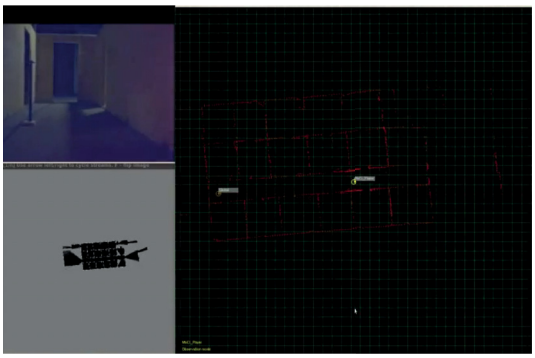

**FIGURE 10.** Teleoperation view for mobile robot.

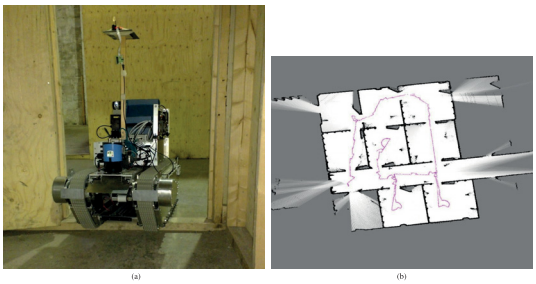

**FIGURE 11.** (a) The robot in the test environment. (b) An example map from the test scenario.

been shown to provide robust, sub-resolution pose estimates even with very large search spaces [34] and being able to map accurately even in the presence of large loops [29]. In this use-case, the map is incrementally built, and thus the search space is relatively small. The robot mapping and tracking inside the target area is shown in Fig. 11(a).

Fig. 11(b) provides an example map from the test scenario. The map is built in real-time by the robot and shows an exploration through eight rooms. The map is published to the other subsystems using ICEStorm as an image every 10 seconds. The map is then used in the command post and overlaid with the a priori map and global geographical information in the COP server. The map is also provided to the robot operator in order to help in keeping spatially oriented while driving the robot, as shown in Fig. 10. The pose of the robot is published to ICEStorm continuously, for the other subsystems, specifically the robot operator and the node localization system.

## IV. SYSTEMS FOR LOCALIZATION

Localization of wireless nodes in Wireless Sensor Networks has been researched extensively, because in spatially distributed systems, sensor data is only meaningful if the location of its origin is known. In the MUSAS, not only node locations are needed, but also locations of field team members, targets and other objects and events, as well as their position in relation to a map. The following subsections briefly present the localization subsystems of the developed MUSAS and explain their technical details and how they produce the required localization information. The interactions of the localization subsystems are described in Section II-C.

### *A. NODE CALIBRATION AND LOCALIZATION*

Due to the ad hoc nature of emergency and rescue situations, the localization systems used in the MUSAS cannot depend on pre-installed infrastructure in the target site. Thus the WSNs used have to be deployed ad hoc. In the most general case, nodes will be placed in random or unknown positions. Once the network has been deployed, the task is then to estimate the position of the nodes, such that the information measured through their sensors can be associated to the known locations.

There are many existing localization methods for WSN [35]. In this work, a maximum likelihood (ML) algorithm based on radial received signal strength (RSS)-distance models is used. Using RSS as a primary source of information for localization has advantages and drawbacks. First, the circuitry to measure RSS is low-cost and most of the radio chips on the market provide an RSS indicator. On the other hand, RSS can be significantly affected by obstacles, and as a consequence, localization using RSS is known to be considerably inaccurate in cluttered environments. However, this sensitivity can be exploited to detect and track objects or persons by monitoring changes in the RSS as is done in Section IV-C. Thus, the same source of information can be used to both locate nodes and track people.

In contrast to RSS-distance model based methods, time based methods using radio signals, such as ultra wide band radios, are less sensitive to the presence of obstacles and gives more accurate position estimates [36]. However, they require expensive circuitry to measure time. Additionally, ranging using time based methods requires dedicated time slots, which can be a limiting factor for tracking [37].

In order to effectively localize the nodes deployed in unknown positions, the MUSAS uses the robot as a mobile beacon. While the robot is exploring the environment, it is communicating with the nodes of the WSN. The robot position is known at all times, and therefore every RSS measurement can be associated to a unique beacon position. Each of the measurements can then be thought of as coming from a fixed beacon placed at the position of the robot at the measurement instant [38]. The advantage of a moving beacon with respect to a limited number of fixed beacons, is that the amount of measurements can be much larger and richer, which allow the localization algorithms to produce more accurate position estimates.

The performance of the localization algorithm depends strongly on the ability of the model to make good predictions of the RSS. In cluttered environments, the RSS can vary significantly, and thus the RSS is modeled as a random

variable. Perhaps the most used RSS-distance model is the log-normal model, which describes the RSS as a normally distributed variable with a mean, decaying proportionally to the logarithm of the distance and with a variance characterizing the variability of the observed RSS [39]. The decaying factor and the standard deviation are well known to depend strongly on the particular environment, and need thus to be estimated. However, the local inhomogeneity of the environment and the hardware differences among the nodes influence significantly the model parameters, which in turn have a strong negative effect on the localization accuracy [40]. Thus, instead of using one model for all the nodes, each node has its own model whose parameters are tuned specifically for that node and the environment.

Because the MUSAS is designed for ad hoc situations, it is not possible to assume the availability of models calibrated a priori or to calibrate the models before the operation. Therefore, algorithms that calibrate the model simultaneously as the node locations are being estimated are needed.

The problem of simultaneous node localization and model parameter estimation can be posed using ML or least-squares (LS) principles, leading in general to a nonlinear optimization problem. The problem can then be solved using any standard nonlinear optimization techniques, such as grid based or Newton-Raphson based. When using the log-normal model, the dependency on the model parameters is linear. Recognizing that the ultimate goal is position estimation, the model parameters can be seen as nuisance parameters, which can be eliminated using the principle of separable least squares [41]. Thus, the search space is reduced to the coordinates of the nodes.

Another conceptually simple approach for simultaneous localization and model calibration is a recursion consisting of 2 steps: starting from an initial guess on the model parameters, first estimate the positions of the nodes. Then, using the estimated positions, re-estimate the model parameters, and start the cycle again. This idea has been proposed in [42] using fixed beacons. In [38] the same principle is exploited using a robot as a mobile beacon to locate the nodes of a WSN in three different environments. With the system used in the MUSAS, a mode localization accuracy of 47 cm was achieved in a large uncluttered space and approximately 1 meter accuracy in a semi-open lobby and a typical office environment [38].

### B. TEAM LOCALIZATION SYSTEM

During operation, it is beneficial to know where own team members are located at any given time. This information can be used in operative planning and execution to increase effectiveness and direct the operation where necessary. For the MUSAS, a team localization system exploiting wearable sensors is developed to produce location information of own team members. In addition, the developed system also provides information about the physical state of the person who is wearing the sensor.

Localization of people has been studied extensively, and various different technologies have been proposed [43]–[47]. Commercially ready solutions for outdoor localization already exist such as GPS and GLONASS. On the contrary, indoor localization is more challenging since line-of-sight to GPS satellites is not available and readily available solutions fulfilling the MUSAS requirements do not exist. In most use-case scenarios of the MUSAS, the team operates both indoors and outdoors. Therefore, the proposed system is designed to have a set of complementary positioning technologies that enable localization in versatile urban environments.

The developed system is based on wearable wireless sensor nodes, which are installed on the clothing and equipment of the team members. Outdoors, the location estimates are provided by GPS. Indoors, the localization is carried out by exploiting either inertial navigation, radio based solutions or both simultaneously. Physical condition monitoring is


(a) (b)

**FIGURE 12.** **(a) The architecture of the team localization system. (b) Wearable sensor node installation on a soldier.**

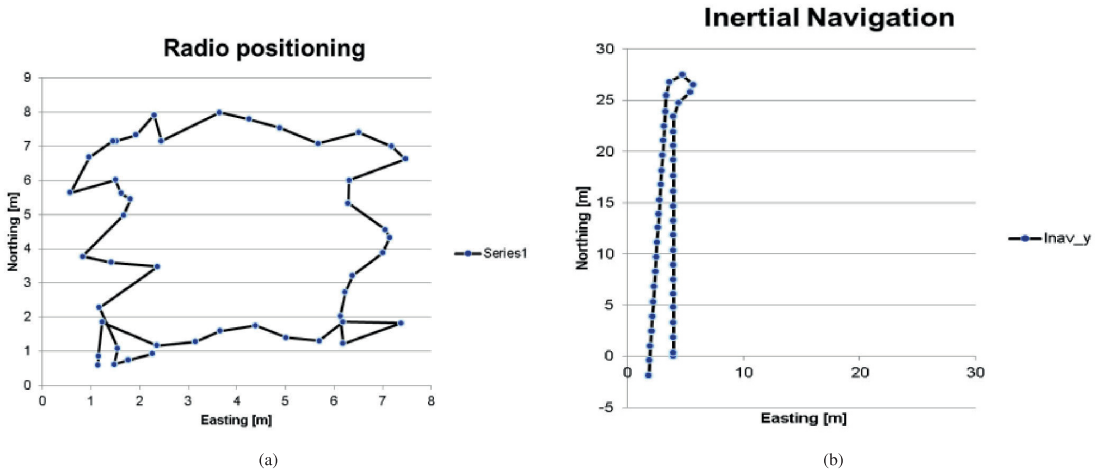


(a) (b)

**FIGURE 13.** **(a) Radio and (b) Inertial navigation in deployment environment.**

implemented by an inertial based activity recognition algorithm that is able to classify some common activities during operation such as: walking, standing, ascending or descending stairs. The algorithm provides the general intensity level of the current activity.

The team localization system, shown in Fig. 12(a), uses inertial navigation and radio based ranging for localization in indoor environments. Ranging is optional and utilized only if radio positioning base stations are deployed in the environment. Each wearable sensor node has an embedded microcontroller based computing unit for running the localization algorithms, radios for data transmission and ranging, and an IMU (Inertial Measurement Unit) with a 3D gyroscope, magnetometer and acceleration sensors for inertial navigation. The wearable sensors are installed on the back of the person as shown in Fig. 12(b), the antennas and IMU on the shoulders, and the acceleration sensors are placed on the right and left boots. Nanotron 2.4 GHz, IEEE 802.15.4a short range radios are used for radio based ranging and relative distance measurement between team members. Wireless communication with the MUSAS is performed using the RC232, 868 MHz RC1180HP long range radios. The wearable sensors are described in more detail in [48].

Inertial navigation of the system is based on estimating the step length using acceleration data gathered from the boots. This information is combined with heading information provided by the gyroscope and magnetometer. Radio based localization relies on time-of-flight (TOF) based distance measurements to fixed base stations, with known locations.

Both localization methods have been implemented separately in the proposed system. The accuracy of the radio-based localization system depends on the used positioning algorithm and the operating environment. Highest accuracy is achieved in unobstructed environments and in line-of-sight conditions. The accuracy decreases in cluttered environments where multipath propagation is common. Inertial navigation is bound to drift during operation and needs regular position and heading corrections. Radio based positioning does not drift, and in future developments, the inertial navigation drift will be compensated by data fusion algorithms taking benefit of GPS or radio based positioning estimates, when available.

Fig. 13 shows some test results gathered during the deployment. Using radio positioning, a test walking trip is done near the walls inside a room approximately $90m^2$. The radio positioning base stations are installed at the corners of the room. The radio based system is capable of localizing a person with an accuracy of 2 m. In the inertial navigation test, a back and forth route was done in a corridor. In the activity recognition test, a stair case was walked, first downstairs and returning back to the start position, as indicated in Fig. 14. The activity recognition algorithm classifies different types of activities. The current type of activity is indicated in color in the end user interface.

### C. DEVICE FREE LOCALIZATION

The MUSAS requires localizing targets in the operation area, rendering a need for utilizing a non-cooperative positioning technology that can operate in various ambient conditions. Device-free localization (DFL) is an emerging technology based on RSS measurements of a dense wireless network. DFL fulfills the target localization requirements of the MUSAS, since it is independent of ambient conditions such as lighting, temperature, humidity, etc., it can operate in

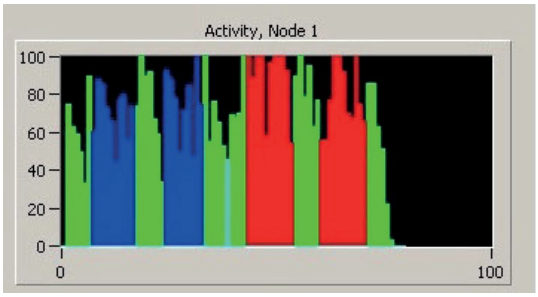


**FIGURE 14.** Activity recognition test results (green=level walk, blue=descending the stairs, red=ascending the stairs).

obstructed environments, and it can be used in through-wall scenarios. Most notably, this technology does not require that the targets to be localized carry any device.

DFL is based on the fact that wireless communication is affected by people [49], [50], which can be observed in RSS measurements of low-cost wireless devices [51]. Generally, a change in RSS is observed when the link line of two communicating nodes is blocked. Further, the presence of a person causes correlated changes in nearby links, enabling a collaborative localization effort. Since the radio is used for extracting localization information, these systems are referred to as radio frequency (RF) sensor networks [52].

One approach to RSS-based DFL is to estimate the changes in the propagation field of the monitored area, and then form an image of this field, a process referred to as radio tomographic imaging (RTI) [24], [25]. The formed image can then be used to infer the locations of people within the deployed wireless network as shown in Fig. 15(a). Use cases of the MUSAS, set strict demands on the used wireless sensor network and the RSS-based DFL system operation. In the following, these demands are addressed and the applied solutions introduced.

A network monitoring and management framework is essential to manage a WSN as argued by Tolle et. al. [53]. In addition, numerous works have shown that the communication conditions vary significantly over time [54], making network management mandatory to ensure functionality in the long-run. Network management serves two purposes in RSS-based DFL: first, the network can be configured easily, reducing the deployment time; second, it offers the possibility to adapt to changing communication conditions, for instance, the network can change the frequency channel of operation if needed. For these reasons, a network monitoring and management framework is designed and utilized for the purpose of the MUSAS [55].

Similarly, as in the case of the node localization system, the locations of the sensors and RSS-based DFL could be calculated simultaneously as proposed in [56]. However, the MUSAS, take advantage of the robot and the proposed solutions in Section IV-A for obtaining the node locations, and then performs DFL using the known positions of the nodes.

Most RSS-based DFL algorithms require that the RSS statistics are known when the link line is not obstructed by a person. In the current case, there is no possibility for empty-area calibration, thus the system must learn the RSS statistics while running and adapt to the changing environment. Several possibilities exist: first, methods that do not require calibration could be applied [57]; second, online algorithms capable of learning the RSS-statistics when the link is not affected by a person could be used [58], [59]; or third, methods for online calibration could be applied [60], [61]. The methods proposed in [61] are used in the MUSAS.

In an urban environment, it is not always possible to deploy sensors inside the same space where the targets are located. Therefore, through-wall localization capability is desired, which is enabled by the RF-based approach. Previous DFL attempts in through-wall scenarios have used variance-based RTI (VRTI) [57], [62]. However, VRTI is not able to localize a stationary target, since it is based on a windowed variance of the RSS. Kernel distance-based RTI (KRTI) has been demonstrated to localize both stationary and moving targets, even through walls of a building [63]. In the MUSAS, the algorithms presented in [64] are exploited, where a multi-scale spatial model and a novel measurement model are utilized. The results demonstrate high accuracy localization (0.3 m) in a through-wall environment as shown in Fig. 15(b).

It is often required to localize and track multiple targets. In [65]–[67], particle filters are used to track multiple targets simultaneously. However, these works assume that the number of targets is known a priori and that the target trajectories do not intersect. These systems struggle also in estimating the locations in real-time, because of the complexity of particle filters. The above drawbacks are addressed in [68], in which machine vision algorithms are adapted for the purpose of imaging-based DFL, and exploited in the MUSAS. The algorithms are able to estimate the number of people correctly 97% of the time. Furthermore, experiments demonstrate that the system is capable of tracking up to four targets with intersecting trajectories with an average error of 0.55 m or lower in a cluttered indoor office.

## V. TEST DEPLOYMENT IN AN URBAN HOSTAGE SITUATION

The implemented MUSAS system was tested, demonstrated and evaluated in an urban military training facility at Santahamina, Finland, in November 2012 as described in this section. The experiment was conducted in a testing yard, consisting of a plywood maze for training troops in urban area warfare. A platoon of soldiers, specialized in urban area warfare, served as a field team and as hostile forces, targets. The evaluation case was a hostage situation, where hostile forces and hostages resided in an unknown indoor environment.

In this event, the system formed a COP using a mobile robot, the device-free localization system, and the wearable sensor nodes. The network was built and localized automat-

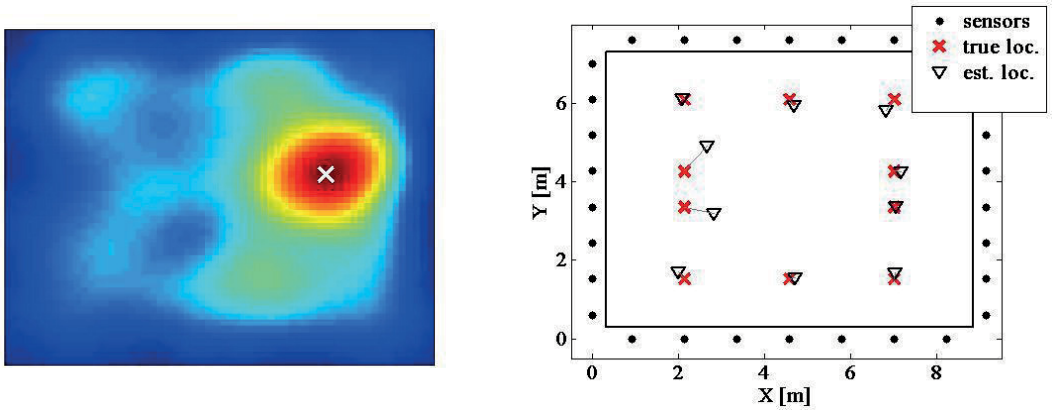


**FIGURE 15.** **(a) The estimated RF propagation field image. The estimated distribution coincides with the true location of the person (white cross). (b) The position estimates obtained with RSS-based DFL in a through-wall scenario.**

ically as the troops advanced inside the building. During the test a WLAN infrastructure network of approximately 300 × 600 meters was achieved, including the interior of the building, by using only four access points. The soldiers were able to carry the hand-held devices and expand the WLAN network when needed. The robot used two different 3G connections for the remote operator, to ensure connection during the operation. 20 IEEE 802.15.4 sensor nodes where used for DFL. The robot deployed 5 nodes inside the building during the demonstration. Three team localization beacon nodes were used to localize the field team.

The indoor environment map was built online as the robot mapped the building. The MUSAS produced real-time results and delivered information to the field team, including the map, the locations of individual solders and other localized objects and relevant information. In the COP model, rooms were colored red if hostile elements were in a room. After the space was cleared out of danger, the color was changed to green.

Attaching the mobile devices to the soldier's equipment and using it during action were evaluated. Two options were studied: attachment to the left hand (for a right-handed user) and to the upper left torso, using a specific pouch. The first impression was that the hand attachment was better, but the torso attachment proved more reliable. The device is vulnerable when used in the hand, consuming more of the user's attention and also possibly preventing other activities during battle. The torso attachment is slightly more difficult to reach, but, on the other hand, the device is well protected and unobtrusive. After some training, the soldiers got used to carrying and using the device attached to the torso. Later, the mobile device will probably be developed to fit to this attachment more effectively. The soldiers also used glows, specially designed for tactical use with touch screen capability.

During the tests it was recognized that it is inconvenient for the soldier to operate the hand-held device displaying the COP when in action. For this reason, the device was only used for supporting situation awareness, not for active use, such as marking discovered objects to the COP model. During the tests, a short movie was shot [69], which explains the operational concept of the MUSAS. The users gave good feedback about the usability of the mobile devices and also on the speed of the system. In further test the system can be used to evaluate the use of a common operational picture for situation awareness in critical tasks and operations.

## VI. CONCLUSIONS

The presented framework provides a novel and scalable solution for creating, hosting and delivering a common operational picture in a multisensory environment focused on localization and position based information in an urban environment. The proposed system is demonstrated by the implemented MUSAS and tested in a realistic urban environment in a military hostage situation.

Compared to other similar systems, the MUSAS focuses on multiple localization services and localized information presentation. The system can be deployed in search-and-rescue and earthquake disaster situations to map the environment and localize people. It has also applications in police hostage situation, indoor fire-fighting scenarios and military operations.

The next step in research is to use a distributed server architecture [70] and distributed computation, to increase modularity and robustness of the overall system. The MUSAS has the architectural solutions which enable distribution of vital services throughout the network and subsystems. Future plans for development include also the implementation of a 3D environment model for localization, as well as improved views for the Android devices.

## REFERENCES


[1] M. D. McNeese, M. S. Pfaff, E. S. Connors, J. F. Obieta, I. S. Terrell, and M. A. Friedenberg, "Multiple vantage points of the common operational picture: Supporting international teamwork," in *Proc. 50th Annu. Meeting Human Factors Ergonom. Soc.*, 2006, pp. 467–471.

[2] R. Virrankoski, "Wireless sensor systems in indoor situation modeling II (WISM II)," Dept. Comput. Sci., Univ. Vaasa, Vaasa, Finland, Tech. Rep. 188, 2013.

[3] M. R. Endsley, "Toward a theory of situation awareness in dynamic systems," *J. Human Factors Ergonom. Soc.*, vol. 37, no. 1, pp. 32–64, 1995.

[4] R. S. Hager, "Current and future efforts to vary the level of detail for the common operational picture," Naval Postgraduate School, Monterey, CA, USA, 1997.

[5] A. Deschamps, D. Greenlee, T. J. Pultz, and R. Saper, "Geospatial data integration for applications in flood prediction and management in the Red River Basin," in *Proc. Geosci. Remote Sens. Symp.*, vol. 6. Jan. 2002, pp. 3338–3340.

[6] U. G. P. Office, *Joint Vision 2020*. Washington, DC, USA: Government Printing Office, 2001.

[7] (2012). *Programmes at a Glance* [Online]. Available: http://www.soldiermod.com/volume-10/pdfs/articles/programmes-overview-may-2013.pdf

[8] A. Taylor, *Future Soldier 2030 Initiative*. New York, NY, USA: US Army RDECOMM, 2009.

[9] R. Dietterle, "The future combat systems (FCS) overview," in *Proc. Military Commun. Conf.*, vol. 5. Oct. 2005, pp. 17–20.

[10] R. Balfour, "Next generation emergency management common operating picture software/systems (COPSS)," in *Proc. LISAT*, May 2012, pp. 1–4.

[11] L. J. Williams, "Small unit operations situation awareness system (SUO SAS): An overview," in *Proc. Military Commun. Conf.*, vol. 1. Oct. 2003, pp. 13–16.

[12] V. Kaul, C. Makaya, S. Das, D. Shur, and S. Samtani, "On the adaptation of commercial smartphones to tactical environments," in *Proc. Military Commun. Conf.*, Nov. 2011, pp. 7–10.

[13] N. Suri, L. Pochet, J. Sterling, R. Kohler, E. Casini, J. Kovach, *et al.*, "Middleware, and applications for portable cellular devices in tactical edge networks," in *Proc. Military Commun. Conf.*, Nov. 2011, pp. 7–10.

[14] S. M. George, W. Z. C. H. Myounggyu Won, Y. O. L. A. Pazarloglou, R. Stoleru, and P. Barooah "Distressnet: A wireless ad hoc and sensor network architecture for situation management in disaster response," *IEEE Commun. Mag.*, vol. 48, no. 3, pp. 128–136, Mar. 2010.

[15] T. He, S. Krishnamurthy, L. Luo, T. Yan, L. Gu, R. Stoleru, *et al.*, "Vigilnet: An integrated sensor network system for energy-efficient surveillance," *ACM Trans. Sensor Netw.*, vol. 2, pp. 1–38, Feb. 2006.

[16] S. M. Diamond and M. G. Ceruti, "Application of wireless sensor network to military information integration," in *Proc. 5th IEEE Int. Conf. Ind. Informat.*, vol. 1. Jun. 2007, pp. 317–322.

[17] N. Michael, S. Shen, K. Mohta, Y. Mulgaonkar, V. Kumar, K. Nagatani, *et al.*, "Collaborative mapping of an earthquake-damaged building via ground and aerial robots," *J. Field Robot.*, vol. 29, no. 5, pp. 832–841, Sep./Oct. 2012.

[18] F. Driewer, H. Baier, K. Schilling, J. Pavlicek, L. Preucil, N. Ruangpayoongsak, *et al.*, "Hybrid telematic teams for search and rescue operations," in *Proc. IEEE Int. Workshop Safety, Security, Rescue Robot.*, May 2004, pp. 2–4.

[19] M. Kulich, J. Kout, L. Preucil, R. Mazl, J. Chudoba, J. Saarinen, *et al.*, "PeLoTe—A heterogeneous telematic system for cooperative search and rescue missions," in *Proc. IEEE/RSJ IROS*, Sep. 2004, pp. 1–8.

[20] J. Saarinen, S. Heikkila, M. Elomaa, J. Suomela, and A. Halme, "Rescue personnel localization system," in *Proc. IEEE Int. Workshop Safety, Security Rescue Robot.*, Jun. 2005, pp. 218–223.

[21] N. Ruangpayoongsak, H. Roth, and J. Chudoba, "Mobile robots for search and rescue," in *Proc. IEEE Int. Workshop Safety, Security Rescue Robot.*, Jan. 2005, pp. 212–217.

[22] J. Lee, "Enabling network management using Java technologies," *IEEE Commun. Mag.*, vol. 38, no. 1, pp. 116–123, Jan. 2000.

[23] M. Henning, "A new approach to object-oriented middleware," *IEEE Internet Comput.*, vol. 8, no. 1, pp. 66–75, Feb. 2004.

[24] N. Patwari and P. Agrawal, "Effects of correlated shadowing: Connectivity, localization, and RF tomography," in *Proc. Int. Conf. IPSN*, 2008, pp. 82–93.

[25] J. Wilson and N. Patwari, "Radio tomographic imaging with wireless networks," *IEEE Trans. Mobile Comput.*, vol. 9, no. 5, pp. 621–632, May 2010.

[26] M. Matusiak, J. Paanajärvi, P. Appelqvist, M. Elomaa, M. Ylikorpi, and A. Halme, "A novel marsupial robot society: Towards long-term autonomy," in *Proc. 9th Int. Symp. DARS*, Nov. 2008, pp. 523–532.

[27] J. Saarinen, A. Maula, R. Nissinen, H. Kukkonen, J. Suomela, and A. Halme, "GIMnet—Infrastructure for distributed control of generic intelligent machines," *Provider (Server)*, vol. 586, no. 29, pp. 525–530, 2007.

[28] A. Maula, M. Myrsky, and J. Saarinen, "GIMnet 2.0-enhanced communication framework for distributed control of generic intelligent machines," in *Proc. 1st IFAC Conf. Embedded Syst., Comput. Intell. Telemat. Control*, 2012, pp. 62–67.

[29] M. Myrsky, A. Maula, J. Saarinen, and I. Kankkunen, "Teleoperation tests for large-scale indoor information acquisition," in *Proc. Comput. Intell. Telemat. Control Embedded Syst.*, vol. 1. 2012, pp. 13–18.

[30] M. W. M. G. Dissanayake, P. Newman, S. Clark, H. Durrant-Whyte, and M. Csorba, "A solution to the simultaneous localization and map building (SLAM) problem," *IEEE Trans. Robot. Autom.*, vol. 17, no. 3, pp. 229–241, Jun. 2001.

[31] H. Durrant-Whyte and T. Bailey, "Simultaneous localization and mapping: Part I," *IEEE Robot. Autom. Mag.*, vol. 13, no. 2, pp. 99–110, Jun. 2006.

[32] T. Bailey and H. Durrant-Whyte, "Simultaneous localization and mapping (SLAM): Part II," *IEEE Robot. Autom. Mag.*, vol. 13, no. 3, pp. 108–117, Sep. 2006.

[33] H. P. Moravec, "Sensor fusion in certainty grids for mobile robots," *AI Mag.*, vol. 9, no. 2, pp. 61–74, 1988.

[34] J. Saarinen, J. Paanajärvi, and P. Forsman, "Best-first branch and bound search method for map based localization," in *Proc. IEEE/RJS Int. Conf. Intell. Robot. Syst.*, Sep. 2011, pp. 59–64.

[35] F. Seco, A. R. Jimenez, C. Prieto, J. Roa, and K. Koutsou, "A survey of mathematical methods for indoor localization," in *Proc. IEEE Int. Symp. Intell. Signal Process. WISP*, Aug. 2009, pp. 9–14.

[36] N. Patwari, A. O. Hero, M. Perkins, N. S. Correal, and R. J. O'Dea, "Relative location estimation in wireless sensor networks," *IEEE Trans. Signal Process.*, vol. 51, no. 8, pp. 2137–2148, Aug. 2003.

[37] G. E. Garcia, L. Muppirisetty, and H. Wymeersch, "On the trade-off between accuracy and delay in cooperative UWB navigation," in *Proc. IEEE WCNC*, Apr. 2013, pp. 1603–1608.

[38] J. Vallet, O. Kaltiokallio, M. Myrsky, J. Saarinen, and M. Bocca, "Simultaneous RSS-based localization and model calibration in wireless networks with a mobile robot," *Proc. Comput. Sci.*, vol. 10, pp. 1106–1113, Aug. 2012.

[39] S. Seidel and T. Rappaport, "914 MHz path loss prediction models for indoor wireless communications in multifloored buildings," *IEEE Trans. Antennas Propag.*, vol. 40, no. 2, pp. 207–217, Feb. 1992.

[40] J. Vallet, O. Kaltiokallio, J. Saarinen, M. Myrsky, and M. Bocca, "On the sensitivity of RSS based localization using the log-normal model: An empirical study," in *Proc. 10th WPNC*, 2013, pp. 1–6.

[41] F. Gustafsson and F. Gunnarsson, "Localization in sensor networks based on log range observations," in *Proc. 10th Int. Conf. Inf. Fusion*, Jul. 2007, pp. 1–8.

[42] R. Zemek, D. Anzai, S. Hara, K. Yanagihara, and K.-I. Kitayama, "RSSI-based localization without a prior knowledge of channel model parameters," *Int. J. Wireless Inf. Netw.*, vol. 15, nos. 3–4, pp. 128–136, 2008.

[43] A. Amanatiadis, D. Chrysostomou, D. Koulouriotis, and A. Gasteratos, "A fuzzy multi-sensor architecture for indoor navigation," in *Proc. IEEE Int. Workshop IST*, Jul. 2010, pp. 452–457.

[44] H. Muller, C. Randell, and A. Moss, "A 10 mW wearable positioning system," in *Proc. 10th IEEE ISWC*, Oct. 2010, pp. 47–50.

[45] S. Holm, "Hybrid ultrasound–RFID indoor positioning: Combining the best of both worlds," in *Proc. IEEE Int. Conf. RFID*, Apr. 2009, pp. 155–162.

[46] R. Tenmoku, M. Kanbara, and N. Yokoya, "A wearable augmented reality system for navigation using positioning infrastructures and a pedometer," in *Proc. 2nd IEEE/ACM ISMAR*, Oct. 2003, pp. 344–345.

[47] S. Lee, B. Kim, H. Kim, R. Ha, and H. Cha, "Inertial sensor-based indoor pedestrian localization with minimum 802.15.4a configuration," *IEEE Trans. Ind. Informat.*, vol. 7, no. 3, pp. 455–466, Aug. 2011.

[48] M. Korkalainen, P. Tukeva, M. Lindholm, and J. Kaartinen, "Hybrid localization system for situation awareness applications," in *Proc. 3rd WOWCA*, Apr. 2012.
[49] H. Hashemi, "The indoor radio propagation channel," *Proc. IEEE*, vol. 81, no. 7, pp. 943–968, Jul. 1993.
[50] H. Hashemi, "A study of temporal and spatial variations of the indoor radio propagation channel," in *Proc. 5th IEEE Int. Symp. Pers., Indoor Mobile Radio Commun., Wireless Netw., Catch. Mobile Future*, vol. 1. Sep. 1994, pp. 127–134.
[51] K. Woyach, D. Puccinelli, and M. Haenggi, "Sensorless sensing in wireless networks: Implementation and measurements," in *Proc. 4th Int. Symp. Model. Optim. Mobile, Ad Hoc Wireless Netw.*, 2006, pp. 1–8.
[52] N. Patwari and J. Wilson, "RF sensor networks for device-free localization: Measurements, models, and algorithms," *Proc. IEEE*, vol. 98, no. 11, pp. 1961–1973, Nov. 2010.
[53] G. Tolle and D. Culler, "Design of an application-cooperative management system for wireless sensor networks," in *Proc. 2nd Eur. Workshop Wireless Sensor Netw.*, 2005, pp. 121–132.
[54] A. Cerpa, J. Wong, L. Kuang, M. Potkonjak, and D. Estrin, "Statistical model of lossy links in wireless sensor networks," in *Proc. 4th Int. Symp. Inf. Process. Sensor Netw.*, 2005, pp. 81–88.
[55] H. Yigitler, O. Kaltiokallio, and R. Jäntti, "A management framework for device-free localization," in *Proc. IEEE IJCNN*, Aug. 2013.
[56] X. Chen, A. Edelstein, Y. Li, M. Coates, M. Rabbat, and A. Men, "Sequential Monte Carlo for simultaneous passive device-free tracking and sensor localization using received signal strength measurements," in *Proc. 10th Int. Conf. IPSN*, 2011, pp. 342–353.
[57] J. Wilson and N. Patwari, "See-through walls: Motion tracking using variance-based radio tomography networks," *IEEE Trans. Mobile Comput.*, vol. 10, no. 5, pp. 612–621, May 2011.
[58] Y. Zheng and A. Men, "Through-wall tracking with radio tomography networks using foreground detection," in *Proc. IEEE WCNC*, Apr. 2012, pp. 3278–3283.
[59] A. Edelstein and M. Rabbat, "Background subtraction for online calibration of baseline RSS in RF sensing networks," *IEEE Trans. Mobile Comput.*, vol. 99, p. 1, 2012, doi: http://doi.ieeecomputersociety.org/10.1109/TMC.2012.206
[60] O. Kaltiokallio, M. Bocca, and N. Patwari, "Follow @grandma: Long-term device-free localization for residential monitoring," in *Proc. IEEE 37th Conf. LCN Workshops*, Oct. 2012, pp. 991–998.
[61] M. Bocca, O. Kaltiokallio, and N. Patwari, "Radio tomographic imaging for ambient assisted living," in *Evaluating AAL Systems Through Competitive Benchmarking* (Communications in Computer and Information Science), vol. 362, S. Chessa and S. Knauth, Eds. Berlin Heidelberg, Germany: Springer-Verlag, 2013, pp. 108–130.
[62] Y. Zhao and N. Patwari, "Noise reduction for variance-based device-free localization and tracking," in *Proc. 8th Annu. IEEE Commun. Soc. Conf. SECON*, Jun. 2011, pp. 179–187.
[63] Y. Zhao, N. Patwari, J. M. Phillips, and S. Venkatasubramanian, "Radio tomographic imaging and tracking of stationary and moving people via kernel distance," in *Proc. 12th Int. Conf. Inf. Process. Sensor Netw.*, 2013, pp. 229–240.
[64] O. Kaltiokallio, M. Bocca, and N. Patwari. (2013, Feb.). *A Multi-Scale Spatial Model for RSS-based Device-Free Localization* [Online]. Available: http://arxiv.org/abs/1302.5914
[65] J. Wilson and N. Patwari, "A fade-level skew-laplace signal strength model for device-free localization with wireless networks," *IEEE Trans. Mobile Comput.*, vol. 11, no. 6, pp. 947–958, Jun. 2012.
[66] F. Thouin, S. Nannuru, and M. Coates, "Multi-target tracking for measurement models with additive contributions," in *Proc. 14th Int. Conf. Inf. Fusion*, 2011, pp. 1–8.
[67] S. Nannuru, Y. Li, M. Coates, and B. Yang, "Multi-target device-free tracking using radio frequency tomography," in *Proc. 7th Int. Conf. ISSNIP*, 2011, pp. 508–513.
[68] M. Bocca, O. Kaltiokallio, N. Patwari, and S. Venkatasubramanian, "Multiple target tracking with RF sensor networks," *IEEE Trans. Mobile Comput.*, vol. PP, no. 99, p. 1, 2013, doi: 10.1109/TMC.2013.92.
[69] (2013, Apr.). *Finnish Combat Camera Team* [Online]. Available: http://www.youtube.com/watch?v=9v1fFIHRWGE
[70] J. Timonen, "Distributed information system for tactical network," in *Proc. 3rd Workshop Wireless Commun. Appl.*, Vaasa, Finland, Apr. 2012.

**MIKAEL BJÖRKBOM** received the M.Sc. degree with distinction in control engineering from the Helsinki University of Technology, Finland, in 2006, and the Doctoral degree from Aalto University, Finland, in 2010. He continues as a postdoctoral researcher and the research coordinator for the Wireless Sensor Systems Group, Aalto University, which consists of about 15 researchers. His main research interests include wireless process control, adaptive control, and simulation of wireless control systems.

**JUSSI TIMONEN** is a Ph.D. Student and Researcher with the Finnish National Defence University, Department of Military Technology. His main research areas are information fusion and visualization of common operational picture. The main fields of research are urban area warfare and cyber warfare.

**HÜSEYIN YIĞITLER** received the B.Sc. and M.Sc. degrees in electrical engineering from Middle East Technical University, Ankara, Turkey, in 2004 and 2006, respectively. He has been pursuing the Ph.D. degree with the Department of Communications and Networking, Aalto University School of Electrical Engineering, since 2011. His current research interests include real-world wireless sensor network development and deployments, wireless automation, network management, and indoor localization technologies.

**OSSI KALTIOKALLIO** received the B.Sc. and M.Sc. degrees in electrical engineering from Aalto University, School of Electrical Engineering, Helsinki, Finland, in 2011. He is currently pursuing the Ph.D. degree with the Department of Communications and Networking, Aalto University School of Electrical Engineering. He is a member of the Wireless Sensor Systems Group, Aalto University. His current research interests include indoor propagation channel, real-world wireless sensor network deployments, signal processing, and indoor localization and tracking technologies.

**JOSÉ M. VALLET GARCÍA** received the M.Sc. degree with distinction in automation and electronics from the Carlos III University of Madrid, Spain, in 2002. He is a Researcher and Ph.D. candidate at Aalto University. His main research areas are home automation, fuel cell automation, and localization systems in WSN.

**MATTHIEU MYRSKY** received the M.Sc. degree in automation technology from Aalto University in 2010. He continued as a Ph.D. student with the Finnish Centre of Excellence, Generic Intelligent Machines Research Group, Department of Automation and Systems Technology, Aalto University. His main research interests include machine abstraction, multi-machine systems, path planning, and system integration.

**JARI SAARINEN** received the M.Sc. and Ph.D. degrees in automation technology from the Helsinki University of Technology in 2002 and 2009, respectively. He has acted as a Senior Researcher with the Center of Excellence in Generic Intelligent Machines, Aalto University, Finland, and as a Researcher with the Centre for Applied Autonomous Sensor Systems, Örebro University, Sweden. His research interests include long-term autonomy, 3-D perception, localization, and mapping.

**MARKO KORKALAINEN** received the M.Sc. degree in electrical engineering from the University of Oulu in 2003. Since 2004, he has been with Industrial M2M Systems, VTT, as a Research Scientist. His research interests include wireless sensor network technologies and embedded sensor systems.

**CANER ÇUHAC** was born in Tekirdağ, Turkey, in 1986. He received the B.E. degree in electronics and communication engineering from Yildiz Technical University, Istanbul, Turkey, in 2008, and the M.Sc. degree in telecommunication engineering from the University of Vaasa, Finland, in 2011.

He joined the Department of Computer Science, University of Vaasa, in 2010, as a Research Assistant, and he became a Researcher in 2011. His current research interests include wireless embedded systems, image processing, and automation.

**RIKU JÄNTTI** (M'02–SM'07) is an Associate Professor (tenured) of communications engineering and the Head of the Department of Communications and Networking, Aalto University School of Electrical Engineering, Finland. He received the M.Sc. degree (with distinction) in electrical engineering and the D.Sc. degree (with distinction) in automation and systems technology from the Helsinki University of Technology (TKK) in 1997 and 2001, respectively. Prior to joining Aalto (formerly known as TKK) in 2006, he was a Professor Pro Tem at the Department of Computer Science, University of Vaasa. He is an Associate Editor of the IEEE Transactions on Vehicular Technology. His research interests include radio resource control, spectrum management, and performance optimization of wireless communication systems.

**REINO VIRRANKOSKI** is a Senior Researcher with the University of Vaasa, Finland. After graduating from the University of Helsinki in 2000, he was a Researcher with the Helsinki University of Technology (now Aalto University) from 2000 to 2007, as a Visiting Assistant Researcher with Yale University from 2004 to 2005 as a Lecturer of telecommunications with the University of Vaasa from 2007 to 2010, and has been a Senior Researcher with the University of Vaasa since 2010. His research interests cover communication and control in wireless networks, wireless automation, and wireless networks in defense and security.

**JOUKO VANKKA** received the M.S. and Ph.D. degrees in electrical engineering from the Helsinki University of Technology in 1991 and 2000, respectively, and the bachelor's degree in social sciences from Helsinki University in 1994. He was a Researcher at the Helsinki University of Technology from 1994 to 2005. Since 2005, he has been with the Finnish Defence Forces. He has been a Professor of military technology with National Defence University since 2012.

His current research interests include cyber warfare, satellite communications, and situation awareness. He is the author or co-author 90 technical papers in the area of software radio and communication systems. He is the author of *Direct Digital Synthesizers: Theory, Design and Applications* (Kluwer Academic Publishers, 2001), *Digital Synthesizers and Transmitters for Software Radio* (Springer-Verlag New York, 2005), *Tactical Networks* (Finnish, 2009), and *Cyber Warfare* (Editor, 2013).

**HEIKKI N. KOIVO** (S'67–M'71–SM'86) received the B.S.E.E. degree from Purdue University, West Lafayette, IN, USA, and the M.S. degree in electrical engineering and the Ph.D. degree in control sciences from the University of Minnesota, Minneapolis. He is an Emeritus Professor at Aalto University, formerly Helsinki University of Technology (HUT), Espoo, Finland. Before joining HUT in 1995, he served in various professorial positions at the University of Toronto, Toronto, ON, Canada, and Tampere University of Technology, Tampere, Finland. His research interests include study of complex systems, adaptive and learning control, mechatronics, microsystems, and cyber-physical systems. He has authored or co-authored over 400 scientific publications. He has been the principal investigator in more than 100 research projects. He is a member of the Editorial Boards of the *Journal of Intelligent and Fuzzy Systems* and the *Journal of Intelligent Automation and Soft Computing*.

He was an Associate Editor of the IEEE Transactions on Robotics and Automation and a member of the Administrative Council of the IEEE Robotics and Automation Society. He is a fellow of the Finnish Academy of Technology.

# Feasibility Study on Solar Energy Harvesting from Asphalt Surface in Cold Climate Region

Caner Çuhac[a], Anne Mäkiranta[a,*], Petri Välisuo[a], Erkki Hiltunen[a], Mohammed Elmusrati[a]

[a]*School of Technology and Innovations, University of Vaasa, P.O. Box 700, FI-65101 Vaasa, Finland*

**Abstract**

Solar heat, already captured by vast asphalt fields in urban areas, provides a large potential energy source. Solar irradiation, vertical soil temperature profile, and heat flow measurements reveal how efficiently the irradiation was absorbed, where the heat is accumulated, and how large a proportion of the energy is radiated back to the atmosphere during the night. In this study, those variables were studied by long term measurements in an open-air platform. To compensate for night time heat loss the soil-accumulated heat could be harvested during the sunny daytime periods and delivered to deeper layers beneath the surface for seasonal storage. A cumulative heat flow over one year, from asphalt to the ground was 70% of the cumulative irradiance measured during the same period. However, due to the night time heat losses, the net heat flow during 5 days period was only 18% of the irradiance in spring and negative during autumn, when the soil is cooling. Certain adaptive heat transfer and storage mechanisms could be used to minimize the loss and turn the asphalt layer to an efficient solar heat collector connected with a seasonal storage system.

*Keywords:* asphalt solar collector, solar energy harvesting, heat flux, distributed temperature sensing, renewable energy, soil temperature profile

## 1. Introduction

Today‘s society is obliged to search for new low carbon energy sources to fight against global climate change. In cold-climate regions, fossil fuels are often used for producing the heat needed. Solar energy, which is one of the most important inexhaustible sustainable energy sources, can be

*Corresponding author

*Email addresses:* caner.cuhac@univaasa.fi (Caner Çuhac), anne.makiranta@univaasa.fi (Anne Mäkiranta), petri.valisuo@univaasa.fi (Petri Välisuo), erkki.hiltunen@univaasa.fi (Erkki Hiltunen), mohammed.elmusrati@univaasa.fi (Mohammed Elmusrati)

harvested using heat collectors or solar panels. Solar heat is renewable and therefore can potentially reduce dependency on fossil fuels, but solar radiation is most easily received during the summer when the need for heat is minimal. In addition, after sunset, the high surface temperatures degrade exponentially with a time constant of a few hours due to the heat flowing back into the atmosphere. The accumulation of the daily gains or losses in terms of solar energy leads to small temperature increases in the deeper layers of the soil, creating long-term warming or cooling of the soil [1, 2]. A diurnal and/or seasonal storage is necessary for a solar heating system in cold climate region.

The simple systems are operating without heat pumps, only solar collectors and panels are connected with seasonal heat storage [3]. Solar heat collectors, together with heat pumps and seasonal heat storage systems, are frequently used in heating real estate, industrial buildings, and greenhouses [4, 5]. Drake Landing Solar Community in Canada has experience in the harvesting and storing of solar energy [6]. In Drake Landing, 52 detached houses are heated using 2293 $m^2$ of flat plate solar collectors. The storage area used for seasonal storage consisted of 144 boreholes, each being the depth of 35 m. The temperature of the Borehole Thermal Energy Storage system (BTES) reached above 65°C in summer after three years of operation, and the temperature dropped nearly 40°C during the winter [7, 8]. Experimental measurements and a Comsol simulation model of heat energy from solar collectors injected in the ground heat storage was studied also by Haq and Hiltunen [9]. The theories and models used by Haq and Hiltunen can be used to optimize the parameters of the asphalt heat collection and seasonal storage system. In addition to collect heat from the hot asphalt layers, the possibilities of using the temperature differences for electricity production, are studied by Kisgyörgy *et al.* [10] and Datta et al. [11]. The temperature differences in the ground and the efficiency of the thermoelectric devices are low, and therefore the power produced is rather modest, but for example for communication devices it can be high enough.

The flat plate solar heat collectors form a considerable amount of the costs of the solar heating system. Urban structures, such as asphalt layers, pavements and buildings, can effectively collect and store solar heating, participating in the formation of the urban heat island (UHI) effect [12, 13, 14]. Asphalt pavements equipped with liquid heat transfer mechanism, so-called hydronic asphalt pavements (HAP), can be used for harvesting solar energy, in addition to conventional solar collectors. By collecting excessive heat from asphalt pavements in summer to BTES, the HAP systems can also mitigate the UHI effect [15]. The focus of this research is to find out if asphalt layers, abundant in urban areas, could replace flat plate heat collectors to reduce the costs

of solar heating systems. Previous research on asphalt heat collection is also reviewed by Bobes-Jesus *et al.* in [16]. According to the review, asphalt heat collectors may be competitive, because they are cheaper than conventional solar heat collectors and the area occupied by the collectors can be used also for other purposes. The review concludes that more research is needed in larger samples in realistic weather conditions since existing research is often performed in laboratory conditions and small areas. Some temperature-profile measurements indicate that soil temperatures can be above 30°C in the surface layer and up to 1 m deep in latitudes near 40-51°N. Pavement heating systems were tested in an experimental study in Tianjin, China [17], where the heat absorbtivity of the pavement was 37% and the total storage effectiveness was 17%. The researchers observed that the maximum temperature of the pavement was below 60°C on the surface and about 47°C at 10 cm depth. These temperatures are lower than those from actual solar collectors, so heat pumps may be needed to efficiently utilize the heat resources.

The laboratory experiments carried out before this study indicated that dark asphalt is efficient in absorbing solar irradiance and conducting heat to the soil [18]. In this research, the thermal behavior of commonly used asphalt paved soil structures, e.g. parking space is studied in high latitudes above 63°N, which is much farther North than the previous research projects and simulations cited above. The measurement field was planned and implemented in order to benchmark the heat flow and the absorptivity of the asphalt layer at different depths without heat collectors.

## 2. Materials and Methods

The measurements were obtained by three main sources: 1) a pyranometer, 2) a heat flux plate, and 3) a Distributed Temperature Sensing (DTS) system. Combining these three independent methods makes the results more reliable and trustworthy.

### *2.1. Pyranometer measurements*

In this research solar irradiance is measured by using a Hukseflux LP02-TR (Hukseflux Inc, the Netherlands) pyranometer, and those values were sampled using a DataTaker - data logger (Thermo Fisher Scientific Australia Pty Ltd) in 10 second time intervals. The data was logged with a timestamp and stored for analysis. The calibration uncertainty of the pyranometer is less than 1.8%.

*2.2. Heat Flux Measurements on the Asphalt Surface*

The heat flux data was collected using a Hukseflux heat flux plate HFP01-15 (Hukseflux Inc, the Netherlands) buried 5 cm below the asphalt surface. This sensor plate generates a small analog output voltage proportional to the net heat flux passing through it. The heat flux towards the ground is interpreted as positive and the heat flow from the ground to the surface is interpreted as negative. The aim of taking the heat flux measurements was to quantify the net energy from solar radiation absorbed by the asphalt during the day and the amount of heat released back to the atmosphere during the night. These energy flows depend on multiple factors, such as irradiance, air temperature, weather, and current soil temperature [19]. The uncertainty of calibration is ±3%.

A data collection system was developed for reading, transferring, and storing the ground heat flux plate data. This system consisted of an analog-to-digital converter (ADC) and a wireless sensor platform, a wireless gateway, and an embedded PC. The analog voltage provided by the sensor was digitized by an ADC and the wireless sensor platform sampled the value every 10 seconds and sent the value to the wireless gateway platform located inside the building. The wireless gateway was connected to the embedded PC, which stores the data on the hard drive. During the data collection period the measurement devices faced cold temperatures as low as −30 °C and continued operating.


Figure 1: Installation of heat flux plate "Hukseflux".

The collected data was analyzed using the mathematical computing software MATLAB (The MathWorks Inc, Massachusetts, USA) to extract information about the net flux of the heat depend-

Figure 2: Heat flux data collection site.

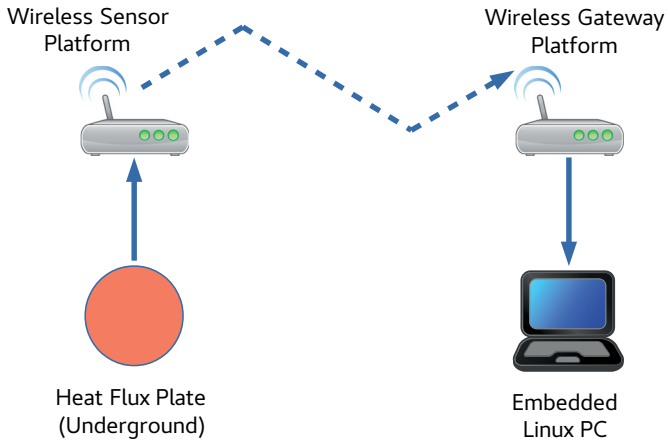


Figure 3: Network structure for heat flux sensor data collection.

ing on the meteorological conditions of the season and the time of day. Statistical computations were used to make estimations of future heat transfers.

*2.3. Underground Temperature Measurements*

The Distributed Temperature Sensing (DTS) method is used to measure the temperatures in soil layers under the asphalt pavement. This method is based on optical light scattering in fiber [20]. Short pulses of laser light are sent to the optical fiber by the DTS measurement device. Part of the incident light pulse is scattered by elastic–or Raman–scattering while it moves along the core of the fiber. The properties of the scattered light are acquired by the DTS measurement device, which then estimates the temperature based on the temperature dependent part of elastic scattering [21, 22]. An optical fiber, therefore, can be used as a linear sensor, observing the temperatures along the fiber even with 1 m spatial resolution.

A measurement fiber was installed under the asphalt in order to measure soil temperatures from the depth of 50 cm down to 10 m at the same time. Temperatures under the asphalt layer were acquired by a DTS device (Oryx DTS, Sensornet Ltd, Hertfordshire, UK) once or twice per month, depending on the season. These measurements were made on site using special instruments in addition to the meteorological data. The accuracy of the DTS device is +/- 0.5 °C.

The structure of an asphalt-paved parking lot is shown in Figure 4. The thickness of the asphalt layer is between 7–10 cm, the gravel and sand layer is about 60 cm, and the clay layer lies beneath those.

## 3. Calculation

The pyranometer and the heat flux plate data were used for estimating the absorption efficiency of the asphalt layer. Changes in the underground temperatures were acquired using the DTS measurement method, and they are relational to the integral sum of the net heat flows.

*3.1. Analyzing Pyranometer and Heat Flux Data*

As an example of daily data analysis, Figure 5 represents the measured solar irradiance and heat flux data on the 23rd of April.

The solar irradiance measured by the pyranometer is always positive since it represents the solar energy received as watts per square meter. The data shown in Figure 5 spans from 00:00 until 23:59. The sunlight on the 23rd of April 2015 started at 3:30 due to the northern latitude of Finland and lasted until 17:00, having a peak of 900 w/m$^2$ at 11:00. The data was sampled every 10 seconds and included relatively large and fast fluctuations due to cloud shadows and reflections.


Figure 4: Soil layers under the asphalt in the measurement field.

Figure 5 also represents the net heat flux through the asphalt surface for the same day. Heat flux can have negative values when the heat is dissipated back onto the surface from the ground. The figure shows that the solar irradiance induces a positive heat flux towards the ground, whereas the heat flow becomes negative when the irradiance is close to zero. The solar irradiance must be greater than the heat loss to achieve positive heat flow. The heat loss depends on the soil temperature, air temperature, and weather conditions. The heat loss is relatively small in spring when the soil is still cool and relatively high in autumn when the soil is warm. Although the peak heat flow is 700 W/m$^2$, the average heat flux, $\overline{\Phi}$, for the given day was only 14 W/m$^2$. The average heat loss was approximately 130 W/m$^2$.

The ratio of the incoming solar radiance leading to a heat flow under the asphalt can be used

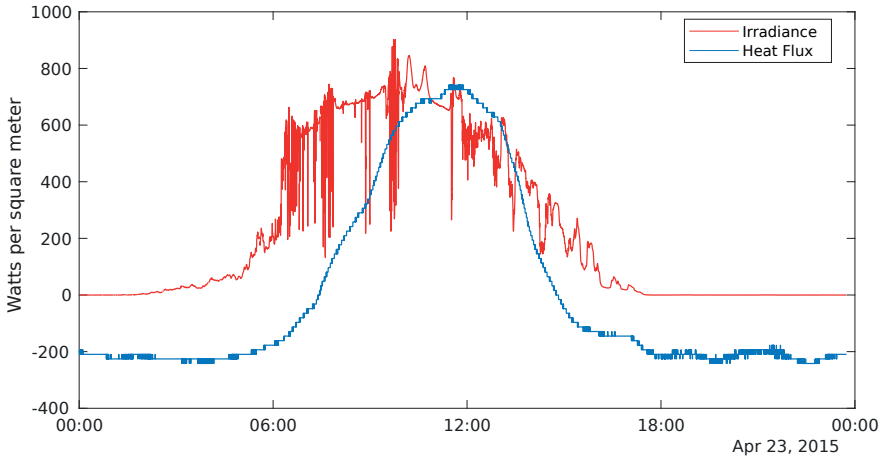


Figure 5: Solar irradiance, $E_e(t)$ (pyranometer) and heat flux under the asphalt $\Phi(t)$ (heat flux plate) for the 23rd of April 2015. The cumulative positive heat flow towards the ground and the net heat flow are 60 % and 5.9 % respectively.

as a measure of the efficiency of the asphalt layer as a heat collector. The daily average absorption ratio, $\sigma$, for the given day was calculated by integrating the solar irradiance, $E_e$, and heat flow, $\Phi$ over a 24 hours period, as follows:

$$\sigma = \frac{(1/T)\int_{t\in T}\Phi(t)\mathrm{dt}}{(1/T)\int_{t\in T}E_e(t)\mathrm{dt}} = \frac{\overline{\Phi}}{\overline{E_e}} \tag{1}$$

This formula applied for the 23th of April gives the following result:

$$\sigma = \frac{14\ \mathrm{W/m^2}}{230\ \mathrm{W/m^2}} = 5.9\%, \tag{2}$$

The net heat flow is rather small due to high negative flow during the night. The escape of the heat can be eliminated by cooling the soil surface temperature below the ambient temperature, by transferring the heat away from the surface. This can be achieved by liquid circulation possibly assisted by heat pumps. Heat escape can be reduced also by many other technical means, such as by selecting optimal materials in different soil layers, or by using an insulating cover during the night. The full potential of the asphalt layer can be estimated by calculating the absorption ratio

in an optimal case where the nighttime heat loss was totally eliminated by accumulating only the positive heat flow. The absorption ratio of this optimal case, $\sigma_p$, is:

$$\sigma_p = \frac{139 \text{ W/m}^2}{230 \text{ W/m}^2} = 60\%, \tag{3}$$

These absorption ratios describe how a large proportion of the solar energy flows to deeper layers of the soil on the given day. As expected, the soil warms up in April, which is usually a spring day in the northern hemisphere. The asphalt was heated at the rate of 139 W/m$^2$ during the day, since 60 % of the irradiance is deposited in the ground but most of the heat evaporated during the night, and the net heating effect is only 14 W/m$^2$, which is only 5.9 % of the original solar irradiance.

### *3.2. Temperature Distribution Measurements Using DTS*

Using the DTS system, temperatures were measured periodically at certain depths. These measurements helped to analyze how the temperature below the surface is distributed. The selected measurement depths in this research are 0.5 m, 1 m, 1.5 m, 3 m, 5 m, and 10 m. Measurements for a period of one year are represented in Figure 6.

Figure 7 represents the temperature changes of the upper layers of the ground from the surface down to 10 m. The data acquired from the DTS system clearly indicates that the higher layers of the soil react to temperature changes faster than the deeper layers. The curves for July and October show that the upper layers have already cooled down in October, but the temperatures of depths below 4 m tend to stay steady. The curves for October and December show that while higher layers keep cooling down, the temperature of deeper layers also drop. After the snow melts in April, the temperature of the highest layer begins to increase but the deeper layers are not affected. During May and the following months of summer, the temperatures continue to increase. Deeper layers are always more steady than the surface and absorb or release heat much slower.

When fast temperature increase occurs on the higher layers, some thermal energy can be delivered to the deeper layers to be stored.

### *3.3. Relation between the cumulative heat flow and soil temperature*

The soil temperature, $T$, is directly proportional to the heat, $Q$, deposited in the soil since $Q = cm\,\Delta T$, where $m$ is the mass of the volume unit of soil and $c$ is the specific heat capacity of the soil. Since the heat, $Q$, is an integral of heat flow, $\Phi$, in time, the following equation is obtained:

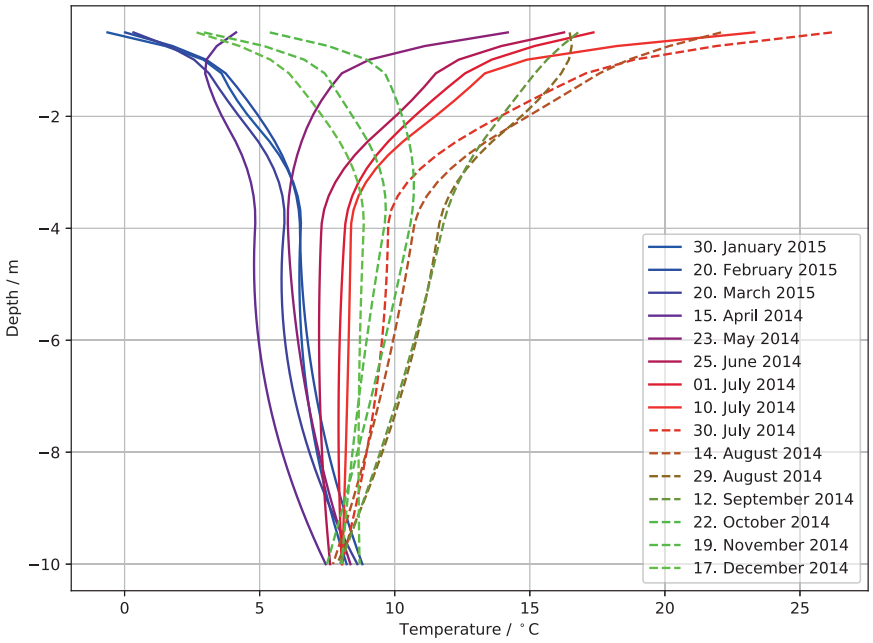


Figure 6: Seasonal soil temperatures according to the DTS measurements

$$\int_o^t (\Phi_{\text{net}})dt = c\, m\, \Delta T, \tag{4}$$

where $\Phi_{\text{net}}$ is the net heat flow into the unit of soil in a certain depth. This equation shows the dependency between soil temperature and heat flow. Figure 7 shows an estimate of the soil temperatures in different depths as a function of time. The temperature change near the surface is positive between April and August and negative from the beginning of August to the beginning of March. The deeper layers of soil keep the temperature longer than the surface layer and therefore the cumulative heat begins decreasing in the middle of October.

Figure 8 shows the solar irradiation and the cumulative heat flow from asphalt to the deeper soil layers. In addition to showing the net heat flow, the negative and positive parts of the heat flow are also integrated separately to obtain a better understanding of the flow. The cumulative

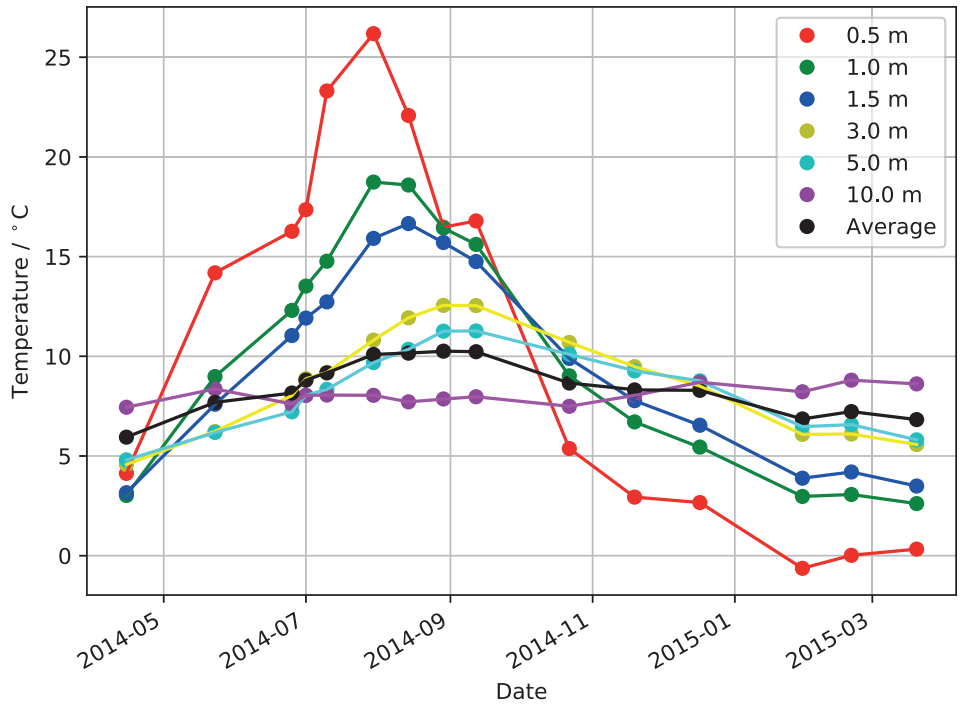


Figure 7: Soil temperatures measured at different depths (0.5 m, 1.0 m, ..., 10 m) and the weighted average temperature of the whole 10 m deep layer.

net flow and the temperature of the soil are increasing until the 26th of September, when the cumulative irradiance is 870 kWh/m$^2$; cumulative positive, negative, and net flows are 610 kWh/m$^2$, 460 kWh/m$^2$ and 150 kWh/m$^2$, respectively. The positive, negative, and net flows correspond to 70%, 53% and 17%, respectively, of the cumulative solar irradiance.

Figures 7 and 8 are not directly comparable since they contain measurements taken in different years, but the overall trends are quite similar. The heat flow through the asphalt layer is not directly relational with the temperature of the surface layer due to the internal heat flows in soil driven by a temperature gradient. Better conformance is obtained by comparing the cumulative heat flow with the average temperature through all soil layers, shown by the black line in Figure 7.

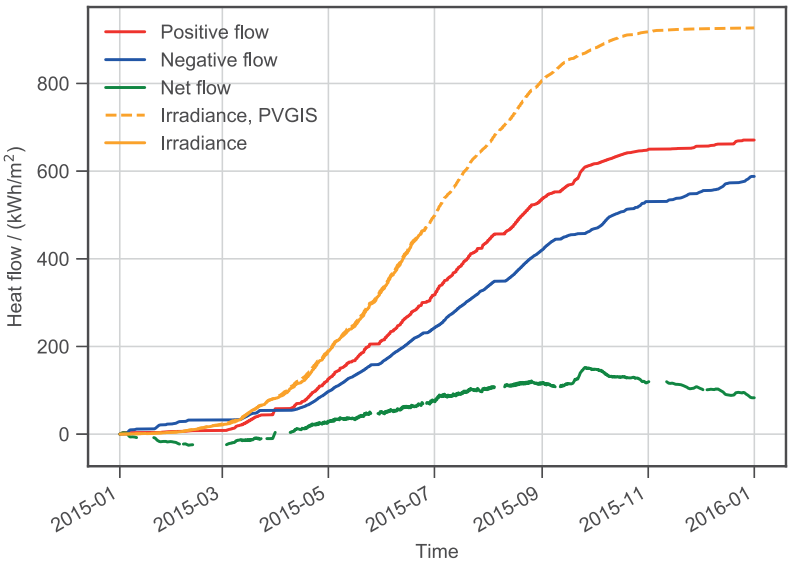


Figure 8: Hourly integrated cumulative irradiance and cumulative heat flows under the asphalt layer over an annual cycle. The net flow consists of the cumulative hourly positive flow into the ground and the cumulative hourly negative flow escaping from the ground. After the warming period, in 26th of September the positive flow is about 70% of the solar irradiance and the net flow is only about 17% of it.

## 4. Results and discussion

The data collected in this research, makes it possible to analyze the performance of the asphalt as a heat collection system during any time period of the year. Selected periods of five days from every season of the year were analyzed and are represented in this section.

First, we can take a look at the temperature gradients in the soil layers. When heat is collected by the asphalt layer, the temperature rises, causing a temperature gradient that drives a heat flow through the soil, according to Fourier's law. $\Phi = -k\nabla T$, where $k$ is the thermal conductivity. The temperature distributions shown in Figure 6 reveal a high gradient in the topmost gravel layer and a more gentle sloping gradient in the next clay layer; there is an even smaller gradient in the

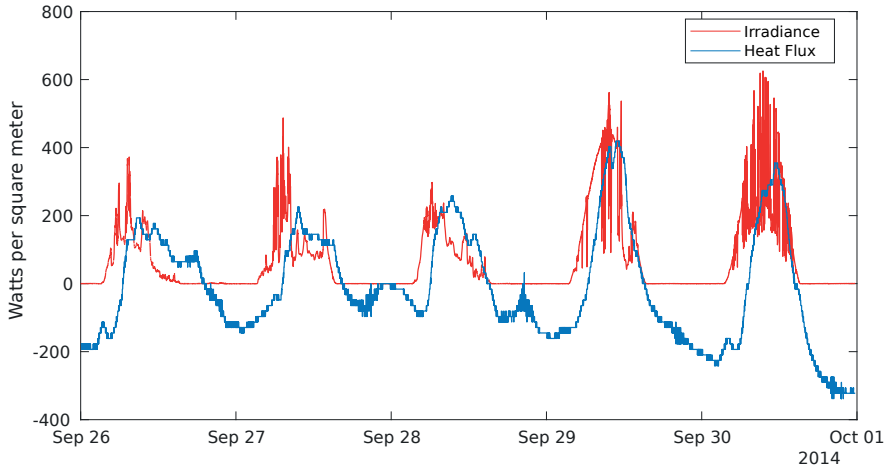


| | |
|---|---|
| Average solar radiation $\overline{E}_e$ | 92 W/m$^2$ |
| Average net heat flux $\overline{\Phi}$ | -27 W/m$^2$ |
| Average positive heat flux $\overline{\Phi}_p$ | 60 W/m$^2$ |
| Absorption ratio $\sigma$ | -30 % |
| Absorption ratio, positive flux $\sigma_p$ | 65 % |

Figure 9: Instantaneous solar irradiation and heat flux from 26 Sep to 01 Oct 2014 (autumn) and estimated average values.

bedrock, implying that the bedrock has the highest conductivity and the gravel layer the lowest. The same observation was seen in the preceding laboratory measurements as well, as reported in [18]. This structure is designed for preventing ground frosting during winters, but not desirable for storing solar heat. We found that the heat flowing through the asphalt is not efficiently distributed in the bigger soil volume, but stays too long in the surface layer and is therefore easily dissipated back to the atmosphere during the night. The ground structure could be optimized by increasing the conductivity of the surface by changing the materials or by irrigation.

Figures (7 - 8) indicate that the net heat flow becomes positive during March or April, depending on the year, and turns back to negative in September or October. The surface reaches its peak temperature at the end of July but remains warm enough to continue driving positive net heat flow

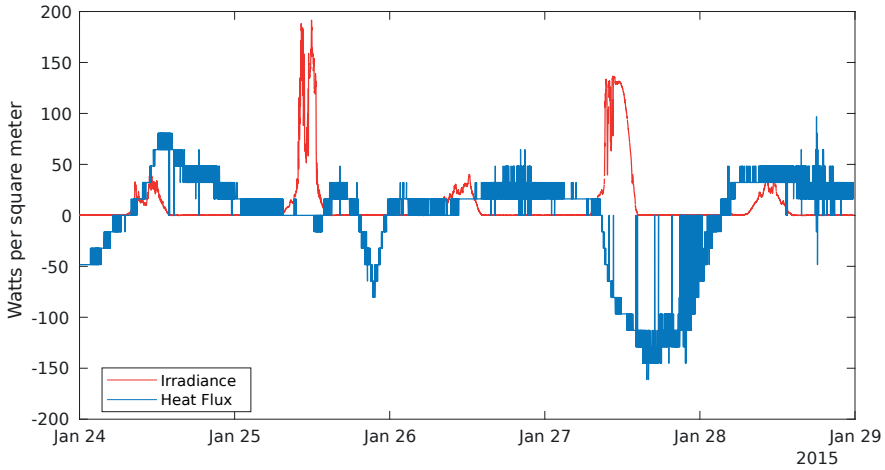


| | |
|---|---|
| Average solar radiation $\overline{E}_e$ | 11 W/m$^2$ |
| Average net heat flux $\overline{\Phi}$ | -1.9 W/m$^2$ |
| Absorption ratio $\sigma$ | -18 % |
| Average positive heat flux $\overline{\Phi}_p$ | 15 % |
| Absorption ratio, positive flux $\sigma_p$ | 150 % |

Figure 10: Instantaneous solar irradiation and heat flux from 24 to 29 Jan 2015 (winter) and estimated average values. Both irradiance and heat flux are negligible and heat flux is more dependent on the temperature than irradiance.

to the ground until 26th of September. The average net heat flow is less than 15% of the available irradiance due to the nighttime heat losses, while the average positive heat is 64% of the irradiance. This positive heat flow could be more efficiently utilized by reducing nighttime losses, which were, according to Table (1), 3/4 of the positive heat flux during spring and summer, and even higher during autumn.

Figures (9 - 12) illustrate the instantaneous balance during 5 days periods of heat flow and irradiance in four different seasons. The data shown in the figures is summarized in Table (1). Heat flux value for autumn is negative because the soil is still warm but is cooling down continuously. In winter, the positive heat flux is small, depending more on the air temperature than negligible irradiance, and losses are small due to the annual soil temperature minimum and the insulating

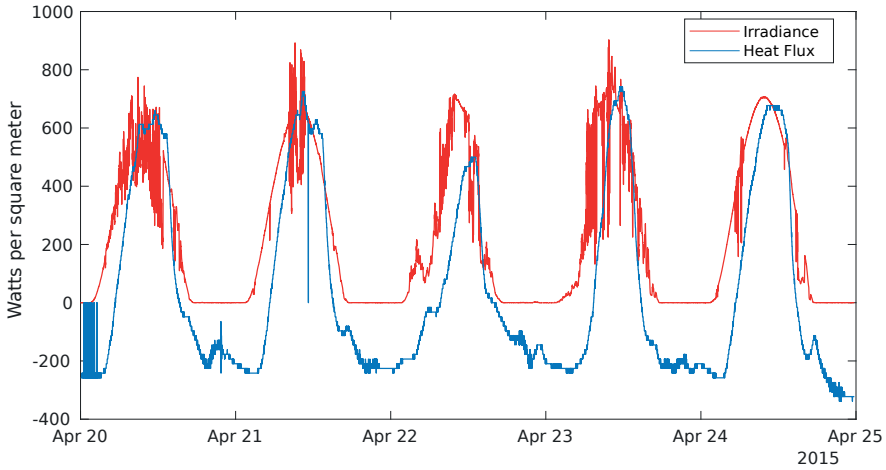


| | |
|---|---|
| Average solar radiation $\overline{E}_e$ | 230 W/m$^2$ |
| Average net heat flux $\overline{\Phi}$ | 42 W/m$^2$ |
| Absorption ratio $\sigma$ | 18% |
| Average positive heat flux $\overline{\Phi}_p$ | 150 W/m$^2$ |
| Absorption ratio, positive flux $\sigma_p$ | 67 % |

Figure 11: Instantaneous solar irradiation and heat flux from 20 to 25 Apr 2015 (spring) and estimated average values.

snow cover. The soil starts warming quickly during spring when the irradiance is increasing but the soil temperature is still low, keeping losses small. Solar irradiance is strongest during the summer, but the net heat flux is not very strong because the soil is already warm and the losses are also high.

Because heat loss due to radiation and convection also occur during daylight, the positive heat flow could be further improved by lowering the temperature of the surface during daylight hours; for example, by collecting and transferring the heat to seasonal storage. This would allow the utilization of this urban renewable energy even in cold climate regions. Further research is needed to find the full potential of the asphalt heat collection and storage system.

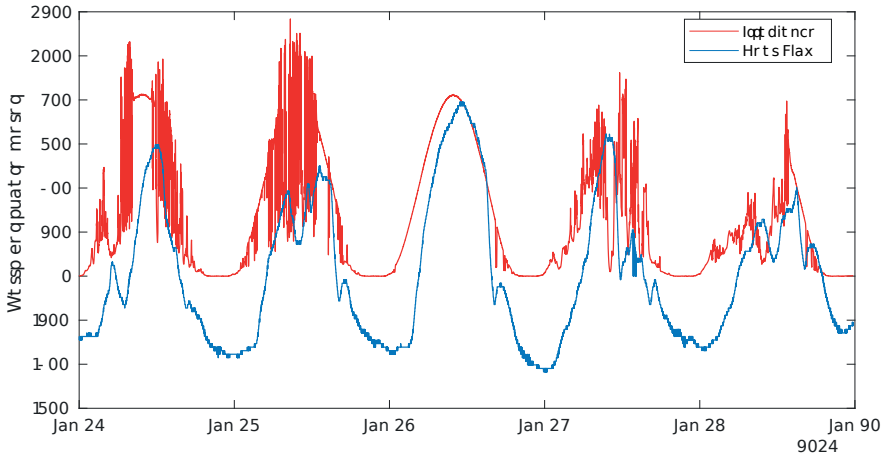


| | |
|---|---|
| Average solar radiation $\overline{E}_e$ | 260 W/m$^2$ |
| Average net heat flux $\overline{\Phi}$ | 8.4 W/m$^2$ |
| Absorption ratio $\sigma$ | 3.3 % |
| Average positive heat flux $\overline{\Phi}_p$ | 190 W/m$^2$ |
| Absorption ratio, positive flux $\sigma_p$ | 53 % |

Figure 12: Instantaneous solar irradiation and heat flux from 15 to 20 Jun 2015 (summer) and estimated average values.

Table 1: Average solar irradiance, heat flux and absorption ratios over five day periods in all seasons. The first three rows represent the average net heat collection values over the whole period and the next two rows represent the corresponding values for positive vlues.

| *Parameter* | *Autumn* | *Winter* | *Spring* | *Summer* | *Year* |
|---|---|---|---|---|---|
| Average solar irradiance $\overline{E}_e$ | 92 W/m$^2$ | 11 W/m$^2$ | 230 W/m$^2$ | 260 W/m$^2$ | 110 W/m$^2$ |
| Average net heat flux $\overline{\Phi}$ | -28 W/m$^2$ | -1.9 W/m$^2$ | 42 W/m$^2$ | 8.4 W/m$^2$ | 9.5 W/m$^2$ |
| Absorption ratio $\sigma$ | -30 % | -18 % | 18 % | 3.3 % | 8.9 % |
| Average positive heat flux $\overline{\Phi}_p$ | 60 W/m$^2$ | 16 W/m$^2$ | 150 W/m$^2$ | 140 W/m$^2$ | 73 W/m$^2$ |
| Absorption ratio, positive flux $\sigma_p$ | 65 % | 150 % | 67 % | 53 % | 70 % |

Some unexpected environmental factors occurred while taking the measurements, such as shadows of cars parking over the measurement area. The long time needed to take the measurements also caused some interruption in data acquisition. These interruptions were mainly caused by battery depletion, software resets due to power shortages, and other unknown reasons. In the future, these losses could be estimated and compensated for using Kalman filters and other estimation methods.

## 5. Conclusions

In this research, three independent methods were used to measure the solar irradiance, heat flux, and soil temperature, to explain the behavior of the asphalt layer of pavement for collecting solar heat. The measurements revealed that the current efficiency of asphalt pavement in absorbing solar irradiation during the soil warming period between 1st of January and 26th of September is about 17%. If the nighttime escape of heat can be eliminated by covering the asphalt field with insulating cover during the night or by transferring the heat away from the surface, the efficiency could be up to 70% in the same time period. The cumulative irradiance, net heat flow and positive heat flow in the asphalt field during the soil warming period were 870 kWh/m$^2$, 150 kWh/m$^2$ and 610 kWh/m$^2$, respectively. Cumulative irradiance, net heat flow and positive heat flow during the whole year are 930 kWh/m$^2$, 83 kWh/m$^2$ and 670 kWh/m$^2$, respectively. These results imply that the asphalt layer could potentially collect up to 670 kWh/m$^2$, provided that the losses can be properly handled.

The temperature of the surface layer is relatively low, exceeding +20°C in half meter depth only in the middle of the summer. The temperature of the heat collection liquid usually needs to be elevated using heat pumps before it can be used for heating purposes. In some applications, such as melting the snow on the asphalt field, it could be used without heat pumps. The temperature of the surface is probably higher in summer closer to the surface, but these temperatures were not covered by current data.

DTS measurements show that the annual changes in the soil temperature, caused by the solar radiation, mostly occur within the first 10 m below the ground level.

In this research, the heat collecting properties of the existing asphalt fields were analyzed and some suggestions for improving the collection efficiency were made. Further research using thermal simulations and experiments are needed to study how much the active and passive heat transfer

mechanisms, like under asphalt soil structures, could improve the net heat collection efficiency in a practical case.

## 6. Acknowledgements

The authors gratefully acknowledge the financial support of the City of Vaasa and the Graduate School of the University of Vaasa.

[1] Canbing Li, Jincheng Shang, Yijia Cao, Discussion on energy-saving taking urban heat island effect into account, in: 2010 International Conference on Power System Technology, IEEE, Zhejiang, Zhejiang, China, 2010, pp. 1–3. doi:10.1109/POWERCON.2010.5666391.
URL http://ieeexplore.ieee.org/document/5666391/

[2] A. Mäkiranta, E. Hiltunen, Utilizing Asphalt Heat Energy in Finnish Climate Conditions, Energies 12 (11) (2019) 2101. doi:10.3390/en12112101.
URL https://www.mdpi.com/1996-1073/12/11/2101

[3] G. Hailu, P. Hayes, M. Masteller, Long-Term Monitoring of Sensible Thermal Storage in an Extremely Cold Region, Energies 12 (9) (2019) 1821. doi:10.3390/en12091821.
URL https://www.mdpi.com/1996-1073/12/9/1821

[4] M. Mehrpooya, H. Hemmatabady, M. H. Ahmadi, Optimization of performance of Combined Solar Collector-Geothermal Heat Pump Systems to supply thermal load needed for heating greenhouses, Energy Conversion and Management 97 (2015) 382–392. doi:10.1016/j.enconman.2015.03.073.
URL http://www.sciencedirect.com/science/article/pii/S0196890415002915

[5] A. Hesaraki, S. Holmberg, F. Haghighat, Seasonal thermal energy storage with heat pumps and low temperatures in building projects—A comparative review, Renewable and Sustainable Energy Reviews 43 (2015) 1199–1213. doi:10.1016/j.rser.2014.12.002.
URL http://www.sciencedirect.com/science/article/pii/S1364032114010545

[6] B. Sibbitt, D. McClenahan, R. Djebbar, J. Thornton, B. Wong, J. Carriere, J. Kokko, The Performance of a High Solar Fraction Seasonal Storage District Heating System – Five Years of Operation, Energy Procedia 30 (2012) 856–865. doi:10.1016/j.egypro.2012.11.097.
URL http://www.sciencedirect.com/science/article/pii/S187661021201613X

[7] B. Sibbitt, D. McClenahan, R. Djebbar, J. Thornton, B. Wong, J. Carriere, J. Kokko, The Performance of a High Solar Fraction Seasonal Storage District Heating System – Five Years of Operation, Energy Procedia 30 (2012) 856–865. doi:10.1016/j.egypro.2012.11.097.
URL http://www.sciencedirect.com/science/article/pii/S187661021201613X

[8] L. Mesquita, D. McClenahan, J. Thornton, J. Carriere, B. Wong, Drake Landing Solar Community: 10 Years of Operation, in: Proceedings of SWC2017/SHC2017, International Solar Energy Society, Abu Dhabi, 2017, pp. 1–12. doi:10.18086/swc.2017.06.09.
URL http://proceedings.ises.org/citation?doi=swc.2017.06.09

[9] H. M. K. U. Haq, E. Hiltunen, An inquiry of ground heat storage: Analysis of experimental measurements and optimization of system's performance, Applied Thermal Engineering 148 (2019) 10–21. doi:10.1016/j.applthermaleng.2018.11.029.
URL http://www.sciencedirect.com/science/article/pii/S1359431118323342

[10] L. Kisgyörgy, B. Plesz, Thermal Energy of Asphalt Pavements, Magyar Építőipar 64 (1) (2014) 3–7.

[11] U. Datta, S. Dessouky, A. T. Papagiannakis, Thermal Energy Harvesting from Asphalt Roadway Pavement, in: L. Mohammad (Ed.), Advancement in the Design and Performance of Sustainable Asphalt Pavements, Sustainable Civil Infrastructures, Springer International Publishing, 2018, pp. 272–286.

[12] J. Suomi, J. Käyhkö, The impact of environmental factors on urban temperature variability in the coastal city of Turku, SW Finland, International Journal of Climatology 32 (3) (2012) 451–463. doi:10.1002/joc.2277.
URL http://doi.wiley.com/10.1002/joc.2277

[13] A. Gonçalves, G. Ornellas, A. Castro Ribeiro, F. Maia, A. Rocha, M. Feliciano, Urban Cold and Heat Island in the City of Bragança (Portugal), Climate 6 (3) (2018) 70. doi:10.3390/cli6030070.
URL https://www.mdpi.com/2225-1154/6/3/70

[14] T. Kershaw, M. Sanderson, D. Coley, M. Eames, Estimation of the urban heat island for UK climate change projections, Building Services Engineering Research and Technology 31 (3)

(2010) 251–263. doi:10.1177/0143624410365033.
URL https://doi.org/10.1177/0143624410365033

[15] P. Pan, S. Wu, Y. Xiao, G. Liu, A review on hydronic asphalt pavement for energy harvesting and snow melting, Renewable and Sustainable Energy Reviews 48 (2015) 624–634. doi:10.1016/j.rser.2015.04.029.
URL http://www.sciencedirect.com/science/article/pii/S1364032115002993

[16] V. Bobes-Jesus, P. Pascual-Muñoz, D. Castro-Fresno, J. Rodriguez-Hernandez, Asphalt solar collectors: A literature review, Applied Energy 102 (2013) 962–970. doi:10.1016/j.apenergy.2012.08.050.
URL http://www.sciencedirect.com/science/article/pii/S030626191200637X

[17] Z. Zhou, X. Wang, X. Zhang, G. Chen, J. Zuo, S. Pullen, Effectiveness of pavement-solar energy system – An experimental study, Applied Energy 138 (2015) 1–10. doi:10.1016/j.apenergy.2014.10.045.
URL http://www.sciencedirect.com/science/article/pii/S0306261914010952

[18] J. B. Martinkauppi, A. Mäkiranta, J. Kiijärvi, E. Hiltunen, Thermal Behavior of an Asphalt Pavement in the Laboratory and in the Parking Lot, The Scientific World Journal 2015. doi:10.1155/2015/540934.
URL https://www.ncbi.nlm.nih.gov/pmc/articles/PMC4377482/

[19] K. Zhu, P. Blum, G. Ferguson, K.-D. Balke, P. Bayer, The geothermal potential of urban heat islands, Environmental Research Letters 5 (4) (2010) 044002. doi:10.1088/1748-9326/5/4/044002.
URL https://doi.org/10.1088/1748-9326/5/4/044002

[20] Oryx DTS User Manual v4, Sensornet Ltd, 2007.

[21] A. Ukil, H. Braendle, P. Krippner, Distributed Temperature Sensing: Review of Technology and Applications, IEEE Sensors Journal 12 (5) (2012) 885–892. doi:10.1109/JSEN.2011.2162060.
URL http://ieeexplore.ieee.org/document/5955066/

[22] C. Sayde, C. Gregory, M. Gil-Rodriguez, N. Tufillaro, S. Tyler, N. v. d. Giesen, M. English, R. Cuenca, J. S. Selker, Feasibility of soil moisture monitoring with heated fiber optics, Water Resources Research 46 (6). doi:10.1029/2009WR007846.
URL https://agupubs.onlinelibrary.wiley.com/doi/abs/10.1029/2009WR007846